

COHOMOLOGY OF REAL GRASSMANN MANIFOLD AND KP FLOW

LUIS CASIAN AND YUJI KODAMA*

ABSTRACT. We consider a realization of the real Grassmann manifold $\mathrm{Gr}(k, n)$ based on a particular flow defined by the corresponding (singular) solution of the KP equation. Then we show that the KP flow can provide an explicit and simple construction of the incidence graph for the integral cohomology of $\mathrm{Gr}(k, n)$. It turns out that there are two types of graphs, one for the trivial coefficients and other for the twisted coefficients, and they correspond to the homology groups of the orientable and non-orientable cases of $\mathrm{Gr}(k, n)$ via the Poincaré-Lefschetz duality. We also derive an explicit formula of the Poincaré polynomial for $\mathrm{Gr}(k, n)$ and show that the Poincaré polynomial is also related to the number of points on a suitable version of $\mathrm{Gr}(k, n)$ over a finite field \mathbb{F}_q with q being a power of a prime. In particular, we find that the number of \mathbb{F}_q points on $\mathrm{Gr}(k, n)$ can be computed by counting the number of singularities along the KP flow.

CONTENTS

1. Introduction	2
2. The real Grassmann manifold $\mathrm{Gr}(k, n)$	8
2.1. The Schubert decomposition	8
2.2. The Plücker embedding and the moment polytope	10
3. The KP flow on $\mathrm{Gr}(k, n)$	11
3.1. The KP flow on the moment polytope	11
3.2. The KP equation and the Toda lattice	13
3.3. Remark on the Toda lattice description	15
4. The set $\mathcal{S}_n^{(k)}$ and the graph $\mathcal{G}_n^{(k)}$	16
4.1. The decomposition of $\mathcal{S}_n^{(k)}$	18
4.2. The decomposition of $\mathrm{Gr}(k, n)$	19
5. The graph $\mathcal{G}(k, n)$	21
5.1. The signed Schubert cells	22
6. Proof of the main Theorem for the incidence graph	25
6.1. The case of $\mathrm{Gr}(2, 4)$	25
6.2. Some standard notation	26
6.3. Connection of the cohomology of G/B with Hecke algebra operators	27
6.4. The edge in the incidence graph associated to $\mathcal{B}_w \cup \mathcal{B}_{s_i w}$	28
6.5. K -equivariant local systems on G/B and their Toda signs	28
6.6. Computation of the signs $\epsilon(\sigma, \mathcal{L})$	29
6.7. Proof of Theorem	31
7. The Poincaré polynomials	34
7.1. The polynomials $P_{(k, n)}^*(t)$	34
7.2. The polynomials $P_{(k, n)}(t)$	36
8. The \mathbb{F}_q points on $\mathrm{Gr}(k, n)$ and the Poincaré polynomials	39
8.1. The q -weighted Schubert cells	39

*Partially supported by NSF grant DMS0806219.

8.2. The number of \mathbb{F}_q -points on $\text{Gr}(k, n)$	43
8.3. Frobenius eigenvalues calculation	46
References	46

1. INTRODUCTION

This paper attempts to extract the topology of real Grassmannians based on a *realization* of the manifolds related to the KP hierarchy. As in the case of the real flag manifolds discussed in [8] using the Toda lattice hierarchy, we here show that the KP equation can be used to obtain similar results for the real Grassmannians.

The KP equation is a two-dimensional extension of the well-known KdV equation, and it was introduced by Kadomtsev and Petviashvili in 1970 to study the stability of one KdV soliton under the influence of weak two-dimensional perturbations [18]. The equation provides also a model to describe a two-dimensional shallow water wave phenomena (see for example [1, 27, 20, 11]). The KP equation is a dispersive wave equation for the scalar function $u = u(x, y, t)$ with spatial variables (x, y) and time variable t , and is given by

$$\frac{\partial}{\partial x} \left(-4 \frac{\partial u}{\partial t} + 6u \frac{\partial u}{\partial x} + \frac{\partial^3 u}{\partial x^3} \right) + 3 \frac{\partial^2 u}{\partial y^2} = 0.$$

We write the solution in the form

$$u(x, y, t) = 2 \frac{\partial^2}{\partial x^2} \ln \tau(x, y, t),$$

where the function τ is called the *tau* function of the KP equation [26, 25]. It is also well-known that some of the exact solutions can be written in the Wronskian determinant form (see for example [15]),

$$(1.1) \quad \tau = \text{Wr}(f_1, f_2, \dots, f_k) := \begin{vmatrix} f_1 & f_2 & \cdots & f_k \\ f'_1 & f'_2 & \cdots & f'_k \\ \vdots & \ddots & \ddots & \vdots \\ f_1^{(k-1)} & f_2^{(k-1)} & \cdots & f_k^{(k-1)} \end{vmatrix},$$

where $f_j^{(l)} := \partial^l f_j / \partial x^l$, and each of the functions $\{f_i(x, y, t) : i = 1, 2, \dots, k\}$ satisfies the simple linear equations,

$$\frac{\partial f_i}{\partial y} = \frac{\partial^2 f_i}{\partial x^2}, \quad \frac{\partial f_i}{\partial t} = \frac{\partial^3 f_i}{\partial x^3}.$$

We then take the following finite dimensional solutions, (i.e. finite Fourier series),

$$f_i = \sum_{j=1}^n a_{i,j} E_j, \quad \text{with} \quad E_j := \exp(\lambda_j x + \lambda_j^2 y + \lambda_j^3 t),$$

where $A := (a_{i,j})$ is an $k \times n$ real matrix of rank k , and λ_j 's are real and distinct numbers, say

$$\lambda_1 < \lambda_2 < \cdots < \lambda_n.$$

Since λ_j 's are all distinct, the set of exponential functions $\{E_j : j = 1, \dots, n\}$ is linearly independent and forms a basis of \mathbb{R}^n . Then the set of $\{f_i : i = 1, \dots, k\}$ defines a k -dimensional subspace in \mathbb{R}^n . This implies that each solution defined by the τ -function (1.1) can be characterized by the A -matrix, hence the solution parametrizes a point of the real Grassmannian. Note here that the Grassmannian denoted by $\text{Gr}(k, n, \mathbb{R})$ can be described as

$$\text{Gr}(k, n, \mathbb{R}) = \text{GL}_k(\mathbb{R}) \setminus M_{k \times n}(\mathbb{R}),$$

where $M_{k \times n}(\mathbb{R})$ is the set of all $k \times n$ matrices of rank k , and $\mathrm{GL}_k(\mathbb{R})$ is the general linear group of $k \times k$ matrices. We then expect that some particular solutions of the KP equation contain certain information on the cohomology of $\mathrm{Gr}(k, n, \mathbb{R})$. This is our main motivation for the present study. In the previous paper [8], we found the similar results for the case of real flag variety using the Toda lattice equation.

Let us explain how some solutions contain information of the cohomology of $\mathrm{Gr}(k, n, \mathbb{R})$ by taking simple example with $k = 1$ and $n = 4$. That is, we recover the cohomology of real variety $\mathbb{R}P^3 \cong \mathrm{Gr}(1, 4, \mathbb{R})$ from a KP flow. We consider the τ -function in the form,

$$(1.2) \quad \tau = \epsilon_1 E_1 + \epsilon_2 E_2 + \epsilon_3 E_3 + \epsilon_4 E_4,$$

where ϵ_j are arbitrary non-zero real constants. Since $|\epsilon_j|$ can be absorbed in the exponential term, we only consider their signs, and here we assume $\epsilon_j \in \{\pm\}$ (which we refer to as *KP signs*). Let us consider the case with the specific signs $(\epsilon_1, \dots, \epsilon_4) = (+, -, -, +)$. Using simple asymptotic argument, one can easily find that each $E_j(x, y, t)$ becomes dominant in certain region of the xy -plane for a fixed t . Figure 1 illustrates the contour plots of the solution $u(x, y, t)$ at $t > 0$ and $t < 0$. Each region marked by the number (i) indicates the dominant exponential E_i , and at the boundary of the region, the τ -function can be expressed by two exponential functions E_i and E_j (which is dominant in the adjacent region), i.e. writing $E_i = e^{\theta_i}$ with $\theta_i = \lambda_i x + \lambda_i^2 y + \lambda_i^3 t$,

$$\begin{aligned} \tau &\approx \epsilon_i E_i + \epsilon_j E_j \\ &= \pm 2e^{\frac{1}{2}(\theta_i + \theta_j)} \begin{cases} \cosh \frac{1}{2}(\theta_i - \theta_j) & \text{if } \epsilon_i \epsilon_j = +, \\ \sinh \frac{1}{2}(\theta_i - \theta_j) & \text{if } \epsilon_i \epsilon_j = -. \end{cases} \end{aligned}$$

Then at the boundary, the solution has the following form depending on the sign $\epsilon_i \epsilon_j$,

$$u = \frac{1}{2}(\lambda_i - \lambda_j)^2 \begin{cases} \operatorname{sech}^2 \frac{1}{2}(\theta_i - \theta_j) & \text{if } \epsilon_i \epsilon_j = +, \\ \operatorname{csch}^2 \frac{1}{2}(\theta_i - \theta_j) & \text{if } \epsilon_i \epsilon_j = -. \end{cases}$$

In Figure 1, the sech-part (regular) of the solution is shown by the dark colored contour, and the csch-part (singular) is shown in the light colored contour. We construct a polytope whose vertices are labeled by the dominant exponentials. The polytope for our example is a tetrahedron as shown in Figure 1. We then consider a KP flow choosing a particular parameter set (x, y, t) , so that the flow is passing near the edges of the polytope. The flow might be expressed as a graph,

$$(1.3) \quad (1) \longrightarrow (2) \implies (3) \longrightarrow (4),$$

where \longrightarrow shows the singular flow, and the \implies shows the regular one. It is then interesting to note that the graph is the incidence graph of the real projective space $\mathbb{R}P^3$, if the arrows are identified as the coboundary operators and their incidence numbers are assigned as 0 for \longrightarrow and ± 2 for \implies .

This kind of graph, exemplified by graph (1.3), was introduced in [8] in an initial attempt to compute the number of connected components carved up by the zero divisors of the τ -function, i.e. $\tau_i = 0$ for some i , within a moment polytope for the Toda flow. In the case of the KP flow Figure 1 shows that this graph does not contain enough information to attempt to do this (one would have to connect (1) and (4) with an edge \implies). Still the main results in [8], which then motivated this paper, were the result of an observation that such a graph, exclusively defined in terms of the flow crossing or not crossing singularities, agrees, in the case of the Toda flow, with the incidence graph of real flag manifolds. The results in this paper extend this type of results to the KP flow.

As in [8] a polynomial can be defined by counting singularities crossed and taking an alternating sum. In this case we obtain $1 - q^2$, and now $q(q^2 - 1)$, with q a power of a prime number, counts the number of points over a finite field, \mathbb{F}_q , of a variety closely related to $\mathrm{Gr}(1, 4, \mathbb{R})$. This is explained in more detail below and generalized. The cohomology calculation can be thought of as actually

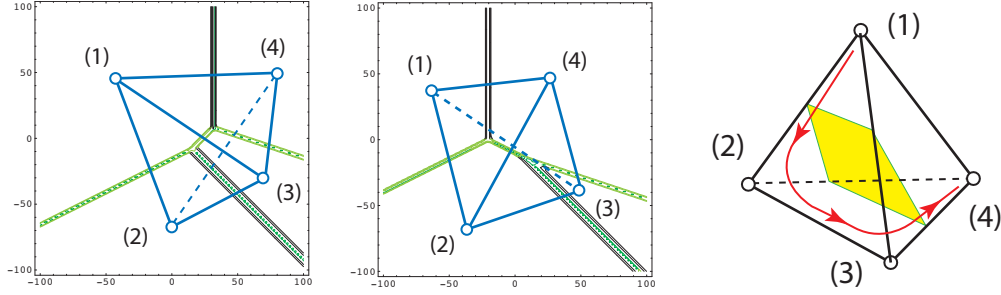


FIGURE 1. The contour plot of the KP solution with the τ -function given by (1.2). The signs are chosen as $(\epsilon_1, \dots, \epsilon_4) = (+, -, -, +)$. In the left two figures, the number (i) of each region represents the dominant exponential E_i , and the dark (light) colored contour shows the regular (singular) part of the solution. The left figure shows the contour plot of the solution at $t = -5$ and the middle one is at $t = 5$. The tetrahedron in the figures indicates as a dual graph of the solution pattern, that is, the vertices of the polytope are labeled by the dominant exponentials. The directed curve in the right figure shows a flow of the KP equation, and this flow blows up twice by crossing the boundary between the regions with different signs, which corresponds to $\tau = 0$.

taking place over a field of positive characteristic (etale cohomology) so that these q^i , i counting singularities crossed, appear as Frobenius eigenvalues in cohomology.

One should note in the graph that the numbers (i) representing the dominant exponential E_i label the Schubert cells of the variety $\mathbb{R}P^3$, i.e.

$$\mathbb{R}P^3 = X(1) \sqcup X(2) \sqcup X(3) \sqcup X(4),$$

where $X(i)$ is the Schubert cell of dimension $i - 1$ (see Section 2). In this paper, we intend to show that this view of the KP flow can be used to construct the incidence graph of the real Grassmann variety $\text{Gr}(k, n, \mathbb{R})$ in general.

We simply denote $\text{Gr}(k, n, \mathbb{R})$ by $\text{Gr}(k, n)$. Here we present an overview of the paper. Let \mathcal{S}_n be the symmetric group with the simple reflections s_j for $j = 1, \dots, n - 1$, and \mathcal{P}_k be the parabolic subgroup of \mathcal{S}_n generated by $\{s_j : j = 1, \dots, n, j \neq k\}$. We then have the Schubert decomposition of $\text{Gr}(k, n)$,

$$\text{Gr}(k, n) = \bigsqcup_{w \in \mathcal{S}_n^{(k)}} X_w,$$

where $\mathcal{S}_n^{(k)}$ is the set of minimal coset representatives of $\mathcal{S}_n / \mathcal{P}_k$ ([2], see also Section 4). In this paper, we are interested in the integral cohomology of $\text{Gr}(k, n)$ which we find by constructing the corresponding incidence graph (Section 5). The co-chain complex may be expressed as follows: The set of the co-chains are defined by

$$\mathcal{C}^* = \bigoplus_{j=0}^{k(n-k)} \mathcal{C}^j, \quad \text{with} \quad \mathcal{C}^j = \bigoplus_{j=l(w)} \mathbb{Z}\langle w \rangle,$$

where $l(w)$ is the length of $w \in \mathcal{S}_n^{(k)}$, and $\langle w \rangle := \overline{X_w}$, the Schubert cycle. For each j , we define an operator $\delta_j : \mathcal{C}^j \rightarrow \mathcal{C}^{j+1}$ in the form, for $\langle w \rangle \in \mathcal{C}^j$ and $\langle w' \rangle \in \mathcal{C}^{j+1}$,

$$\delta_j \langle w \rangle = \sum_{l(w')=l(w)+1} [w; w'] \langle w' \rangle.$$

where $w' = s_i w$ for all s_i with $l(s_i w) = l(w) + 1$. The coefficient $[w, w']$ takes the value either 0 or ± 2 ([19], see also Section 5). Then we define a graph $\mathcal{G}(k, n)$, which can be described along the KP flow, and which consists of the vertices given by $\langle w \rangle$ for $w \in \mathcal{S}_n^{(k)}$ and the edges given by the (double) arrows between $\langle w \rangle$ and $\langle w' \rangle$ when $[w, w'] \neq 0$, that is, there is no blow up. For example, in the case of $\text{Gr}(1, 4) \cong \mathbb{R}P^3$, we have $\mathcal{C}^* = \mathbb{Z}[\langle e \rangle] \oplus \mathbb{Z}[\langle s_1 \rangle] \oplus \mathbb{Z}[\langle s_2 s_1 \rangle] \oplus \mathbb{Z}[\langle s_3 s_2 s_1 \rangle]$, and the graph $\mathcal{G}(1, 4)$ is given by

$$\langle e \rangle \longrightarrow \langle s_1 \rangle \implies \langle s_2 s_1 \rangle \longrightarrow \langle s_3 s_2 s_1 \rangle.$$

This graph is the incidence graph for $\mathbb{R}P^3$ when we assign the coefficients as $[e; s_1] = 0$, $[s_1; s_2 s_1] = \pm 2$ and $[s_2 s_1; s_3 s_2 s_1] = 0$ (cf. (1.3)). This can be extended to the general case, and in Section 6, we prove the main theorem,

Theorem 1.1. *The graph $\mathcal{G}(k, n)$ is the incidence graph for the real Grassmannian $\text{Gr}(k, n)$.*

The proof of this theorem is based on [9] and a simplified description of these results for the real split case which are described in terms of the Toda lattice in [8]; finally an adaptation of [8] so that incidence graphs are expressed exclusively in terms of the KP flow, which, it turns out, further simplifies the case of real Grassmannians allowing easy explicit calculation of Betti numbers.

Based on the graph $\mathcal{G}(k, n)$, we then derive explicit formulas for Betti numbers of real Grassmannians, and discuss relations of these Betti numbers to the number of points over a finite field of certain related varieties. For this computation, we first replace the real Grassmannian manifold $\text{Gr}(k, n)$ with a complex manifold, a Zariski open subset $\text{Gr}(k, n)_{\mathbb{C}} \subset \text{Gr}(k, n, \mathbb{C})$ with the same homotopy type (see subsection 8.2 for the details). The variety $\text{Gr}(k, n)_{\mathbb{C}}$ can be considered over other fields, for example, a finite field \mathbb{F}_q with q elements. The number of \mathbb{F}_q points i.e. the number of points on $\text{Gr}(k, n)_{\mathbb{F}_q}$, is given by a polynomial of q denoted by $|\text{Gr}(k, n)_{\mathbb{F}_q}|$. In section 8, we show that the polynomial $|\text{Gr}(k, n)_{\mathbb{F}_q}|$ is related to the Poincaré polynomial of the real variety $\text{Gr}(k, n)$. The cohomology of $\text{Gr}(k, n)$ is much more complicated than the cohomology of the complex variety $\text{Gr}(k, n, \mathbb{C})$, since it involves torsion. However we find that, the Betti numbers of $\text{Gr}(k, n, \mathbb{C})$ and $\text{Gr}(k', n')$ for some (k', n') determined from (k, n) , agree after taking into account a change in degrees. Recall that the Poincaré polynomial of the complex variety $\text{Gr}(k, n, \mathbb{C})$, denoted by $P_{(k, n)}^{\mathbb{C}}(t)$, is simply obtained by the number of \mathbb{F}_q points, $|\text{Gr}(k, n, \mathbb{C})|$. That is, we have

$$P_{(k, n)}^{\mathbb{C}}(t) = |\text{Gr}(k, n, \mathbb{F}_q)|_{q=t^2} = \sum_{w \in \mathcal{S}_n^{(k)}} t^{2l(w)} = \left[\begin{matrix} n \\ k \end{matrix} \right]_{t^2},$$

Here the polynomial $\left[\begin{matrix} n \\ k \end{matrix} \right]_q$ is a q -analog of the binomial coefficient $\binom{n}{k}$ (see section 2).

The simplest example is the case of $\text{Gr}(1, 2) \cong \mathbb{R}P^1$ which is a circle S^1 and can be described with an equation $x^2 + y^2 = 1$. The number of \mathbb{F}_q points of $\text{Gr}(1, 2)$, that is the number of the solutions of $x^2 + y^2 = 1$ for $x, y \in \mathbb{F}_q$, is $q - 1$ (see Remark 1.1 below). We thus have a polynomial in q , namely,

$$|\text{Gr}(1, 2)_{\mathbb{F}_q}| = q - 1,$$

and we note that this gives the Betti numbers β_k as coefficients of $(-1)^{1-j} q^j$, $j = 0, 1$, in the polynomial, i.e. $|\text{Gr}(1, 2)_{\mathbb{F}_q}| = \sum_{j=0}^1 (-1)^{1-j} \beta_j q^j$. Namely the Poincaré polynomial for $\text{Gr}(1, 2)$ denoted by $P_{(1, 2)}(t)$ is given by

$$P_{(1, 2)}(t) = \sum_{j=0}^1 \beta_j t^j = 1 + t.$$

Remark 1.1. In fact, there are two formulas for the number of points of $x^2 + y^2 = 1$ over \mathbb{F}_q depending on q (q not a power of 2). For instance over \mathbb{F}_3 we have $|S^1(\mathbb{F}_3)| = q + 1 = 4$; however over F_5

there $|S^1; (\mathbb{F}_5)| = q - 1 = 4$. By extending \mathbb{F}_3 to \mathbb{F}_{3^2} (adding $\sqrt{-1}$), the number of \mathbb{F}_q points with $q = 3^2 = 9$ becomes $q - 1$. We assume in this paper $\sqrt{-1} \in \mathbb{F}_q$.

In a similar computation (see the subsection 8.2), we obtain the number of \mathbb{F}_q points of $\mathbb{R}P^3 \cong \text{Gr}(1, 4)$ as

$$|\text{Gr}(1, 4)_{\mathbb{F}_q}| = q(q^2 - 1).$$

The Poincaré polynomial for this case is given by

$$P_{(1,4)}(t) = 1 + t^3,$$

and the relation with $|\text{Gr}(1, 4)_{\mathbb{F}_q}|$ is not obvious, but we note that the replacement $q^2 - 1$ to $1 + t^3$ gives the relation between those polynomials. It turns out that the similar replacement can be done for the general cases of $\text{Gr}(2j + 1, 2m)$ (see the subsection 8.1).

A more interesting example is $\text{Gr}(2, 4)$ which is discussed in Example 2.2 below. The polynomial that results in this case is $q^2(1 + q^2)$ giving the number of \mathbb{F}_q points on $\text{Gr}(2, 4)$. Notice that the polynomial $1 + q^2$ is also $\text{Gr}(1, 2, \mathbb{F}_{q^2})$ i.e., we have

$$|\text{Gr}(2, 4)_{\mathbb{F}_q}| = q^2 |\text{Gr}(1, 2, \mathbb{F}_{q^2})| = q^2 P_{(1,2)}^{\mathbb{C}}(q) = q^2 \begin{bmatrix} 2 \\ 1 \end{bmatrix}_{q^2}.$$

The Poincaré polynomial is obtained from $1 + q^2$ by replacing q with t^2 , and is related to $P_{(1,2)}^{\mathbb{C}}(q)$ i.e.

$$P_{(2,4)}(t) = P_{(1,2)}^{\mathbb{C}}(t^2) = 1 + t^4.$$

Remark 1.2. This relation of the Poincaré polynomials suggests that the ring of polynomials for the real cohomology for $\text{Gr}(2, 4)$ be expressed by

$$H^*(\text{Gr}(2, 4), \mathbb{R}) \cong \frac{\mathbb{R}[p]}{\{p^2\}},$$

where p is the Pontrjagin class $p \in H^4(\text{Gr}(2, 4), \mathbb{R})$. We discuss this more in section 7.

This paper generalizes those low dimensional examples to any real Grassmannians $\text{Gr}(k, n)$ introducing explicit polynomials $p_{(k,n)}(q)$ in q (see the subsection 8.1). The polynomial $p_{(k,n)}(q)$ has an interesting connection with the KP flow. For example, in the case of $\text{Gr}(1, 4)$ discussed above, the flow blows up twice along the orbit considered (see Figure 1). Then we consider the following polynomial

$$p_{(1,4)}(q) = \sum_{w \in \mathcal{S}_4^{(1)}} (-1)^{l(w)} q^{\eta(w)} = 1 - q^2,$$

where $\eta(w)$ counts the number of blow-ups from $e = (1)$ to $w = (i) = s_{i-1} \cdots s_1$, i.e. $\eta(e) = 0$, $\eta(s_1) = \eta(s_2 s_1) = 1$ and $\eta(s_3 s_2 s_1) = 2$. Namely, we also assign powers $q^{\eta(w)}$ to the vertex labeled by $w \in \mathcal{S}_n^{(k)}$ which keep track of the number of blow-ups from e to w . Then each vertex in the graph $\mathcal{G}(k, n)$ would have additional label $q^{\eta(w)}$, which defines the *weighted* Schubert cell (see subsection 8.1). In the case of $\text{Gr}(1, 4)$, we have the graph with the weighted Schubert cells $(\sigma_i) = (i)$ (see Figure 1),

$$((1); q^0) \longrightarrow ((2); q^1) \implies ((3); q^1) \longrightarrow ((4); q^2).$$

The polynomial $p_{(k,n)}(q)$ appears in $|\text{Gr}(k, n)_{\mathbb{F}_q}|$ given above, and in section 8.2, we show that this is true in general. Without technicalities, the main result is that these polynomials $p_{(k,n)}(q)$ times certain power of q compute the number of \mathbb{F}_q points. The polynomial in t given by $p_{(k,n)}(t^2)$ is the corresponding Poincaré polynomial. The cases of the form $(k, n) = (2j + 1, 2m)$ turn out to be exceptions obeying a slightly different formula. Excluding the exceptional cases $(k, n) = (2j + 1, 2m)$, the relation between the complex Grassmannians $\text{Gr}(j, m, \mathbb{C})$ and the real Grassmannians $\text{Gr}(k, n)$ with $k = 2j, 2j + 1$, $n = 2m, 2m + 1$ is given by $p_{(k,n)}(q^{1/2})$ vs. $p_{(k,n)}(q)$.

We then obtain the following Theorems in Section 8:

Theorem 1.2. *The number of \mathbb{F}_q points of $\text{Gr}(k, n)$ is given as follows:*

(i) *If (k, n) equals $(2j, 2m)$, $(2j, 2m+1)$ or $(2j+1, 2m+1)$, we have*

$$|\text{Gr}(k, n)_{\mathbb{F}_q}| = q^r \begin{bmatrix} m \\ j \end{bmatrix}_{q^2} \quad \text{with} \quad r = k(n-k) - 2j(m-j).$$

(ii) *If $(k, n) = (2j+1, 2m)$, then we have*

$$|\text{Gr}(k, n)_{\mathbb{F}_q}| = q^r \begin{bmatrix} m-1 \\ j \end{bmatrix}_{q^2} (q^m - 1) \quad \text{with} \quad r = k(n-k) - 2j(m-j-1) - m.$$

One should note here that $\begin{bmatrix} m \\ j \end{bmatrix}_{q^2} = |\text{Gr}(j, m, \mathbb{F}_{q^2})|$ for any $m \geq j \geq 1$. Let $P_{(k,n)}(t)$ denote the Poincaré polynomial of $\text{Gr}(k, n)$, i.e.

$$P_{(k,n)}(t) = \sum_{i=0}^{k(n-k)} \beta_i t^i \quad \text{with} \quad \beta_i := \dim H^i(\text{Gr}(k, n), \mathbb{Q}).$$

We also show that those \mathbb{F}_q points are related to the Poincaré polynomials of $\text{Gr}(k, n)$:

Theorem 1.3. *The Poincaré polynomial of $\text{Gr}(k, n)$ is given as follows:*

(i) *If (k, n) equals $(2j, 2m)$, $(2j, 2m+1)$ or $(2j+1, 2m+1)$, we have*

$$P_{(k,n)}(t) = \begin{bmatrix} m \\ j \end{bmatrix}_{t^4}.$$

(ii) *If $(k, n) = (2j+1, 2m)$, we have*

$$P_{(k,n)}(t) = (1 + t^{2m-1}) \begin{bmatrix} m-1 \\ j \end{bmatrix}_{t^4}.$$

This then gives the well-known formulas on the Euler characteristic for $\text{Gr}(k, n)$.

Corollary 1.4. *The Euler characteristic $\chi(\text{Gr}(k, n))$ has the following form.*

(i) *If (k, n) equals $(2j, 2m)$, $(2j, 2m+1)$ or $(2j+1, 2m+1)$, we have*

$$\chi(\text{Gr}(k, n)) = P_{(k,n)}(-1) = \begin{pmatrix} m \\ j \end{pmatrix}.$$

(ii) *If $(k, n) = (2j+1, 2m)$, then we have*

$$\chi(\text{Gr}(k, n)) = P_{(k,n)}(-1) = 0.$$

It is interesting to note in particular that for the case (i), we have

$$P_{(k,n)}(t) = P_{(\lfloor k/2 \rfloor, \lfloor n/2 \rfloor)}^{\mathbb{C}}(t^2),$$

which gives an information on the structure of the cohomology ring $H^*(\text{Gr}(k, n), \mathbb{R})$ (see [3, 24]).

Let us summarize the results for low dimensional cases, $\text{Gr}(1, 2)$, $\text{Gr}(1, 3)$ and $\text{Gr}(2, 4)$.

(a) The case $\text{Gr}(1, 2) \cong S^1$: From Theorem 1.2 with $(k, m) = (1, 2)$, we recover the polynomial

$$|\text{Gr}(1, 2)_{\mathbb{F}_q}| = (q-1) \begin{bmatrix} 1 \\ 0 \end{bmatrix}_{q^2} = q-1.$$

The Poincaré polynomial is then obtained from Theorem 1.3 as

$$P_{(1,2)}(t) = (1+t) \begin{bmatrix} 1 \\ 0 \end{bmatrix}_{t^4} = 1+t.$$

Notice in general that $\text{Gr}(1, n) \cong \mathbb{R}P^{n-1}$ and $P_{(1,n)}(t) = 1 + t^{2m-1}$ when $n = 2m$.

(b) The case $\text{Gr}(1, 3) \cong \mathbb{R}P^2$: We have

$$|\text{Gr}(1, 3)_{\mathbb{F}_q}| = q^2 \begin{bmatrix} 1 \\ 0 \end{bmatrix}_{q^2} = q^2.$$

The Poincaré polynomial is

$$P_{(1,3)}(t) = 1.$$

that is, the $\text{Gr}(1, 3)$ is connected but not orientable. In general, we have $P_{(1,n)}(t) = 1$ when n is odd.

(c) The case $\text{Gr}(2, 4)$: We have

$$|\text{Gr}(2, 4)_{\mathbb{F}_q}| = q^2 \begin{bmatrix} 2 \\ 1 \end{bmatrix}_{q^2} = q^2(1 + q^2).$$

The Poincaré polynomial is then given by

$$P_{(2,4)}(t) = \begin{bmatrix} 2 \\ 1 \end{bmatrix}_{t^4} = 1 + t^4,$$

which shows that the manifold is connected and orientable.

2. THE REAL GRASSMANN MANIFOLD $\text{Gr}(k, n)$

Let $G = \text{SL}_n(\mathbb{R})^\pm$, the set of $n \times n$ real matrices of determinant ± 1 . We have $\text{Gr}(k, n) = G/P_k$ for a maximal parabolic subgroup P_k stabilizing the k -dimensional subspace $V_0(k) = \text{Span}_{\mathbb{R}}\{E_1, \dots, E_k\}$ with the standard basis $\{E_j : j = 1, \dots, n\}$. In this section, we give an elementary introduction of the Grassmann manifolds and the Schubert decompositions.

The vector spaces $\mathbb{R}^n = V(E_1, \dots, E_n)$ and $\bigwedge^k \mathbb{R}^n = \bigwedge^k V(E_1, \dots, E_n)$ for $k = 1, \dots, n$ are also the *fundamental* representations of G with the standard action of G on $V(E_1, \dots, E_n)$. Note that the real Grassmannian can be also expressed as a (unoriented) homogeneous space,

$$\text{Gr}(k, n) \cong \frac{\text{O}_n(\mathbb{R})}{\text{O}_k(\mathbb{R}) \times \text{O}_{n-k}(\mathbb{R})}.$$

2.1. The Schubert decomposition. Let $\{E_j : j = 1, \dots, n\}$ be a basis of \mathbb{R}^n . Then a k -dimensional vector subspace is expressed by a set of vectors $\{f_i : i = 1, \dots, k\}$ with

$$(2.1) \quad f_i = \sum_{j=1}^n a_{i,j} E_j \quad i = 1, \dots, k,$$

With the $k \times n$ real matrix $A := (a_{i,j})$,

$$A = \begin{pmatrix} a_{1,1} & a_{1,2} & \cdots & a_{1,n} \\ \vdots & \vdots & \ddots & \vdots \\ a_{k,1} & a_{k,2} & \cdots & a_{k,n} \end{pmatrix} \in M_{k \times n}(\mathbb{R}),$$

we write

$$(f_1, \dots, f_k)^T = A \cdot (E_1, \dots, E_n)^T.$$

Here $M_{k \times n}(\mathbb{R})$ is the set of $k \times n$ matrices of the maximal rank k . Each A matrix gives a label of a point of $\text{Gr}(k, n)$, and it can be put in a unique form called the row reduced echelon form (RREF): For some $g \in \text{GL}_k(\mathbb{R})$,

$$g \cdot (f_1, \dots, f_k)^T = g \cdot A \cdot (E_1, \dots, E_n)^T,$$

expresses the same k -dimensional subspace. Choosing an appropriate matrix g , one can put A in the RREF. This implies

$$\text{Gr}(k, n) \cong \text{GL}_k(\mathbb{R}) \backslash M_{k \times n}(\mathbb{R}).$$

To each RREF we can associate a set of ordered integers $(\sigma_1, \dots, \sigma_k)$, σ_j indicating that the σ_j -th column has a pivot. This parametrizes the cells in a cell decomposition of $\text{Gr}(k, n)$ which is called the Schubert decomposition,

$$\text{Gr}(k, n) = \bigsqcup_{1 \leq \sigma_1 < \dots < \sigma_k \leq n} X(\sigma_1, \dots, \sigma_k),$$

where $X(\sigma_1, \dots, \sigma_k)$ is the Schubert cell defined by the set of all matrices whose pivot ones are at $(\sigma_1, \dots, \sigma_k)$ places. The ordered set $(\sigma_1, \dots, \sigma_k)$ is called the Schubert symbol for the corresponding Schubert cell, and we sometime denote the cell simply by the symbol.

Example 2.1. The Grassmannian $\text{Gr}(2, 4)$, the space consisting of two dimensional vector spaces inside the four dimensional space $V(E_1, \dots, E_4)$, has six Schubert cells, $X(i, j)$ with $1 \leq i < j \leq 4$, which are given by

$$\begin{aligned} X(1, 2) &= \left\{ \begin{pmatrix} 1 & 0 & 0 & 0 \\ 0 & 1 & 0 & 0 \end{pmatrix} \right\} & X(1, 3) &= \left\{ \begin{pmatrix} 1 & 0 & 0 & 0 \\ 0 & * & 1 & 0 \end{pmatrix} \right\} \\ X(2, 3) &= \left\{ \begin{pmatrix} * & 1 & 0 & 0 \\ * & 0 & 1 & 0 \end{pmatrix} \right\} & X(1, 4) &= \left\{ \begin{pmatrix} 1 & 0 & 0 & 0 \\ 0 & * & * & 1 \end{pmatrix} \right\} \\ X(2, 4) &= \left\{ \begin{pmatrix} * & 1 & 0 & 0 \\ * & 0 & * & 1 \end{pmatrix} \right\} & X(3, 4) &= \left\{ \begin{pmatrix} * & * & 1 & 0 \\ * & * & 0 & 1 \end{pmatrix} \right\} \end{aligned}$$

Each “*” indicates a free parameter for RREF, and the number of free parameters gives the dimension of the cell.

The dimension of the cell is given by

$$\dim X(\sigma_1, \dots, \sigma_k) = \sum_{j=1}^k (\sigma_j - j),$$

Let n_j be the total number of cells of j dimension. Then the generating function $\sum_{j=0}^{k(n-k)} n_j q^j$ is given by counting the number of points in $\text{Gr}(k, n, \mathbb{F})$ over a finite field $\mathbb{F} = \mathbb{F}_q$, i.e.

$$(2.2) \quad \sum_{j=0}^{k(n-k)} n_j q^j = |\text{Gr}(k, n, \mathbb{F}_q)|.$$

The number $|\text{Gr}(k, n, \mathbb{F}_q)|$ can be obtained from the complex Grassmannian $\text{Gr}(k, n, \mathbb{C})$ restricted on \mathbb{F}_q , i.e.

$$|\text{Gr}(k, n, \mathbb{F}_q)| = \begin{bmatrix} n \\ k \end{bmatrix}_q = \frac{[n]_q!}{[k]_q! [n-k]_q!},$$

where $[n]_q! = [n]_q [n-1]_q \cdots [2]_q [1]_q$ with $[j]_q = (1 - q^j)/(1 - q)$, the q -analog of the number j . For example, we have

$$|\text{Gr}(2, 4, \mathbb{F}_q)| = \begin{bmatrix} 4 \\ 2 \end{bmatrix}_q = 1 + q + 2q^2 + q^3 + q^4,$$

(see Example 2.1).

We also note that the polynomial $|\text{Gr}(k, n, \mathbb{F}_q)|$ with $q = t^2$ is the Poincaré polynomial for the cohomology of $\text{Gr}(k, n, \mathbb{C})$, denoted by $P_{(k,n)}^{\mathbb{C}}(t)$, that is,

$$P_{(k,n)}^{\mathbb{C}}(t) = \sum_{j=0}^{k(n-k)} \beta_{2j}^{\mathbb{C}} t^{2j},$$

and each coefficient $\beta_i^{\mathbb{C}}$ gives the Betti number for i -cycles,

$$\beta_i^{\mathbb{C}} := \dim H^i(\mathrm{Gr}(k, n, \mathbb{C}); \mathbb{R}) = \begin{cases} 0 & \text{if } i = \text{odd} \\ n_j & \text{if } i = 2j. \end{cases}$$

2.2. The Plücker embedding and the moment polytope. In order to describe the points of $\mathrm{Gr}(k, n)$, we can use the Plücker embedding,

$$\begin{aligned} \mathrm{Gr}(k, n) &\longrightarrow P\left(\bigwedge^k \mathbb{R}^n\right) \\ [f_1, \dots, f_k] &\longmapsto \mathbb{R}f_1 \wedge \dots \wedge f_k \end{aligned}$$

where the wedge product can be expressed as

$$(2.3) \quad f_1 \wedge \dots \wedge f_k = \sum_{1 \leq j_1 < \dots < j_k \leq n} \xi(j_1, \dots, j_k) E_{j_1} \wedge \dots \wedge E_{j_k},$$

Here the coefficients $\xi(j_1, \dots, j_k)$ are the Plücker coordinates given by the $k \times k$ minor of the coefficient matrix A , i.e.

$$(2.4) \quad \xi(j_1, \dots, j_k) = \left| (a_{l, j_m})_{1 \leq l, m \leq k} \right|.$$

Those coordinates satisfy the Plücker relations,

$$(2.5) \quad \sum_{r=1}^{k+1} (-1)^r \xi(\alpha_1, \dots, \check{\alpha}_r, \dots, \alpha_{k+1}) \xi(\alpha_r, \beta_1, \dots, \beta_{k-1}) = 0,$$

for any set of numbers $\{\alpha_1, \dots, \alpha_{k+1}, \beta_1, \dots, \beta_{k-1}\} \subset \{1, \dots, n\}$. Here the notation $\check{\alpha}_r$ implies the deletion of this number.

Example 2.2. In the case of $\mathrm{Gr}(2, 4)$, there is one Plücker relation,

$$(2.6) \quad \xi(1, 2)\xi(3, 4) - \xi(1, 3)\xi(2, 4) + \xi(1, 4)\xi(2, 3) = 0.$$

Then $\mathrm{Gr}(2, 4)$ can be expressed as

$$\mathrm{Gr}(2, 4) = \left\{ [v] = \mathbb{R} \sum_{1 \leq i, j \leq 4} \xi(i, j) E_i \wedge E_j : \begin{array}{l} \xi(i, j) \text{ satisfy (2.6)} \\ \sum_{1 \leq i < j \leq 4} |\xi(i, j)|^2 \neq 0 \end{array} \right\}.$$

This variety can be also expressed as the following, which may be useful for counting the \mathbb{F}_q points of $\mathrm{Gr}(2, 4)$. Let $(x_1, x_2, x_3, y_1, y_2, y_3)$ be a new coordinate defined by

$$\begin{aligned} \xi(1, 2) &= x_1 - y_1, & \xi(1, 3) &= -x_2 + y_2, & \xi(1, 4) &= x_3 - y_3, \\ \xi(3, 4) &= x_1 + y_1, & \xi(2, 4) &= x_2 + y_2, & \xi(2, 3) &= x_3 + y_3. \end{aligned}$$

Then one can express $\mathrm{Gr}(2, 4)$ as the set of *isotropic* vectors in $\mathbb{R}P^5$,

$$(2.7) \quad \mathrm{Gr}(2, 4) = \left\{ \mathbb{R}(x_1, x_2, x_3, y_1, y_2, y_3) : \begin{array}{l} x_1^2 + x_2^2 + x_3^2 - y_1^2 - y_2^2 - y_3^2 = 0 \\ x_1^2 + x_2^2 + x_3^2 \neq 0 \end{array} \right\} \subset \mathbb{R}P^5.$$

Here the first condition is the Plücker relation (2.6) and the second one shows the maximal rank (i.e. at least one $\xi(i, j) \neq 0$).

With the expression of the wedge product $f_1 \wedge \dots \wedge f_k$, one can define the moment map $\mu : \mathrm{Gr}(k, n) \rightarrow \mathfrak{h}_{\mathbb{R}}^*$ (see [12]),

$$(2.8) \quad \mu(f_1 \wedge \dots \wedge f_k) = \frac{\sum_{1 \leq i_1 < \dots < i_k \leq n} |\xi(\sigma_1, \dots, \sigma_k)|^2 (L_{\sigma_1} + \dots + L_{\sigma_k})}{\sum_{1 \leq \sigma_1 < \dots < \sigma_k \leq n} |\xi(\sigma_1, \dots, \sigma_k)|^2}$$

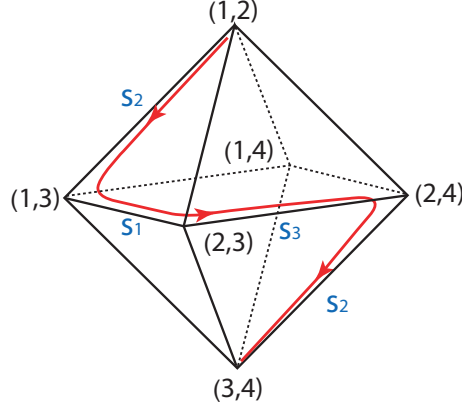


FIGURE 2. The moment polytope of $\text{Gr}(2, 4)$. Each weight is marked by (σ_1, σ_2) with $L = L_{\sigma_1} + L_{\sigma_2}$. The highest weight is given by $(1, 2)$, and all the weights are in the $\mathcal{S}_4^{(2)}$ -orbit of highest weight. The arrowed curve indicates a KP flow, which approximates the Weyl group action. Each s_j shows the simple reflection $j \leftrightarrow j+1$.

where L_σ are the weights of the standard representation V of $\text{SL}_n(\mathbb{R})$, and $\mathfrak{h}_{\mathbb{R}}^*$ is defined by

$$\mathfrak{h}_{\mathbb{R}}^* = \text{Span}_{\mathbb{R}} \left\{ L_1, \dots, L_k : \sum_{i=1}^n L_i = 0 \right\} \cong \mathbb{R}^{n-1}.$$

The image under the moment map is a convex polytope whose vertices are marked by the elements of $\mathcal{S}_n^{(k)}$. In the representation theory, this polytope is a weight polytope of the fundamental representation of $\mathfrak{sl}(n)$ on $\bigwedge^k V(E_1, \dots, E_n)$. The set $\{E_{\sigma_1} \wedge \dots \wedge E_{\sigma_k} : 1 \leq \sigma_1 < \dots < \sigma_k \leq n\}$ then corresponds to a basis of weight vectors of the representation $\bigwedge^k V$ (see for example [13]).

In Figure 2, we illustrate the moment polytope of $\text{Gr}(2, 4)$, which is an octahedron whose vertices are labeled by the Schubert symbols (σ_1, σ_2) .

3. THE KP FLOW ON $\text{Gr}(k, n)$

In this section, we give a realization of $\text{Gr}(k, n)$ in terms of finite dimensional solutions of the KP equation (see, for example, [10, 11, 20] for the recent development of the classification problem of soliton solutions of the KP equation). The purpose of this section is to give a dynamical system, called a KP flow, on the moment polytope (2.8). In particular, we consider the flows which approximate Weyl group action along the weak Bruhat order (see section 4). For example, a KP flow in $\text{Gr}(2, 4)$ is illustrated in Figure 2, which gives the orbit $(1, 2) \xrightarrow{s_2} (1, 3) \xrightarrow{s_1} (2, 3) \xrightarrow{s_3} (2, 4) \xrightarrow{s_2} (3, 4)$ with the simple reflections $s_j \in \mathcal{S}_4$, the symmetric group of permutations. Those flows contain the information of the cohomology of the real variety $\text{Gr}(k, n)$, which is the main motivation of the present paper.

3.1. The KP flow on the moment polytope. Let us start to fix the set of independent vectors $\{E_i : i = 1, \dots, n\}$ as given by the exponential functions of multi-variables $\mathbf{t} = (t_1, t_2, \dots, t_{n-1}) \in \mathbb{R}^{n-1}$,

$$E_i(\mathbf{t}) = e^{\theta(\lambda_i; \mathbf{t})} \quad \text{with} \quad \theta(\lambda_i; \mathbf{t}) = \sum_{r=1}^{n-1} \lambda_i^r t_r,$$

where $\lambda_i \in \mathbb{R}$ are all distinct, and we assume the ordering,

$$\lambda_1 < \lambda_2 < \dots < \lambda_n.$$

With the set of functions $\{f_j : j = 1, \dots, k\}$ defined in (2.1), i.e. $(f_1, \dots, f_k)^T = A(E_1, \dots, E_n)^T$ with the $k \times n$ coefficient matrix A , we define the following function, called the τ -function, given by the Wronskian determinant of those functions,

$$(3.1) \quad \tau_A(\mathbf{t}) = \text{Wr}(f_1, \dots, f_k) = \begin{vmatrix} f_1 & \cdots & f_k \\ \vdots & \ddots & \vdots \\ f_1^{(k-1)} & \cdots & f_k^{(k-1)} \end{vmatrix},$$

Here the index A indicates the matrix A defined in (2.1). We then have:

Lemma 3.1. *The τ -function can be expressed in the form,*

$$\tau_A(\mathbf{t}) = \sum_{1 \leq \sigma_1 < \cdots < \sigma_k \leq n} \xi(\sigma_1, \dots, \sigma_k) E(\sigma_1, \dots, \sigma_k; \mathbf{t}),$$

where $\xi(\sigma_1, \dots, \sigma_k)$ are the Plücker coordinates given by (2.4), and

$$E(\sigma_1, \dots, \sigma_k; \mathbf{t}) = \text{Wr}(E_{\sigma_1}, \dots, E_{\sigma_k}) = \prod_{i < j} (\lambda_{\sigma_j} - \lambda_{\sigma_i}) \exp \theta(\sigma_1, \dots, \sigma_k; \mathbf{t}),$$

with $\theta(\sigma_1, \dots, \sigma_k; \mathbf{t}) := \sum_{i=1}^k \theta(\lambda_{\sigma_i}; \mathbf{t})$.

This Lemma is a direct consequence of the Binet-Cauchy theorem (see p.9 in [14]). With the formula for $f_1 \wedge \cdots \wedge f_k$ in (2.3), the τ_A -function gives a realization of the corresponding point on $\text{Gr}(k, n)$ with the identification $\tau_A \equiv c\tau_A$ for any nonzero constant c (the projectivization). Namely, the Wronskian-map can be considered as the Plücker embedding, $\text{Wr} : \text{Gr}(k, n) \hookrightarrow \mathbb{RP}^{\binom{n}{k}-1}$. Here one should note that $\sum_{i=1}^k \lambda_{\sigma_i}$ should be distinct for all $(\sigma_1, \dots, \sigma_k)$. Then one can identify the set $\{E(\sigma_1, \dots, \sigma_k; \mathbf{t})\}$ as the basis $\{E_{\sigma_1} \wedge \cdots \wedge E_{\sigma_k}\}$ of $\wedge^k \mathbb{R}^n$.

One can also define a map $\varphi_A : \mathbb{R}^{n-1} \rightarrow \mathfrak{h}_{\mathbb{R}}^*$ as the composite map, $\varphi_A = \mu \circ \tau_A$, with

$$\varphi_A(\mathbf{t}) = \frac{\sum_{1 \leq \sigma_1 < \cdots < \sigma_k \leq n} |\xi(\sigma_1, \dots, \sigma_k) E(\sigma_1, \dots, \sigma_k; \mathbf{t})|^2 (L_{\sigma_1} + \cdots + L_{\sigma_k})}{\sum_{1 \leq \sigma_1 < \cdots < \sigma_k \leq n} |\xi(\sigma_1, \dots, \sigma_k) E(\sigma_1, \dots, \sigma_k; \mathbf{t})|^2}.$$

Then if A is in the top cell, one can see that the closure of the set $\{\varphi(\mathbf{t}) : \mathbf{t} \in \mathbb{R}^{n-1}\}$ is a convex hull with the vertices given by the weights $\{L_{\sigma_1} + \cdots + L_{\sigma_k} : 1 \leq \sigma_1 < \cdots < \sigma_k \leq n\}$, denoted by $\text{Conv}(k, n)$, i.e.

$$\text{Conv}(k, n) = \overline{\{\varphi_A(\mathbf{t}) : \mathbf{t} \in \mathbb{R}^{n-1}\}}.$$

This map defines a flow on the polytope, and we are interested in studying the zero set of the τ_A function which is determined by a particular choice of the coefficient matrix A .

Example 3.1. Let us consider the case $\text{Gr}(2, 4)$ to show how one can see the polytope in Figure 2 from the KP flow. Figure 3 illustrates the contour plots of the t -evolution of the solution $u(x, y, t)$. Then as we explained in the introduction, the polytope can be seen from the dual graph of the solution pattern as shown in the figure. Here we take the matrix A in the form,

$$A = \begin{pmatrix} 1 & 1 & 1 & 1 \\ \lambda_1 & \lambda_2 & \lambda_3 & \lambda_4 \end{pmatrix}.$$

Note here that the 2×2 minors of A are all positive, i.e. $\xi(i, j) = \lambda_j - \lambda_i > 0$ with the ordering in λ_j 's, and this implies the τ -function is positive definite and no blow-up in the KP flow. We then extend this example to the case with some signs in the Plücker coordinates, and show that the

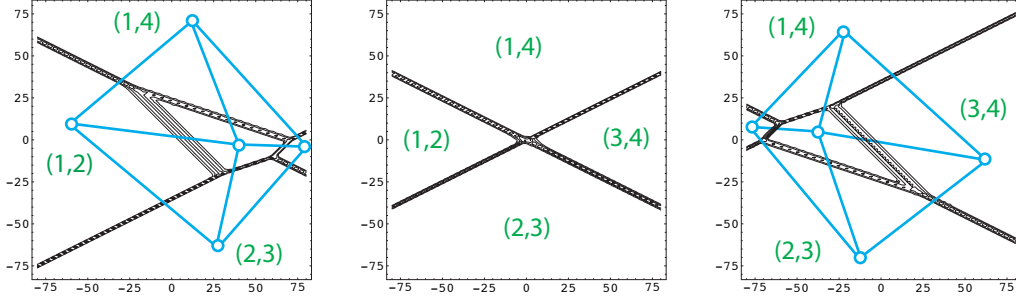


FIGURE 3. Soliton solution of the KP equation on $\text{Gr}(2, 4)$. The figures show the contour plot of the solution $u(x, y, t)$ for $t < 0$ (left), $t = 0$ (middle) and $t > 0$ (right). Each pair of numbers (i, j) indicates the dominant exponential $E(i, j)$, i.e. the Plücker coordinates. The bounded region in the left (right) figure corresponds to $E(1, 3)$ ($E(2, 4)$). The light colored graph in the figures shows the dual graph whose vertices represent those dominant exponentials, and is the moment polytope (tetrahedron) shown in Figure 2.

flow associated with a particular choice of the signs can provide topological information of the real Grassmannians.

3.2. The KP equation and the Toda lattice. As we explained in Introduction, the function

$$u(x, y, t) = 2 \frac{\partial^2}{\partial x^2} \ln \tau_A(x, y, t),$$

satisfies the KP equation with the identification $t_1 = x, t_2 = y$ and $t_3 = t$. The higher times, t_j for $j > 3$, give the symmetry parameters of the KP equation, and the set of all the flows parametrized by t_j 's forms the so-called KP hierarchy (see for example [25, 11, 20]).

In this paper, we consider a particular set of independent functions $\{f_i : i = 1, \dots, k\}$ such that

$$f_i = \frac{\partial^{i-1}}{\partial t_1^{i-1}} f =: f^{(i-1)}, \quad \text{with} \quad f = \sum_{j=1}^n \epsilon_j E_j,$$

where we take $\epsilon_j \in \{\pm 1\}$, and the set of signs $(\epsilon_1, \dots, \epsilon_n)$ is referred to as the KP sign. Note here that the $k \times n$ coefficient matrix A is then given by

$$(3.2) \quad A = \begin{pmatrix} 1 & 1 & \cdots & 1 \\ \lambda_1 & \lambda_2 & \cdots & \lambda_n \\ \vdots & \vdots & \ddots & \vdots \\ \lambda_1^{k-1} & \lambda_2^{k-1} & \cdots & \lambda_n^{k-1} \end{pmatrix} h_\epsilon,$$

where h_ϵ is the diagonal matrix whose entries are ± 1 , i.e. $h_\epsilon := \text{diag}(\epsilon_1, \dots, \epsilon_n)$. This matrix specifies the blow-ups of the KP flow, and plays an important role for our study (subsection 5.1). Because of the ordering $\lambda_1 < \dots < \lambda_n$, the sign of each Plücker coordinate is given by

$$(3.3) \quad \text{sign}(\xi(\sigma_1, \dots, \sigma_k)) = \prod_{j=1}^k \epsilon_{\sigma_j} =: \epsilon(\sigma_1, \dots, \sigma_k),$$

which will be used as the sign for the Schubert cell $X_{w_\sigma} = (\sigma_1, \dots, \sigma_k)$ (see subsection 5.1).

Without loss of generality, we choose the parameters λ_j in E_j with $\sum_{j=1}^n \lambda_j = 0$ (since the matrix L can be shifted by a constant in the diagonal, i.e. $L \rightarrow L + cI$ with the identity matrix I does not change the equation). Then the set of τ -functions,

$$(3.4) \quad \tau_k := \text{Wr}(f, f', \dots, f^{(k-1)}), \quad k = 1, 2, \dots, n.$$

gives the solution of the Toda lattice equation for $\text{SL}_n(\mathbb{R})$, which is defined with the $n \times n$ tri-diagonal matrix L ,

$$L = \begin{pmatrix} b_1 & 1 & 0 & \cdots & 0 \\ a_1 & b_2 & 1 & \cdots & 0 \\ \vdots & \ddots & \ddots & \ddots & \vdots \\ 0 & \cdots & \cdots & b_{n-1} & 1 \\ 0 & \cdots & \cdots & a_{n-1} & b_n \end{pmatrix}$$

The Toda lattice equation is then expressed by the matrix equation (i.e. the Lax equation),

$$\frac{dL}{dt} = [L, L_-],$$

where L_- represents the (strictly) lower triangular part of the matrix L . The solution is then given by

$$(3.5) \quad a_j = \frac{\tau_{j+1}\tau_{j-1}}{\tau_j^2}, \quad b_j = \frac{d}{dt} \ln \frac{\tau_j}{\tau_{j-1}},$$

with $\tau_0 = 1$. The Toda lattice equation has several commuting flows, and the set of those flows forms the Toda lattice hierarchy which can be defined as

$$\frac{\partial L}{\partial t_j} = [L, L_-^j] \quad \text{with} \quad L_-^j := (L^j)_-, \quad j = 1, 2, \dots, n-1.$$

Note that each τ_k then gives a solution of the KP equation on $\text{Gr}(k, n)$ with the identifications $t_1 = x, t_2 = y$ and $t_3 = t$. The solution of the Toda lattice hierarchy is given by the set $(\tau_1, \dots, \tau_{n-1})$ (note τ_n is just a constant, since $\sum_{j=1}^n \lambda_j = 0$). Since each τ_k can be considered as a point of $\text{Gr}(k, n)$, the solution of the Toda lattice equation defines a point of the flag manifold $\mathcal{B} := \text{SL}_n(\mathbb{R})/B$ with the Borel subgroup B . This is just a consequence of the diagonal embedding, denoted by ι , of \mathcal{B} into the product of the Grassmannians, i.e.

$$\iota : \mathcal{B} \hookrightarrow \text{Gr}(1, n) \times \text{Gr}(2, n) \times \cdots \times \text{Gr}(n-1, n).$$

We then define a map $\varphi : \mathbb{R}^{n-1} \rightarrow \mathfrak{h}_{\mathbb{R}}^*$ as the composite map $\varphi = \mu \circ \iota$,

$$\varphi(\mathbf{t}) = \sum_{k=1}^{n-1} \mu(\tau_k(\mathbf{t})),$$

where $\mu : \text{Gr}(k, n) \rightarrow \mathfrak{h}_{\mathbb{R}}^*$ is the moment map defined in (2.8). The moment polytope for the Toda lattice hierarchy is the permutohedron of the symmetric group \mathcal{S}_n , whose vertices are labeled by the elements of \mathcal{S}_n . In [8], we used this fact, and described the cohomology of the real flag variety in terms of the Toda flow and its blow-ups. We basically follow the arguments given in that paper. However we have found several new structures for the case of $\text{Gr}(k, n)$, not just by a projection $\pi : \mathcal{B} \rightarrow \text{Gr}(k, n)$, and in fact, we found the explicit form of the Poincaré polynomials for $\text{Gr}(k, n)$. Figure 4 illustrates the moment polytope (permutohedron) for $\text{SL}_4(\mathbb{R})$ Toda lattice hierarchy. The figure shows the incidence graph of the real flag variety $\mathcal{B} = \text{SL}_4(\mathbb{R})/B$ as shown in [8].

Each τ -function gives the zero divisor on the polytope which corresponds to the singular solution of the Toda lattice hierarchy. Although one can recover the incidence graph of $\text{Gr}(k, 4)$ from the

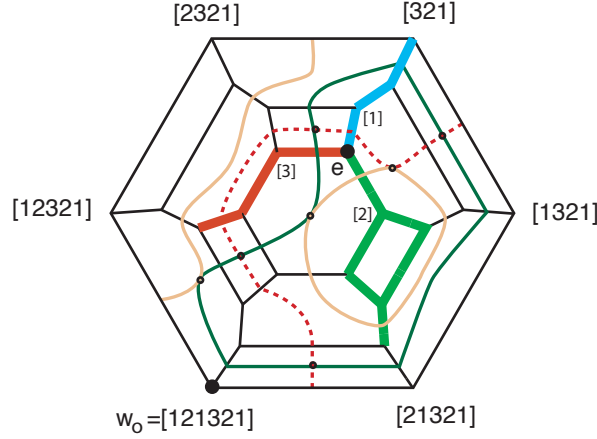


FIGURE 4. The moment polytope of $SL_4(\mathbb{R})$ Toda lattice hierarchy with the signs $\tilde{\epsilon}_j := \text{sign}(a_j) = -$ for all $j = 1, 2, 3$. Each vertex is marked by the element of the symmetric group \mathcal{S}_4 , which is denoted by $[i_1 i_2 \dots i_j] = s_{i_1} s_{i_2} \dots s_{i_j}$. The three subgraphs indicated by the thick edges with different colors correspond to the incidence graphs of $Gr(k, 4)$. Namely, the edges connecting with the vertices $\{e, [1], [21], [321]\}$ corresponds to $Gr(1, 4)$, the edges with $\{e, [2], [12], [32], [312], [2312]\}$ corresponds to $Gr(2, 4)$, and those with $\{e, [3], [23], [123]\}$ for $Gr(3, 4)$. The zero sets of the τ -functions are shown by the curves crossing the edges (see [8]). For example, the dotted curve shows $\tau_1 = 0$, the light color curve shows $\tau_2 = 0$, and the dark one shows $\tau_3 = 0$.

Figure as the subgraph of this flag picture, in this paper we give an alternative construction based on the KP low which leads to explicit cohomology calculations. We do use the flag picture based on the Toda flow to prove our main theorem 1.1. Below we explain the links, similarities and differences between the Toda and the KP approaches with an example.

3.3. Remark on the Toda lattice description. Here using the $SL_4(\mathbb{R})$ Toda lattice, we give a brief overview of the results in [8] on the incidence graph of the real flag manifold $\mathcal{B} = SL_4(\mathbb{R})/B$. The cohomology of \mathcal{B} then arises from the Toda lattice with the *Toda signs* $\tilde{\epsilon}_j = \text{sign}(a_j)$ (see Definition 6.2 below) attached to the vertex e given by $\tilde{\epsilon}_j = -$ for all $j = 1, 2, 3$. Since the solution (a_j, b_j) of the Toda lattice is given in the form (3.5), the τ_1 -function has the form,

$$\tau_1 = E_1 - E_2 + E_3 - E_4,$$

that is, we have the KP signs $(\epsilon_1, \dots, \epsilon_4) = (+, -, +, -)$ (the solution corresponding to this choice of the signs has the maximum number of blow-ups from $t \rightarrow -\infty$ to $t \rightarrow \infty$, see [21]). Note that from (3.5), the Toda signs are defined with the ϵ_j 's in the τ_1 -function in the form,

$$\tilde{\epsilon}_j := \text{sign}(a_j) = \epsilon_j^{-1} \epsilon_{j+1}.$$

This corresponds to the relation between the roots α and the fundamental weights ω , i.e. with the character χ of the group, they are defined by $\tilde{\epsilon} = -\chi_\alpha(h)$ and $\epsilon = -\chi_\omega(h)$ for $h \in H$, the Cartan subgroup [5] (see also subsection 6.5). Then the sign change along the edge $w \rightarrow s_i w$ is given by (Proposition 5.1 in [8], see also Proposition 6.1)

$$\tilde{\epsilon}'_j = \tilde{\epsilon}_j \tilde{\epsilon}_i^{-C_{i,j}},$$

where $C_{i,j}$ is the Cartan matrix for $\mathrm{SL}_4(\mathbb{R})$. The co-boundaries involving two vertices w and $s_i w$ are zero when one crosses a blow-up (singularity), that is, the edge crosses $\tau_i = 0$, (i.e. $\tilde{\epsilon}_j \tilde{\epsilon}'_j = -$).

Then the incidence graph of $\mathrm{Gr}(k, 4)$ is obtained as a subgraph of the incidence graph for the flag manifold. If we consider $\mathrm{Gr}(1, 4)$ then the incidence graph is the subgraph containing the vertices $\{e, s_1, s_2 s_1, s_3 s_2 s_1\}$. In Figure 4, this is the subgraph connecting with the vertices $\{e, [1], [21], [321]\}$ which crosses curves of the form $\tau_i = 0$ twice. That is, along s_1 one crosses $\tau_1 = 0$, then along the edge from $[1]$ to $[21]$ none of the $\tau_k = 0$ are crossed, hence there is a non-zero co-boundary. Finally along the edge connecting $[21]$ and $[321]$, τ_3 becomes zero, i.e. the co-boundary is zero. This gives the incidence graph giving the cohomology of $\mathrm{Gr}(1, 4)$, that is, we have the graph, $e \rightarrow s_1 \Rightarrow s_2 s_1 \rightarrow s_3 s_2 s_1$. In general, the incidence graph of the partial flag G/P appears as a subgraph of the incidence graph of the flag G/B (see [9] and Remark 6.1 below).

In this paper, we consider the cohomology of $\mathrm{Gr}(k, n)$ directly from the KP flow, that is, we construct the incidence graph based on a single τ -function, i.e. τ_k . One should then note that for example, the incidence graph of $\mathrm{Gr}(1, 4)$ from the KP flow is obtained by the choice of the τ -function in (1.2), i.e. we have $(\epsilon_1, \dots, \epsilon_4) = (+, -, -, +)$ as we discussed above. Notice that the corresponding Toda sign is $(\tilde{\epsilon}_1, \tilde{\epsilon}_2, \tilde{\epsilon}_3) = (-, +, -)$, which is *not* the same as the Toda signs used for the flag picture of Figure 4. The Toda sign $(-, +, -)$ would give an incidence graph for cohomology with twisted coefficients of the real flag manifold and this is not described by Figure 4. (See Figure 4 in [6] for the moment polytopes with different signs $(\tilde{\epsilon}_1, \tilde{\epsilon}_2, \tilde{\epsilon}_3)$.)

In order to get the incidence graph of $\mathrm{Gr}(1, 4)$ in terms of the KP flow, that is related to the Toda flow with sign $(-, +, -)$ and taking into account only the flow as it crosses $\tau_1 = 0$, we then need to consider the quotient $\mathcal{S}_4/\langle s_2, s_3 \rangle$ corresponding to the natural projection, $\pi : G/B \rightarrow G/P$ with the maximum parabolic P . Namely we are now in $\mathrm{Gr}(1, 4)$ viewed as $\mathrm{SL}_4(\mathbb{R})/P$ and in this quotient $\tau_1 = 0$ is crossed by that edge of the tetrahedron, and so we recover the incidence graph of $\mathrm{Gr}(1, 4)$. This is illustrated in Figure 1. Also note that the projection $\pi : G/B \rightarrow \mathrm{Gr}(2, 4)$ gives the octahedron illustrated in Figures 2 and 3.

It turns out that there are exactly two distinguished Toda signs (and two corresponding distinguished KP signs) which need to be used for the cohomology of all the $\mathrm{Gr}(k, n)$ to be expressed in terms of the KP flow. For example, in the case $\mathrm{Gr}(k, 4)$, these are $(-, +, -)$ for $k = 1, 3$ and $(+, -, +)$ for $k = 2$. Note once more, that the Toda sign $(\tilde{\epsilon}_1, \tilde{\epsilon}_2, \tilde{\epsilon}_3)$ giving the incidence graph in [8] (cohomology with constant coefficients), or in Figure 4, is not one of these two, but rather it is associated to $(-, -, -)$.

A summary of the strategy in the proof of our main theorem given in section 6 can be expressed as follows. The point is to check that the incidence graph of $\mathrm{Gr}(k, n)$, viewed as a subgraph of the incidence graph of the real flag manifold, derived from the Toda lattice and corresponding to the Toda signs $\tilde{\epsilon}_i = -$ for all i , agrees with a graph defined in terms of the KP flow and one of the two distinguished KP signs.

4. THE SET $\mathcal{S}_n^{(k)}$ AND THE GRAPH $\mathcal{G}_n^{(k)}$

In this section, we describe the algebraic structure of the Grassmannian $\mathrm{Gr}(k, n)$. The set of Schubert cells $\{(\sigma_1, \dots, \sigma_k) : 1 \leq \sigma_1 < \dots < \sigma_k \leq n\}$ for $\mathrm{Gr}(k, n)$ forms a partially ordered set (*poset*) with the Bruhat order defined as follows: Let $s_i \in \mathcal{S}_n$ be an adjacent transposition $s_i : i \rightarrow i+1$ for $i = 1, \dots, n-1$ for the symmetric group \mathcal{S}_n . Then there exists s_{σ_i} -action on the cell $(\sigma_1, \dots, \sigma_k)$, if $\sigma_i + 1 < \sigma_{i+1}$ for some i or $\sigma_k < n$. The action gives

$$s_{\sigma_i} : (\sigma_1, \dots, \sigma_i, \dots, \sigma_k) \longrightarrow (\sigma_1, \dots, \sigma_{i-1}, \sigma_i + 1, \sigma_{i+1}, \dots, \sigma_k).$$

Then the arrow given by the action determines the *weak* Bruhat order between those cells. With action defined this way, each cell can be uniquely parametrized by a representative of minimal length

in the quotient $\mathcal{S}_n/\mathcal{P}_k$ (see [2]), that is,

$$\mathcal{S}_n^{(k)} := \{\text{the reduced words of } \text{mod}(\mathcal{P}_k) \text{ ending in } s_k\}.$$

Here \mathcal{P}_k is a Weyl subgroup of \mathcal{S}_n corresponding to the maximal parabolic subgroup, and is generated by $\{s_1, \dots, s_{k-1}, s_{k+1}, \dots, s_{n-1}\}$, denoted as

$$\mathcal{P}_k = \langle s_1, \dots, \check{s}_k, \dots, s_{n-1} \rangle \cong \mathcal{S}_k \times \mathcal{S}_{n-k}.$$

Note here that $\mathcal{P}_n = \mathcal{S}_n$ and $\mathcal{S}_n^{(n)} = \{e\}$. In this sense, we identify an element $w_\sigma \in \mathcal{S}_n^{(k)}$ with the Schubert cell $\sigma = (\sigma_1, \dots, \sigma_k)$. This leads to the Schubert decomposition in terms of $\mathcal{S}_n^{(k)}$, that is, we have

$$\text{Gr}(k, n) = \bigsqcup_{w_\sigma \in \mathcal{S}_n^{(k)}} X_{w_\sigma}, \quad \text{with } X_{w_\sigma} = (\sigma_1, \dots, \sigma_k).$$

We also write X_{w_σ} simply as w_σ , that is, $w_\sigma = (\sigma_1, \dots, \sigma_k)$. With the set $\mathcal{S}_n^{(k)}$, one should also note

$$|\text{Gr}(k, n, \mathbb{F}_q)| = \sum_{w \in \mathcal{S}_n^{(k)}} q^{l(w)},$$

where $l(w)$ is the length of w .

The set of Schubert cells with s_i -actions forms a graph consisting of the vertices given by the cells and the edges given by the weak Bruhat order. We denote this graph by $\mathcal{G}_n^{(k)}$, and call it the weak Bruhat graph of $\text{Gr}(k, n)$. Let us give few examples of $\mathcal{G}_n^{(k)}$.

Example 4.1. We consider the cases with $n = 4$ and $k = 1, 2, 3$:

(1) $\text{Gr}(1, 4) \cong \mathbb{R}P^3$: The graph $\mathcal{G}_4^{(1)}$ is given by

$$(1) \xrightarrow{s_1} (2) \xrightarrow{s_2} (3) \xrightarrow{s_3} (4).$$

Each cell (k) can be parametrized by an element in $\mathcal{S}_4^{(1)}$, the set of minimal length representative in the quotient $\mathcal{S}_4/\langle s_2, s_3 \rangle$, that is, $(1) = e$, $(2) = s_1$, $(3) = s_2s_1$, $(4) = s_3s_2s_1$.

(2) $\text{Gr}(2, 4)$: The graph $\mathcal{G}_4^{(2)}$ is given by

$$\begin{array}{ccccc} (1, 2) & \xrightarrow{s_2} & (1, 3) & \xrightarrow{s_3} & (1, 4) \\ & & \downarrow s_1 & & \downarrow s_1 \\ & & (2, 3) & \xrightarrow{s_3} & (2, 4) \\ & & & & \downarrow s_2 \\ & & & & (3, 4) \end{array}$$

Each cell (i, j) is parametrized by a unique element of $\mathcal{S}_4^{(2)}$, i.e. $(1, 2) = e$, $(1, 3) = s_2$, $(2, 3) = s_1s_2$, $(1, 4) = s_3s_2$, $(2, 4) = s_1s_3s_2$, $(3, 4) = s_2s_1s_3s_2$.

(3) $\text{Gr}(3, 4) \cong \mathbb{R}P^3$: The graph $\mathcal{G}_4^{(3)}$ is given by

$$(1, 2, 3) \xrightarrow{s_3} (1, 2, 4) \xrightarrow{s_2} (1, 3, 4) \xrightarrow{s_1} (2, 3, 4).$$

The parametrization of each cell (i, j, k) is given by $(1, 2, 3) = e$, $(1, 2, 4) = s_3$, $(1, 3, 4) = s_2s_3$, $(2, 3, 4) = s_1s_2s_3$. Those are the elements of $\mathcal{S}_4^{(3)}$.

4.1. The decomposition of $\mathcal{S}_n^{(k)}$. Here we consider a decomposition of the set $\mathcal{S}_n^{(k)}$ into the set $\{\mathcal{S}_{j-1}^{(k-1)} : j = k, k+1, \dots, n\}$. This decomposition is based on the following relation for the binomial coefficients,

$$\binom{n}{k} = \binom{k-1}{k-1} + \binom{k}{k-1} + \dots + \binom{n-1}{k-1} = \sum_{j=k}^n \binom{j-1}{k-1}.$$

which is a direct consequence of the Pascal rule, $\binom{n}{k} = \binom{n-1}{k} + \binom{n-1}{k-1}$. Namely we have:

Proposition 4.1. *The set $\mathcal{S}_n^{(k)}$ has a decomposition,*

$$\mathcal{S}_n^{(k)} = \mathcal{S}_{k-1}^{(k-1)} \cup \bigcup_{j=k}^{n-1} \mathcal{S}_j^{(k-1)} s_j \cdots s_k,$$

where note $\mathcal{S}_{k-1}^{(k-1)} = \{e\}$.

To prove Proposition 4.1, we first state the following Lemma which is similar to the Pascal rule,

Lemma 4.2. *There is a decomposition,*

$$\mathcal{S}_n^{(k)} = \mathcal{S}_{n-1}^{(k)} \cup \mathcal{S}_{n-1}^{(k-1)} s_{n-1} s_{n-2} \cdots s_k.$$

Proof. This corresponds to the decomposition of weight vectors,

$$\bigwedge^k V(E_1, \dots, E_n) = \bigwedge^k V(E_1, \dots, E_{n-1}) \oplus \left[\bigwedge^{k-1} V(E_1, \dots, E_{n-1}) \wedge E_n \right].$$

It is then obvious that the weight vectors in the last part are given by the orbit of $\mathcal{S}_{n-1}^{(k)}$ of the highest weight vector $E_1 \wedge \cdots \wedge E_k$.

Now note that the element $w = s_{n-1} \cdots s_k$ maps the highest weight vector $E_1 \wedge \cdots \wedge E_k$ to $E_1 \wedge \cdots \wedge E_{k-1} \wedge E_n$. Then the weight vectors in $\bigwedge^{k-1} V(E_1, \dots, E_{n-1})$ can be obtained by the orbit of $\mathcal{S}_{n-1}^{(k-1)}$ of the highest weight vector $E_1 \wedge \cdots \wedge E_{k-1}$. \square

Remark 4.1. The decomposition in Proposition 4.1 corresponds to the following decomposition,

$$\bigwedge^k V(E_1, \dots, E_n) = \bigoplus_{j=k}^n \left[\bigwedge^{k-1} V(E_1, \dots, E_{j-1}) \wedge E_j \right].$$

Example 4.2. The set $\mathcal{S}_4^{(2)}$ can be written as $\mathcal{S}_1^{(1)} \cup \mathcal{S}_2^{(1)} s_2 \cup \mathcal{S}_3^{(1)} s_3 s_2$: First we write the sets $\mathcal{S}_m^{(k)}$ which are involved,

$$(4.1) \quad \mathcal{S}_1^{(1)} = \{e\}, \quad \mathcal{S}_2^{(1)} = \{e, s_1\}, \quad \mathcal{S}_3^{(1)} = \{e, s_1, s_2 s_1\}.$$

Hence we have

$$(4.2) \quad \mathcal{S}_1^{(1)} = \{e\}, \quad \mathcal{S}_2^{(1)} s_2 = \{s_2, s_1 s_2\}, \quad \mathcal{S}_3^{(1)} s_3 s_2 = \{s_3 s_2, s_1 s_3 s_2, s_2 s_1 s_3 s_2\}.$$

As in Remark 4.1 we have a decomposition

$$\bigwedge^2 V(E_1, E_2, E_3) = \left[\bigwedge^1 V(E_1) \wedge E_2 \right] \oplus \left[\bigwedge^1 V(E_1, E_2) \wedge E_3 \right] \oplus \left[\bigwedge^1 V(E_1, E_2, E_3) \wedge E_4 \right].$$

For example, $\bigwedge^1 V(E_1, E_2, E_3) \wedge E_4$ corresponds to $\mathcal{S}_3^{(1)} s_3 s_2$. This is given explicitly by associating $E_1 \wedge E_4$, $E_2 \wedge E_4$, $E_3 \wedge E_4$ to the elements $s_3 s_2$, $s_1 s_3 s_2$, $s_2 s_1 s_3 s_2$ respectively (see also Example 4.5 below).

The decomposition of $\mathcal{S}_n^{(k)}$ provides an arrangement of the Schubert decomposition of $\text{Gr}(k, n)$:

$$(4.3) \quad \text{Gr}(k, n) = \bigsqcup_{j=k}^n \left(\bigsqcup_{1 \leq \sigma_1 < \dots < \sigma_{k-1} \leq j-1} X(\sigma_1, \dots, \sigma_{k-1}, j) \right).$$

Each Schubert cell $X(\sigma_1, \dots, \sigma_{k-1}, j)$ can be labeled by an element of $\mathcal{S}_j^{(k-1)} s_j \dots s_k$. For each set $\mathcal{S}_j^{(k-1)}$, we can define the Bruhat graph $\mathcal{G}_j^{(k-1)}$. We then have a decomposition of the graph $\mathcal{G}_n^{(k)}$,

$$\mathcal{G}_n^{(k)} = \left[\mathcal{G}_{k-1}^{(k-1)} \xrightarrow{s_k} \mathcal{G}_k^{(k-1)} \xrightarrow{s_{k+1}} \dots \xrightarrow{s_{n-1}} \mathcal{G}_{n-1}^{(k-1)} \right].$$

Here the s_j -action provides the edges connecting the vertices in $\mathcal{G}_{j-1}^{(k-1)}$ with the corresponding vertices in $\mathcal{G}_j^{(k-1)}$, i.e.

$$\mathcal{G}_{j-1}^{(k-1)} \ni (\sigma_1, \dots, \sigma_{k-1}, \boxed{j}) \xrightarrow{s_j} (\sigma_1, \dots, \sigma_{k-1}, \boxed{j+1}) \in \mathcal{G}_j^{(k-1)},$$

for all $1 \leq \sigma_1 < \dots < \sigma_{k-1} \leq j-1$, and each index in the box is fixed.

Example 4.3. Consider the case of $\text{Gr}(3, 5)$. The graph $\mathcal{G}_5^{(3)}$ is given by

$$\begin{array}{ccccc} (1, 2, \boxed{3}) & \xrightarrow{s_3} & (1, 2, \boxed{4}) & \xrightarrow{s_4} & (1, 2, \boxed{5}) \\ & & \downarrow & & \downarrow \\ & & (1, 3, \boxed{4}) & \xrightarrow{s_4} & (1, 3, \boxed{5}) \longrightarrow (1, 4, \boxed{5}) \\ & & \downarrow & & \downarrow \\ & & (2, 3, \boxed{4}) & \xrightarrow{s_4} & (2, 3, \boxed{5}) \longrightarrow (2, 4, \boxed{5}) \\ & & & & \downarrow \\ & & & & (3, 4, \boxed{5}) \end{array}$$

which has the structure of a sequence of smaller graphs, i.e. the decomposition of the graph $\mathcal{G}_5^{(3)}$,

$$\mathcal{G}_5^{(3)} = \left[\mathcal{G}_2^{(2)} \xrightarrow{s_3} \mathcal{G}_3^{(2)} \xrightarrow{s_4} \mathcal{G}_4^{(2)} \right].$$

4.2. The decomposition of $\text{Gr}(k, n)$. We now describe a decomposition of $\text{Gr}(k, n)$ based on the arrangement (4.3). Let us first define $Y(j)$ for $j = k, k+1, \dots, n$ as the unions of the Schubert cells in (4.3),

$$Y(j) := \bigsqcup_{1 \leq \sigma_1 < \dots < \sigma_{k-1} \leq j-1} X(\sigma_1, \dots, \sigma_{k-1}, j).$$

Then we explain that each $Y(j)$ is a manifold with the structure of a vector bundle. To do this, let us fix vector spaces $\{V_0(j) : j = k-1, k, \dots, n\}$ satisfying

$$V_0(k-1) \subset V_0(k) \subset \dots \subset V_0(n-1) \subset V_0(n) = \mathbb{R}^n,$$

with $\dim(V_0(j)) = j$. Then $Y(j)$ can be described by

$$Y(j) = \{[V] : V \subset V_0(j), \dim(V \cap V_0(j-1)) = k-1\} \quad \text{for } j = k, k+1, \dots, n.$$

Now one can see that $Y(j)$ is a manifold which has the structure of a vector bundle $\mathcal{V}(j)$ with fibers of dimension $j-k$ over the Grassmannian $\text{Gr}(k-1, j-1)$. We have well defined projections $\pi_j : Y(j) \rightarrow \text{Gr}(k-1, j-1)$ which are given by $\pi_j([V]) = [V \cap V_0(j-1)]$. This is because $V \cap V_0(j-1) \subset V_0(j-1)$ is a vector space of dimension $k-1$ inside a fixed vector space which looks like \mathbb{R}^{j-1} . The fibers of this projection can be computed using explicit coordinates (see below). These vector bundles determine the determinant line-bundles over $\text{Gr}(k-1, j-1)$,

$$(4.4) \quad \bigwedge^{j-k} \mathcal{V}(j) = \mathcal{E}(j).$$

Remark 4.2. We have the following:

- (i) The space $Y(j)$ is a union of cells corresponding to $\mathcal{S}_{j-1}^{(k-1)} s_{j-1} \cdots s_k \leftrightarrow \mathcal{G}_{j-1}^{(k-1)}$
- (ii) Each element in $\mathcal{S}_{j-1}^{(k-1)}$ labels a corresponding cell in $\text{Gr}(k-1, j-1)$.
- (iii) The cell of lowest dimension in $Y(j)$ corresponds to $s_{j-1} \cdots s_k$.
 - The union of all these cells $\{s_{j-1} \cdots s_k : j = k+1, \dots, n-1\}$ correspond to the incidence graph of $\mathbb{R}P^{n-k} \cong \text{Gr}(1, n-k+1)$.
 - These cells of $\mathbb{R}P^{n-k}$ are the ones associated to the Schubert symbols

$$(1, 2, \dots, k-1, j), \quad \text{for } j = k, \dots, n.$$

- These are also the elements $s_j \cdots s_k$ in the statement of Proposition 4.1 and in Example 4.2 these are the cells labeled as $e, s_2, s_3 s_2$.
- (iv) The fibers of the vector bundles $\mathcal{V}(j)$ with total space $Y(j)$ and base $\text{Gr}(k-1, j-1)$ correspond to the cells of this $\mathbb{R}P^{n-k}$.

In the following examples, we describe explicitly the cells involved in each piece of this decomposition and the correspondence between a cell decomposition of $Y(j)$ and $\bigwedge^{k-1} V(E_1, \dots, E_{j-1}) \wedge E_j$. The basis element $E_{\sigma_1} \wedge \cdots \wedge E_{\sigma_{k-1}} \wedge E_j$ label a cell with pivots at the positions $(\sigma_1, \dots, \sigma_{k-1}, j)$.

Example 4.4. Explicit decomposition in the case of $\text{Gr}(2, 3) \cong \mathbb{R}P^2$. Let $V_0(2) \subset \mathbb{R}^3$ consist of vectors of the form $(x_1, x_2, 0)$. We let V denote a two dimensional vector space in \mathbb{R}^3 and $[V]$ a corresponding point in $\text{Gr}(2, 3)$. We than have

$$\begin{aligned} Y(2) &= \{[V_0(2)]\} = \left\{ \begin{pmatrix} 1 & 0 & 0 \\ 0 & 1 & 0 \end{pmatrix} \right\}, \\ Y(3) &= \{[V] : V \subset \mathbb{R}^3, \dim(V \cap V_0(2)) = 1\} \\ &= \left\{ \begin{pmatrix} 1 & 0 & 0 \\ 0 & * & 1 \end{pmatrix} \right\} \sqcup \left\{ \begin{pmatrix} * & 1 & 0 \\ * & 0 & 1 \end{pmatrix} \right\}. \end{aligned}$$

Looking at the position of pivots $Y(2)$ should be thought as corresponding to $\bigwedge^1 V(E_1) \wedge E_2$ and $Y(3)$ to the summand $\bigwedge^1 V(E_1, E_2) \wedge E_3$ in a decomposition of $\bigwedge^2 V(E_1, E_2, E_3)$.

If we think of $\text{Gr}(2, 3) \cong \mathbb{R}P^2$ given as a sphere where antipodal points are identified, then this decomposition has a simple description. First $Y(2)$ can be identified with the north and south poles. If we delete this pair of antipodal points we are left with a Möbius band corresponding to $Y(3)$. This is a non-trivial line bundle over the equator and in matrix notation, π_3 projects a matrix to its first row so that $\pi_3(Y(3)) = \{(1 \ 0 \ 0)\} \sqcup \{(* \ 1 \ 0)\} \cong \mathbb{R}P^1$. The one dimensional fibers are given by the second row in a matrix i.e. $(0 \ * \ 1)$ and $(* \ 0 \ 1)$ over $\{(1 \ 0 \ 0)\}$ and $\{(* \ 1 \ 0)\}$, respectively.

The $\mathbb{R}P^1$ in item (iii) of Remark 4.2 is a meridian. Note that the direction along meridians corresponds to the fibers of the fiber bundle over the equator giving the Möbius band.

Example 4.5. Explicit decomposition in the case of $\text{Gr}(2, 4)$. We once more emphasize the connection with a decomposition:

$$(4.5) \quad \bigwedge^2 V(E_1, E_2, E_3, E_4) = \left[\bigwedge^1 V(E_1) \wedge E_2 \right] \oplus \left[\bigwedge^1 V(E_1, E_2) \wedge E_3 \right] \oplus \left[\bigwedge^1 V(E_1, E_2, E_3) \wedge E_4 \right].$$

Let $V_0(2) \subset V_0(3) \subset \mathbb{R}^4$ be two subspaces of dimensions 2 and 3 respectively. We let V denote a two dimensional vector space in \mathbb{R}^4 and $[V]$ a corresponding point in $\text{Gr}(2, 4)$. Set:

$$Y(2) = \{[V_0(2)]\} = \left\{ \begin{pmatrix} 1 & 0 & 0 & 0 \\ 0 & 1 & 0 & 0 \end{pmatrix} \right\},$$

$$\begin{aligned} Y(3) &= \{[V] : V \subset V_0(3), \dim(V \cap V_0(2)) = 1\} \\ &= \left\{ \begin{pmatrix} 1 & 0 & 0 & 0 \\ 0 & * & 1 & 0 \end{pmatrix} \right\} \sqcup \left\{ \begin{pmatrix} * & 1 & 0 & 0 \\ * & 0 & 1 & 0 \end{pmatrix} \right\}, \end{aligned}$$

$$\begin{aligned} Y(4) &= \{[V] : V \subset \mathbb{R}^4, \dim(V \cap V_0(3)) = 1\} \\ &= \left\{ \begin{pmatrix} 1 & 0 & 0 & 0 \\ 0 & * & * & 1 \end{pmatrix} \right\} \sqcup \left\{ \begin{pmatrix} * & 1 & 0 & 0 \\ * & 0 & * & 1 \end{pmatrix} \right\} \sqcup \left\{ \begin{pmatrix} * & * & 1 & 0 \\ * & * & 0 & 1 \end{pmatrix} \right\}. \end{aligned}$$

We have $Y(2) = \text{Gr}(2, 2) \cong \text{Gr}(1, 1)$, $Y(3)$ is a non-trivial line bundle over $\text{Gr}(1, 2)$, and $Y(4)$ is a non-trivial \mathbb{R}^2 bundle over $\text{Gr}(1, 3)$. The projections of these bundles are $\pi_3 : Y(3) \rightarrow \text{Gr}(1, 2)$ with $\pi_3([V]) = [V \cap V_0(2)]$, and $\pi_4 : Y(4) \rightarrow \text{Gr}(1, 3)$ with $\pi_4([V]) = [V \cap V_0(3)]$. More explicitly, we have

$$\pi_3(Y(3)) = \{(1 \ 0 \ 0 \ 0)\} \sqcup \{(* \ 1 \ 0 \ 0)\} = \text{Gr}(1, 2),$$

$$\pi_4(Y(4)) = \{(1 \ 0 \ 0 \ 0)\} \sqcup \{(* \ 1 \ 0 \ 0)\} \sqcup \{(* \ * \ 1 \ 0)\} = \text{Gr}(1, 3).$$

The fiber over $\{(1 \ 0 \ 0 \ 0)\}$ in $Y(3)$ is $(0 \ * \ 1 \ 0)$, and the fiber over $\{(* \ 1 \ 0 \ 0)\}$ is $(* \ 0 \ 1 \ 0)$. This becomes a non-trivial line bundle over the circle $\text{Gr}(1, 2)$. The case of $Y(4)$ is described similarly and results in a non-trivial vector bundle with fiber of dimension 2. The fiber over $\{(1 \ 0 \ 0 \ 0)\}$ is $\{(0 \ * \ * \ 1)\}$, the fiber over $\{(* \ 1 \ 0 \ 0)\}$ is $\{(* \ 0 \ * \ 1)\}$, and the fiber over $\{(* \ * \ 1 \ 0)\}$ is $\{(* \ * \ 0 \ 1)\}$. The fiber of the vector bundle over $\text{Gr}(1, 3)$ is two dimensional because of the two parameters.

5. THE GRAPH $\mathcal{G}(k, n)$

Here we define what will be shown to be the incidence graph for the cohomology of $\text{Gr}(k, n)$ relative to Schubert cells. We first consider the case of $\text{Gr}(1, n) \cong \mathbb{R}P^{n-1}$, and then introduce *signed* Schubert cells to construct what will become the incidence graph. The goal of this section is to show that this graph defined for $\text{Gr}(k, n)$ can be obtained from the results of $\text{Gr}(1, n)$ and its dual $\text{Gr}(n-1, n)$.

Let us recall that $\text{Gr}(1, n) \cong \mathbb{R}P^{n-1}$ has the Schubert decomposition,

$$\text{Gr}(1, n) = \bigsqcup_{1 \leq \sigma_1 \leq n} X(\sigma_1),$$

where $X(\sigma_1)$ is the Schubert cell given by $X(i) = \{(x_1, \dots, x_{i-1}, 1, 0, \dots, 0) : x_j \in \mathbb{R}\} \cong \mathbb{R}^{i-1}$. Then the cochain complex for $\text{Gr}(1, n)$ is expressed by

$$(5.1) \quad \mathbb{Z}[\langle(1)\rangle] \xrightarrow{\delta_0} \mathbb{Z}[\langle(2)\rangle] \xrightarrow{\delta_1} \dots \xrightarrow{\delta_{2m-2}} \mathbb{Z}[\langle(2m)\rangle] \xrightarrow{\delta_{2m-1}} \mathbb{Z}[\langle(2m+1)\rangle] \xrightarrow{\delta_{2m}} \dots$$

with $\langle(i)\rangle = \overline{X(i)}$ and the coboundary operator $\delta_i : \mathbb{Z}[\langle(i+1)\rangle] \rightarrow \mathbb{Z}[\langle(i+2)\rangle]$. Here the single arrow \rightarrow indicates 0 incidence number and the double arrow indicates nonzero incidence number which is either 2 or -2 [19], i.e.

$$\delta_{i-1}\langle(i)\rangle = \begin{cases} 0 & \text{if } i = \text{odd} \\ \pm 2 \langle(i+1)\rangle & \text{if } i = \text{even} \end{cases}$$

Then we recover the well-known formulas of the integral cohomology of $\text{Gr}(1, n) \cong \mathbb{R}P^{n-1}$ as follows:

(a) For $n = 2m + 1$, the last arrow in (5.1) is the double arrow, and we have

$$H^k(\mathbb{R}P^{2m}; \mathbb{Z}) = \begin{cases} \mathbb{Z} & \text{if } k = 0 \\ 0 & \text{if } k = \text{odd} \leq 2m - 1 \\ \mathbb{Z}_2 & \text{if } k = \text{even} \leq 2m \end{cases}$$

The Poincaré polynomial for $\text{Gr}(1, 2m + 1)$ is then just $P_{(1, 2m+1)}(t) = 1$.

(b) For $n = 2m + 2$, the last arrow is the single one, and

$$H^k(\mathbb{R}P^{2m+1}; \mathbb{Z}) = \begin{cases} \mathbb{Z} & \text{if } k = 0 \text{ and if } k = 2m + 1 \\ 0 & \text{if } k = \text{odd} \neq 2m + 1 \\ \mathbb{Z}_2 & \text{if } k = \text{even} \leq 2m \end{cases}$$

The Poincaré polynomial for this case is $P_{(1, 2m+2)}(t) = 1 + t^{2m+1}$.

5.1. The signed Schubert cells. In order to represent the incidence graph in terms of the Schubert cells, we introduce the signed Schubert cells (see also subsection 3.1). Let us first define the signed vectors $e_j := \epsilon_j E_j$ for $j = 1, \dots, n$ where $E_j \in \mathbb{R}^n$ is the j -th standard basis vector, and $\epsilon_j \in \{\pm\}$. Then the k -wedge product $e_{\sigma_1} \wedge \dots \wedge e_{\sigma_k}$ has the sign $\epsilon(\sigma_1, \dots, \sigma_k) = \prod_{j=1}^k \epsilon_{\sigma_j}$ (see (3.3)), i.e.

$$e_{\sigma_1} \wedge \dots \wedge e_{\sigma_k} = \epsilon(\sigma_1, \dots, \sigma_k) E_{\sigma_1} \wedge \dots \wedge E_{\sigma_k}.$$

We then define a (induced) sign of the Schubert cell $(\sigma_1, \dots, \sigma_k)$ as the sign of the wedge product $e_{\sigma_1} \wedge \dots \wedge e_{\sigma_k}$, i.e. $\epsilon(\sigma_1, \dots, \sigma_k)$. Thus we identify the signed cell $(\sigma_1, \dots, \sigma_k)$ as $e_{\sigma_1} \wedge \dots \wedge e_{\sigma_k}$.

Remark 5.1. With the signed bases $\{e_j : j = 1, \dots, n\}$, the τ -function in (3.4) can be written in the

following form with $f = \sum_{j=1}^k \epsilon_j E_j$,

$$\begin{aligned} \tau_k &= \text{Wr}(f, f', \dots, f^{(k-1)}) \\ &= \sum_{1 \leq \sigma_1 < \dots < \sigma_k \leq n} |\xi(\sigma_1, \dots, \sigma_k)| \epsilon(\sigma_1, \dots, \sigma_k) E(\sigma_1, \dots, \sigma_k) \end{aligned}$$

where $|\xi(\sigma_1, \dots, \sigma_k)|$ is the $k \times k$ minor of the Vandermonde matrix in A .

We now define a graph $\mathcal{G}(k, n)$, which depends on the choice of signed vectors e_i and which is obtained from the weak Bruhat graph whose edges indicate that the cells connected by the edge have the same sign. Suppose that we have s_{σ_i} -action on the cell $(\sigma_1, \dots, \sigma_k)$, i.e. $\sigma_i + 1 < \sigma_{i+1}$. Then if the cells connected by the action have the same sign, i.e. $\epsilon(\sigma_1, \dots, \sigma_i, \dots, \sigma_k) \epsilon(\sigma_1, \dots, \sigma_i + 1, \dots, \sigma_k) = +$, we put the double edge for the Bruhat order, i.e.

$$s_{\sigma_i} : (\sigma_1, \dots, \sigma_i, \dots, \sigma_k) \Longrightarrow (\sigma_1, \dots, \sigma_i + 1, \dots, \sigma_k).$$

Otherwise (i.e. sign change), we keep the single edge of the Bruhat order. Thus this new graph is obtained from the Bruhat graph by changing some of the edges to the double ones. The single edges correspond to the cells which have the different signs, i.e. $\epsilon(\sigma) \epsilon(\sigma') = -$ for the Bruhat ordered cells with $\sigma = (\sigma_1, \dots, \sigma_k)$ and $\sigma' = (\sigma'_1, \dots, \sigma'_k)$.

We also impose the signs for particular cells $(\sigma_1, \dots, \sigma_k)$ as follows:

- (a) Assume $\epsilon_1 = +$.
- (b) Assign $\epsilon(1, \dots, k - 1, k + j) = (-)^{\lfloor \frac{j+1}{2} \rfloor}$ for $j = 0, 1, \dots, n - k$.
- (c) Assign $\epsilon(1, \dots, k - j, k - j + 2, \dots, k + 1) = (-)^{\lfloor \frac{j+1}{2} \rfloor}$ for $j = 1, 2, \dots, k - 1$.

The item (b) implies that we have the same sign pattern for $\mathbb{R}P^{n-k} = \text{Gr}(1, n - k + 1)$. The item (c) then corresponds to the pattern of $\mathbb{R}P^k = \text{Gr}(k, k + 1)$. Those cells appear in the upper horizontal line and the left vertical side of the Bruhat graph. Then one can determine uniquely the signs $(\epsilon_1, \dots, \epsilon_n)$ for a given pair of the numbers (k, n) .

Proposition 5.1. *Following the sign assignment given above for $\text{Gr}(k, n)$, the signs ϵ_j are given by*

$$\begin{cases} \epsilon_{2j+1} = (-)^j & \text{for } j = 0, 1, \dots, \lfloor \frac{n-1}{2} \rfloor, \\ \epsilon_{2j+2} = (-)^{k+j} & \text{for } j = 0, 1, \dots, \lfloor \frac{n-2}{2} \rfloor. \end{cases}$$

Proof. First we note that the sign choice in (b) leads to the condition,

$$\epsilon_{k+j-1}\epsilon_{k+j} = (-)^j \quad \text{for } j = 1, 2, \dots, n-k.$$

Also from the choice (c), we have

$$\epsilon_{k-j+1}\epsilon_{k-j+2} = (-)^j \quad \text{for } j = 1, 2, \dots, k.$$

Combining those, we have

$$\epsilon_j\epsilon_{j+1} = (-)^{k+j+1} \quad \text{for } j = 1, 2, \dots, n-1,$$

With the condition (a), i.e. $\epsilon_1 = +$, we obtain the desired formulae. \square

This proposition implies that for $\text{Gr}(k, n)$, if k is *odd*, we choose the signs,

$$(5.2) \quad (\epsilon_1, \epsilon_2, \epsilon_3, \epsilon_4, \dots, \epsilon_n) = (+, -, -, +, \dots, (-)^{\lfloor \frac{n}{2} \rfloor}),$$

and if k is *even*, we choose

$$(5.3) \quad (\epsilon_1, \epsilon_2, \epsilon_3, \epsilon_4, \dots, \epsilon_n) = (+, +, -, -, \dots, (-)^{\lfloor \frac{n-1}{2} \rfloor}).$$

It will be useful to describe those sets of signs using the diagonal matrix h_ϵ defined in (3.2). Namely we define $h(-)$ and $h(+)$ as the $n \times n$ diagonal matrices h_ϵ corresponding to the sets of signs (5.2) and (5.3), respectively, i.e.

$$\begin{aligned} h(-) &:= \text{diag} \left(+, -, -, +, \dots, (-)^{\lfloor \frac{n}{2} \rfloor} \right), \\ h(+) &:= \text{diag} \left(+, +, -, -, \dots, (-)^{\lfloor \frac{n-1}{2} \rfloor} \right). \end{aligned}$$

These act on $V(E_1, \dots, E_n)$. These matrices then belong to the group $\text{SL}(n, \mathbb{R})^\pm$ and also act on $\bigwedge^k V(E_1, \dots, E_n)$. This gives each $E_{j_1} \wedge \dots \wedge E_{j_k}$ (i.e. *each cell*) a sign, namely the corresponding eigenvalue,

$$h(\pm) E_{\sigma_1} \wedge E_{\sigma_2} \wedge \dots \wedge E_{\sigma_k} = \epsilon(\sigma_1, \sigma_2, \dots, \sigma_k) E_{\sigma_1} \wedge E_{\sigma_2} \wedge \dots \wedge E_{\sigma_k}.$$

The graph that has been constructed has vertices $(\sigma_1, \dots, \sigma_k) \longleftrightarrow E_{\sigma_1} \wedge \dots \wedge E_{\sigma_k}$. For k odd, we consider the action $h(-)$, and for k even, the action of $h(+)$. An edge \Rightarrow exists between two vertices related by a simple reflection whenever the signs (eigenvalues of $h(\pm)$) agree for the two elements in $\bigwedge^k V(E_1, \dots, E_n)$.

Remark 5.2. In the identification of the Schubert cell $(\sigma_1, \dots, \sigma_k)$ with the wedge vector $E_{\sigma_1} \wedge \dots \wedge E_{\sigma_k}$, the action between two cells in the weak Bruhat order can be considered as the KP flow through the corresponding two dominant exponentials. Then changing the sign $\epsilon(\sigma_1, \dots, \sigma_k)$ is equivalent to having a zero in the τ -function. That is, the KP flow has a singularity.

Notation 5.1. With the diagonal action of $h(\pm)$, we can refer to this graph denoted by $\mathcal{G}(k, n)$ as the graph associated to the action of $h(\pm)$ on $\bigwedge^k V(E_1, \dots, E_n)$. It will be shown that this graph is an incidence graph computing cohomology of $\text{Gr}(k, n)$ relative to Schubert cells.

We now state the main theorem.

Theorem 5.2. *The graph $\mathcal{G}(k, n)$ of $h(\pm)$ acting on $\bigwedge^k V(E_1, \dots, E_n)$ agrees with the incidence graph of $\text{Gr}(k, n)$.*

We prove the Theorem in the section 6. Before closing this section, we give some lower dimensional examples.

Example 5.1. Let us first consider $\text{Gr}(2, 4)$: With the signs $(\epsilon_1, \dots, \epsilon_4) = (+, +, -, -)$, we obtain

$$\begin{array}{ccccc} (1, 2) & \rightarrow & (1, 3) & \Rightarrow & (1, 4) \\ & & \downarrow & & \downarrow \\ & & (2, 3) & \Rightarrow & (2, 4) \\ & & & & \downarrow \\ & & & & (3, 4) \end{array}$$

This is the incidence graph of $\text{Gr}(2, 4)$ and the nonzero incidence numbers are ± 2 . This graph is, of course, a subgraph of the incidence graph for the real flag manifold shown in Figure 4. The integral cohomology $H^*(\text{Gr}(2, 4), \mathbb{Z})$ is then given by

$$\begin{array}{ll} H^0(\text{Gr}(2, 4), \mathbb{Z}) &= \mathbb{Z}, & H^3(\text{Gr}(2, 4), \mathbb{Z}) &= \mathbb{Z}_2, \\ H^1(\text{Gr}(2, 4), \mathbb{Z}) &= 0, & H^4(\text{Gr}(2, 4), \mathbb{Z}) &= \mathbb{Z}, \\ H^2(\text{Gr}(2, 4), \mathbb{Z}) &= \mathbb{Z}_2, & & \end{array}$$

It is interesting to note that the Betti numbers $\beta_0 = 1$ and $\beta_4 = 1$ are coming from the cells with $(1, 2)$ and $(3, 4)$, respectively. The corresponding Young diagrams for those cells are given by

$$(1, 2) = \emptyset, \quad (3, 4) = \begin{array}{|c|c|} \hline \square & \square \\ \hline \end{array}.$$

Here the Young diagram associated to the cell $(\sigma_1, \dots, \sigma_k)$ is defined by (ν_1, \dots, ν_k) with $\nu_j = \sigma_{k-j+1} - (k - j + 1)$ (note $\nu_j \geq \nu_{j+1}$ as the usual definition of the Young diagram, and each ν_j expresses the number of boxes in the row of the diagram).

Remark 5.3. Note that the top row of the graph corresponds to the elements

$$E_1 \wedge E_2 \rightarrow E_1 \wedge E_3 \Rightarrow E_1 \wedge E_4.$$

These terms E_2, E_3, E_4 already appeared in the decomposition (4.5) in Example 4.5 indicating the position of a pivot. They now corresponds to a portion of the graph of $\mathbb{R}P^3$ with twisted coefficients, which agrees with the graph of $\mathbb{R}P^2$ with constant coefficients, and is indicated with $\overbrace{\cdots}$,

$$E_1 \Rightarrow \overbrace{E_2 \rightarrow E_3 \Rightarrow E_4}.$$

In general the top row of the graph is one of the following depending on whether k is odd or even:

(a) If k is odd, we have $h(-)$ action, and

$$E_1 \wedge \cdots \wedge E_{k-1} \wedge E_k \Rightarrow E_1 \wedge \cdots \wedge E_{k-1} \wedge E_{k+1} \rightarrow E_1 \wedge \cdots \wedge E_{k-1} \wedge E_{k+2} \Rightarrow \cdots$$

(b) If k is even, we have $h(+)$ action, and

$$E_1 \wedge \cdots \wedge E_{k-1} \wedge E_k \rightarrow E_1 \wedge \cdots \wedge E_{k-1} \wedge E_{k+1} \Rightarrow E_1 \wedge \cdots \wedge E_{k-1} \wedge E_{k+2} \rightarrow \cdots$$

We summarize the argument above as the following Lemma.

Lemma 5.3. *We have the following.*

- (i) *The top row of the graph $\mathcal{G}(k, n)$ associated to the action of $h(-)$ on $\bigwedge^k V(E_1, \dots, E_n)$ is the incidence graph of $\mathbb{R}P^{n-k}$ with trivial coefficients if k is odd and with twisted coefficients if k is even.*
- (ii) *The top row of the graph $\mathcal{G}(k, n)$ associated to the action of $h(+)$ on $\bigwedge^k V(E_1, \dots, E_n)$ is the incidence graph of $\mathbb{R}P^{n-k}$ with twisted coefficients if k is even and with trivial coefficients if k is odd.*

Example 5.2. We now consider $\text{Gr}(3, 6)$: The action is then given by $h(-) = \text{diag}(+, -, -, +, +, -)$, and the graph is given by

$$\begin{array}{ccccccc}
 (1, 2, 3)_0 & (1, 2, 4)_1 & \Rightarrow & (1, 2, 5)_2 & & (1, 2, 6)_3 & \\
 & \downarrow & & \downarrow & & \downarrow & \\
 & (1, 3, 4)_2 & \Rightarrow & (1, 3, 5)_3 & (1, 4, 5)_4 & (1, 3, 6)_4 & (1, 4, 6)_5 \Rightarrow (1, 5, 6)_6 \\
 & & & & & & \\
 (2, 3, 4)_3 & \Rightarrow & (2, 3, 5)_4 & (2, 4, 5)_5 & (2, 3, 6)_5 & (2, 4, 6)_6 & \Rightarrow (2, 5, 6)_7 \\
 & & & \downarrow & & \downarrow & \downarrow \\
 & & & (3, 4, 5)_6 & & (3, 4, 6)_7 & \Rightarrow (3, 5, 6)_8 \\
 & & & & & & \\
 & & & & & & (4, 5, 6)_9
 \end{array}$$

Here the single arrows (corresponding to the zero incidence numbers) are all eliminated. The suffix in each cell shows the dimension of the cell, that is, the dimension d is given by $d = \sum_{j=1}^3 (\sigma_j - j)$ for each cell of $(\sigma_1, \sigma_2, \sigma_3)$. The cohomology is then given by

$$\begin{array}{ll}
 H^0(\text{Gr}(3, 6), \mathbb{Z}) = \mathbb{Z}, & H^5(\text{Gr}(3, 6), \mathbb{Z}) = \mathbb{Z}, \\
 H^1(\text{Gr}(3, 6), \mathbb{Z}) = 0, & H^6(\text{Gr}(3, 6), \mathbb{Z}) = \mathbb{Z}_2 \oplus \mathbb{Z}_2, \\
 H^2(\text{Gr}(3, 6), \mathbb{Z}) = \mathbb{Z}_2, & H^7(\text{Gr}(3, 6), \mathbb{Z}) = \mathbb{Z}_2, \\
 H^3(\text{Gr}(3, 6), \mathbb{Z}) = \mathbb{Z}_2, & H^8(\text{Gr}(3, 6), \mathbb{Z}) = \mathbb{Z}_2, \\
 H^4(\text{Gr}(3, 6), \mathbb{Z}) = \mathbb{Z} \oplus \mathbb{Z}_2 \oplus \mathbb{Z}_2, & H^9(\text{Gr}(3, 6), \mathbb{Z}) = \mathbb{Z}.
 \end{array}$$

Note here that the Betti numbers $\beta_0 = 1, \beta_4 = 1, \beta_5 = 1$ and $\beta_9 = 1$ are coming from the Schubert cycles with $(1, 2, 3), (1, 4, 5), (2, 3, 6)$ and $(4, 5, 9)$, and the Young diagrams of those cycles are given by

$$(1, 2, 3) = \emptyset, \quad (1, 4, 5) = \begin{array}{|c|c|} \hline \square & \square \\ \hline \end{array}, \quad (2, 3, 6) = \begin{array}{|c|c|c|} \hline \square & \square & \square \\ \hline \end{array}, \quad (4, 5, 6) = \begin{array}{|c|c|c|c|} \hline \square & \square & \square & \square \\ \hline \end{array}.$$

The Young diagram for $(4, 5, 6)$ may be considered to be a combination of $(1, 4, 5)$ and $(2, 3, 6)$. This pattern is common for the case of $\text{Gr}(k, n)$ with $k = \text{odd}$ and $n = \text{even}$ (see Section 8)

6. PROOF OF THE MAIN THEOREM FOR THE INCIDENCE GRAPH

Here we begin to provide a roadmap of the main argument to prove the main theorem 1.1 through a simple example.

6.1. The case of $\text{Gr}(2, 4)$. Let us describe the example of $\text{Gr}(2, 4)$: First we recall that the graph $\mathcal{G}(2, 4)$ is induced by the KP signs $(+, +, -, -)$ (i.e. $h(+) = \text{diag}(+, +, -, -)$) by Lemma 5.3 or Remark 5.3. We start with the decomposition, $\text{Gr}(2, 4) = Y(2) \cup Y(3) \cup Y(4)$, and observe that if we proceed inductively (either on n or on k), then pieces of the incidence graph are already available. In this case we can assume that we know the graphs corresponding to the $Y(j) \rightsquigarrow \text{Gr}(1, j-1)$ for $j = 2, 3, 4$ (those are the columns in the graph below). We also know the top row, i.e the subgraph associated to a copy of $\mathbb{R}P^2$. Thus we get the following,

$$\begin{array}{ccccc}
 (1, 2) & \longrightarrow & (1, 3) & \implies & (1, 4) \\
 & & \downarrow & & \downarrow \\
 & & (2, 3) & ? & (2, 4) \\
 & & & & \downarrow \\
 & & & & (3, 4)
 \end{array}$$

where we are still missing the edge indicated with “?”. We note two things:

- (a) The incidence graphs associated to the columns $Y(j)$ correspond to *twisted* coefficients.
- (b) To determine the missing edge, we need to show that the arrows on the top row extend to the columns (are “constant” along the columns). The missing edge is \Rightarrow .

We explain (a) and (b) in the rest of this section, which provides the proof of Theorem 1.1. However (a) requires some notation from [8] to encode the structure of K -equivariant local systems on a flag manifold. Keeping in mind this simple example, the roadmap of the proof consists in giving a complete description of the local systems associated to the line bundles $\mathcal{E}(j)$. The description takes place in the context of K -equivariant line bundles on the flag manifold \mathcal{B} for $K = \mathrm{O}_n(\mathbb{R})$ or $K = \mathrm{SO}_n(\mathbb{R})$ with respect to (a). After introducing some notation and Proposition 6.1 below on the sign change under the Weyl group action, the general situation of $\mathrm{Gr}(k, n)$ becomes an issue of bookkeeping. The bookkeeping is done through the Toda signs $\tilde{\epsilon}_i$ which were introduced in [8] and above in subsection 3.3. What determines the (twisted) coefficients in the incidence graph of Grassmanians along the columns, that is item (a), is the structure of the vector bundle described in Example 4.5 in terms of the projections π_3, π_4 and corresponding determinant (line) bundles. The vector bundles, roughly speaking, have fibers corresponding to the cells of the $\mathbb{R}P^2$ along the top row of the graph $\mathcal{G}(2, 4)$.

6.2. Some standard notation. Let G be a real split semi-simple Lie group associated to the real Lie algebra \mathfrak{g} . For this paper the relevant cases will be $G = \mathrm{SL}_n(\mathbb{R})^\pm$ or $G = \mathrm{SL}_n(\mathbb{R})$ but some of the statements in this section apply to the more general situation. We fix H a split Cartan subgroup of G with Lie algebra \mathfrak{h} , $B = HN$ a Borel subgroup and P a maximal parabolic subgroup containing B . We let K denote a maximal compact Lie subgroup with Lie algebra \mathfrak{k} , $T = K \cap H$ is a finite subgroup of H (usually $K = \mathrm{O}_n(\mathbb{R})$, or $K = \mathrm{SO}_n(\mathbb{R})$ here and T the diagonal $n \times n$ matrices with entries ± 1).

Let $\{h_{\alpha_i}, e_{\pm\alpha_i}\}$ is the Cartan-Chevalley basis of \mathfrak{g} with the simple roots $\Pi = \{\alpha_1, \dots, \alpha_l\}$ which satisfy the relations,

$$[h_{\alpha_i}, h_{\alpha_j}] = 0, \quad [h_{\alpha_i}, e_{\pm\alpha_j}] = \pm C_{j,i} e_{\pm\alpha_j}, \quad [e_{\alpha_i}, e_{-\alpha_j}] = \delta_{i,j} h_{\alpha_j},$$

where $(C_{i,j})$ is the $l \times l$ Cartan matrix of \mathfrak{g} .

We first review the computation of integral cohomology of G/B with K -equivariant local coefficients: Let us recall that there is a filtration by Bruhat cells with $\mathcal{B}_j := \sqcup_{l(w) \leq j} NwB/B$,

$$\emptyset \subset \mathcal{B}_0 \subset \mathcal{B}_1 \subset \dots \subset \mathcal{B}_{l(w_o)} = G/B$$

where w_o indicates the longest element of the Weyl group W . We have coboundary maps, $\delta : H^s(\mathcal{B}_s, \mathcal{B}_{s-1}; \mathbb{Z}) \rightarrow H^{s+1}(\mathcal{B}_{s+1}, \mathcal{B}_s; \mathbb{Z})$, and these define a chain complex which computes the cohomology of G/B .

Recall that $\mathrm{Gr}(k, n) = G/P_k$ for a maximal parabolic P_k and that the Weyl group of its Levi factor is denoted \mathcal{P}_k . On the level of cells parametrized by the Weyl group, $W = \mathcal{S}_n$ in this case, there is a bijection, $\mathcal{S}_n^{(k)} \rightarrow W/P_k$.

Notation 6.1. Flag manifold and the Bruhat cells \mathcal{B}_w : Consider the flag manifold for $G = \mathrm{SL}_n(\mathbb{R})$ or $\mathrm{SL}_n(\mathbb{R})^\pm$, G/B with $B = HN$, consisting of all real flags $\{0 \subset V_1 \subset V_2 \subset \dots \subset V_n = \mathbb{R}^n\}$. Let \mathcal{B}_w denote the N orbit NwB/B . Hence $\mathcal{B}_w \cong wN \cap N^-$. There is a decomposition into Bruhat cells, i.e. into N orbits, $G/B = \bigsqcup_{w \in W} \mathcal{B}_w$.

We now recall that in the cases of $G = \mathrm{SL}_n(\mathbb{R})$ or $G = \mathrm{SL}_n(\mathbb{R})^\pm$ studied here, $\mathcal{S}_n^{(k)}$ consists of representatives of cosets in W/P_k of minimal length.

Remark 6.1. The subspace consisting of cells $X(k, n) := \bigsqcup_{w \in \mathcal{S}_n^{(k)}} \mathcal{B}_w$ is *homeomorphic* to $G/P_k \cong \mathrm{Gr}(k, n)$ because the projection $\pi : G/B \rightarrow G/P_k$ is such that π restricted to each \mathcal{B}_w is a bijection

whenever $w \in S_n^{(k)} \subset W$. The fibers of this projection are real flag manifolds associated to the Levi factor and \mathcal{B}_w intersected with this fiber is one point, the lowest dimensional Bruhat cell in this flag manifold. On the level of cells this corresponds to restricting the quotient $W \rightarrow W/\mathcal{P}_k$ to the subset $S_n^{(k)}$ which parametrizes W/\mathcal{P}_k . This explains why the incidence graphs of real Grassmannians are found as subgraphs of the incidence graph of the real flag manifold.

6.3. Connection of the cohomology of G/B with Hecke algebra operators. Here we give a quick summary of [9] on the cohomology of G/B as reformulated in [8].

For the purposes of this paper we consider $K = \mathrm{SO}_n(\mathbb{R})$, its complexification $K_{\mathbb{C}}$ as well as $G = \mathrm{SL}_n(\mathbb{R})$ and $G_{\mathbb{C}} = \mathrm{SL}_n(\mathbb{C})$. However this can be done in the more general context of [23]. We consider the real flag manifold $\mathcal{B} = G/B$ and its complexification $\mathcal{B}_{\mathbb{C}} = G_{\mathbb{C}}/B_{\mathbb{C}}$. For example for $G = \mathrm{SL}_n(\mathbb{R})$, $\mathcal{B}_{\mathbb{C}}$ consists of $\mathbb{C}P^1$. The real flag manifold \mathcal{B} is contained as a circle inside the open $K_{\mathbb{C}}$ orbit $\mathbb{C} \setminus \{0\}$.

Recall that the Hecke algebra \mathcal{H} of the Weyl group defined in [22] is a deformation of the usual group algebra of W . As a set it is given by $\mathcal{H} = \mathbb{Z}[q, q^{-1}] \otimes_{\mathbb{Z}} \mathbb{Z}[W]$, that is, the set of formal linear combinations of elements in W with coefficients in $\mathbb{Z}[q, q^{-1}]$. The multiplication is defined as in p. 189 of [22]. The elements $w \in W$ are denoted by T_w when viewed inside \mathcal{H} and we have $T_x T_y = T_{xy}$ when $l(xy) = l(x) + l(y)$ and for any simple reflection s_i , we have $(T_{s_i} + 1)(T_{s_i} - q) = 0$. This replaces the equation $s_i^2 = 1$.

If \mathcal{D} denotes the set of K -equivariant local systems on the flag manifold $\mathcal{B}_{\mathbb{C}}$ (dextended by zero from local systems on $K_{\mathbb{C}}$ orbits) then $\mathbb{Z}[q, q^{-1}] \otimes_{\mathbb{Z}} \mathbb{Z}[\mathcal{D}]$ becomes a module over the Hecke algebra. The incidence graph of the real flag manifold with local coefficients \mathcal{L}_o can be described in terms of this \mathcal{H} action on local systems. If $\mathcal{D}_o \subset \mathcal{D}$ consists of the elements in \mathcal{D} which are supported on the open dense orbit, then the incidence graph of G/B with local coefficients is given by the relations between the various elements $T_{\tau}^{-1} \mathcal{L}$. Let w_o be the longest element in W , and consider $T_{w_o}^{-1} \mathcal{L}$. Suppose that $\mathcal{L}_o \in \mathcal{D}_o$ occurs in the expression $T_{w_o}^{-1} \mathcal{L}$, (or we set $q = 1$ and obtain \mathcal{L}_o) then the incidence graph that we are describing corresponds to $H^*(G/B; \mathcal{L}_o)$. The vertices correspond to W . We associate “graded characters” to elements of W as follows. We let $\theta(e) = T_{w_o}^{-1} \mathcal{L}$, and then set $T_{\sigma} \theta(e) = \theta(\sigma)$. The element $\theta(\sigma)$ corresponds to cells parametrized by $\sigma^{-1} = w$. Each graded character $\theta(\sigma)$ corresponds to a local system $\mathcal{L}_w \in \mathcal{D}_o$. For example if we set $q = 1$ then $\theta(\sigma)$ reduces to \mathcal{L}_w . Let q^R denote the power of q of \mathcal{L}_e in $\theta(e)$. We let $q^{\eta(w)}$ be the power of q of \mathcal{L}_w in $q^R \theta(\sigma)$. We have readjusted so that $\eta(e) = 0$ and all the $\eta(w)$ are non-negative integers.

Remark 6.2. In [8], the number $\eta(w)$ is described in terms of the number of blow-ups of the Toda flow. Namely, we count the number of singular points in the flow from the top cell (corresponding to the flow for $t \ll 0$) to the Bruhat cell marked by $w \in W$ (see Figure 4).

Now the following is in the case when G is \mathbb{R} split e.g. $G = \mathrm{SL}_n(\mathbb{R})$. We can describe the edges of the incidence graph in the following way (after [8]): We have an edge $w \Rightarrow w'$ whenever $w \leq w'$ in the Bruhat order, $l(w') = l(w) + 1$ and $\eta(w) = \eta(w')$.

Example 6.1. In the case of $G = \mathrm{SL}_2(\mathbb{R})$, $\mathcal{D} = \{\mathcal{C}, \mathcal{L}, \delta_+, \delta_-\}$ where \mathcal{C} denotes a trivial sheaf on $\mathcal{O}_o = \mathbb{C}^*$, δ_{\pm} are sheaves supported on the points $0, \infty$ respectively, and \mathcal{L} is a non-trivial local system on \mathbb{C}^* . We have $T_{s_1} \mathcal{C} = (q - 2)\mathcal{C} + (q - 1)(\delta_- + \delta_+)$ and $T_{s_1} \mathcal{L} = -\mathcal{L}$.

In the Hecke algebra $T_{s_1}^{-1} = q^{-1}(T_{s_1} + (1 - q))$. Hence by applying $T_{s_1}^{-1}$ to \mathcal{C} we obtain $-q^{-1}\mathcal{C} + q^{-1}(q - 1)(\delta_+ + \delta_-)$. We also have $q^{-1}(T_{s_1} \mathcal{L} + (1 - q)\mathcal{L}) = q^{-1}(-\mathcal{L} + (1 - q)\mathcal{L}) = -\mathcal{L}$. Hence if we start with \mathcal{C} , then $\theta(e) = -q^{-1}\mathcal{C} + q^{-1}(q - 1)(\delta_+ + \delta_-)$, $\theta(s) = \mathcal{C}$. Then (setting $q = 1$ in $\theta(e)$) $\mathcal{L}_o = \mathcal{C}$ corresponding to constant coefficients. Since the power of q associated to \mathcal{C} is, respectively, -1 and 0 , or shifting to get non-negative integers $\eta(e) = 0, \eta(s) = 1$. Since $\eta(e) \neq \eta(s)$ there is no edge \Rightarrow joining e and s . This situation corresponds to the existence of one blow up in the Toda lattice. We end up with an incidence graph containing vertices e and s and no edges \Rightarrow . This

gives the cohomology of $\text{Gr}(1, 2)$, a circle, with constant coefficients. If we consider \mathcal{L} then we end up with $e \Rightarrow s$ the incidence graph of $\text{Gr}(1, 2)$ with local coefficients \mathcal{L} . This second case corresponds to an irreducible principal series module or to the case in which there are no blow-ups in the Toda flow.

Finally, we note the connection with the representation theory of $\mathfrak{sl}(2; \mathbb{R})$. By rewriting $T_{s_1}^{-1} q^1 \mathcal{C}$ as $-q^{-1/2} \hat{C}_{\mathcal{C}} + \hat{C}_{\delta_+} + \hat{C}_{\delta_-}$ with $\hat{C}_{\mathcal{C}} = q^{-1/2}(\mathcal{C} + \delta_+ + \delta_-)$, $\hat{C}_{\delta_{\pm}} = \delta_{\pm}$, we recover the weight filtration of the principal series representation containing the trivial representation as submodule (replace $\hat{C}_{\mathcal{C}}$ with a trivial representation C and $\hat{C}_{\delta_{\pm}}$ with two discrete series representations D_{\pm}).

We can now describe the incidence graph $\mathcal{G}(k, n)$ in terms of the description given above using Hecke algebra operators. The incidence graph is a graph with vertices $S_n^{(k)} \subset W$. Only two $K_{\mathbb{C}}$ equivariant local systems $\mathcal{L}(e)$ are considered. One trivial and one non-trivial. Then we have an edge $w \Rightarrow s_i w$ whenever $l(s_i w) = l(w) + 1$ and $\eta(w) = \eta(s_i w)$ (i.e. no sign change).

6.4. The edge in the incidence graph associated to $\mathcal{B}_w \cup \mathcal{B}_{s_i w}$. As in [9] and [7] the edge in the incidence graph corresponding to $\mathcal{B}_w \cup \mathcal{B}_{s_i w}$ is encoded in the action of the Hecke algebra operator T_s on the graded character $\theta(\sigma)$, i.e. whether $\eta(w) = \eta(sw)$ or $\eta(w) \neq \eta(sw)$. In terms of the action of the Weyl group on the set of signs of the Toda flow corresponding to $\text{sgn}(a_i)$ (introduced in [8] and below in Definition 6.2), there is an edge \Rightarrow , precisely when s_i does not change signs. If signs change, we just indicate the relation between w and $s_i w$ on the Bruhat order with \rightarrow , which, does not count as an edge in the graph, and which corresponds to crossing $\tau_i = 0$, a blow-up in the Toda flow.

We recall that each simple root α_i gives rise to a Lie group homomorphism $\Phi_{\alpha_i} : \text{SL}_2(\mathbb{R}) \rightarrow G$. We denote by $z_i = \Phi_{\alpha_i} \left(\begin{pmatrix} -1 & 0 \\ 0 & -1 \end{pmatrix} \right)$. This element can be expressed as $z_i = \exp(\pi \sqrt{-1} h_{\alpha_i})$. We can also consider $\sigma(z_i) = \exp(\pi \sqrt{-1} \sigma h_{\alpha_i})$ associated to σs_i i.e. to $\sigma \alpha_i \in \sigma(\Delta^+)$. The sign of $\chi_w(\sigma(z_i)) = \pm 1$ then determines whether $w \rightarrow s_i w$ (coboundary is zero) or $w \Rightarrow s_i w$ (coboundary is ± 2).

6.5. K -equivariant local systems on G/B and their Toda signs. Borel subgroups $w(B)$ containing H and corresponding to the positive roots systems $w(\Delta^+)$ define points x_w in the flag manifold G/B . These points are, in turn, representatives of Bruhat cells. We follow the notation in [9] which allows us to describe the action of the Weyl group on these local systems.

Definition 6.1. Consider a K -equivariant local system \mathcal{L} determined by a character of T given by $\chi(\mathcal{L})$. We consider the local system \mathcal{L}_w given by the T character $\chi(\mathcal{L}) \otimes \bigwedge^{l(w)} \sigma \mathfrak{n} \cap \mathfrak{n}^*$ ($\sigma = w^{-1}$). These correspond to $K_{\mathbb{C}}$ -equivariant local systems supported on the open $K_{\mathbb{C}}$ orbit on $\mathcal{B}_{\mathbb{C}}$ and have already been described above in terms of the Hecke algebra action.

Given $w \in W$ and the K -equivariant local system \mathcal{L}_w , we associate some signs which describe the local system from the perspective of simple reflections relative to $\sigma(\Delta^+)$. As in Definition 4.3 of [9] to the K -equivariant local system \mathcal{L}_w one associates a list of signs $\epsilon(\sigma, \mathcal{L}) = (\tilde{\epsilon}_1, \dots, \tilde{\epsilon}_l)$. These signs describe the local system relative to x_w i.e. relative to simple roots in $\sigma(\Delta^+)$. Here l the rank of the semi-simple Lie algebra. The signs keep track of triviality or non-triviality along directions corresponding to simple roots for $\sigma(\Delta^+)$. A sign $-$ in the i th place means that along a circle associated to s_i the local system is trivial and a sign $+$ means that it is non-trivial.

Definition 6.2. Let χ be a character of T corresponding to the local system \mathcal{L} . Then $(w^{-1} = \sigma)$ \mathcal{L}_w corresponds to $\chi_w = \chi(\mathcal{L}) \otimes \bigwedge^{l(w)} \sigma \mathfrak{n} \cap \mathfrak{n}^*$. We let $\epsilon(\sigma, \mathcal{L}) = (\tilde{\epsilon}_1, \dots, \tilde{\epsilon}_l)$ where $\tilde{\epsilon}_i = -\chi_{\sigma}(z_i)$. This is $-$ if the local system is trivial along the direction of the i th simple root relative to $\sigma \Delta^+$ and $+$ otherwise. For convenience we will refer to these signs as *Toda signs*, since they have a clear

interpretation in terms of the Toda flow. When $w = e$ we can refer to the Toda sign as *initial* Toda sign. This initial Toda sign determines which local coefficients are being used in cohomology computations.

Example 6.2. Consider the flag manifold $\mathcal{B} = G/B$ of $G = \mathrm{SL}_3(\mathbb{R})$. Recall the four such characters, χ with $\chi\left(\begin{pmatrix} e_1 & 0 & 0 \\ 0 & e_2 & 0 \\ 0 & 0 & e_3 \end{pmatrix}\right) = e_i$ for $i = 1, 2, 3$ and the trivial character. Assume $i = 1$. We compute $\tilde{\epsilon}_i = -\chi_w(z_i)$ where $w = e$. We have

$$z_1 = \begin{pmatrix} -1 & 0 & 0 \\ 0 & -1 & 0 \\ 0 & 0 & 1 \end{pmatrix} \quad \text{and} \quad z_2 = \begin{pmatrix} 1 & 0 & 0 \\ 0 & -1 & 0 \\ 0 & 0 & -1 \end{pmatrix}.$$

If we evaluate $-\chi_e(z_1)$ we get $+$, and if we evaluate $-\chi_e(z_2)$ we get $-$. Hence the two signs associated to \mathcal{L} are $(+, -)$.

We can now compute the correspondence:

$$\begin{aligned} \epsilon(e, \mathcal{L}(\tilde{\epsilon}_2)) &= (+, +) \\ \epsilon(e, \mathcal{L}(\tilde{\epsilon}_3)) &= (-, +) \\ \epsilon(e, \mathcal{L}(1)) &= (-, -) \\ \epsilon(e, \mathcal{L}(\tilde{\epsilon}_1)) &= (+, -) \end{aligned}$$

6.6. Computation of the signs $\epsilon(\sigma, \mathcal{L})$. We first write the well-known action of the Weyl group on roots and coroots:

$$\begin{aligned} s_i \alpha_j &= \alpha_j - C_{j,i} \alpha_i, \\ s_i \check{\alpha}_j &= \check{\alpha}_j - C_{i,j} \check{\alpha}_i \end{aligned}$$

In the first formula the matrix that is involved is the *transpose* of the Cartan matrix $(C_{i,j})$. In the second, using coroots, the matrix that appears is the usual Cartan matrix. Recall that each simple root α_j gives rise to a Lie group homomorphism $\Phi_{\alpha_j} : \mathrm{SL}_2(\mathbb{R}) \rightarrow G$ corresponding to an injection of $\mathfrak{sl}_2(\mathbb{R})$ into the Lie algebra. The elements h_{α_j} correspond to the $\begin{pmatrix} 1 & 0 \\ 0 & -1 \end{pmatrix}$ in the copy of $\mathfrak{sl}_2(\mathbb{R})$ associated to α_j and corresponds to the coroot $\check{\alpha}_j$. The reason to introduce the h_{α_j} is that we then can write $\Phi_{\alpha_j}\left(\begin{pmatrix} -1 & 0 \\ 0 & -1 \end{pmatrix}\right) = \exp(\pi\sqrt{-1}h_{\alpha_j})$. From the correspondence between $\check{\alpha}_i$ and h_{α_i} , we have

$$(6.1) \quad s_i h_{\alpha_j} = h_{\alpha_j} - C_{j,i} h_{\alpha_i}.$$

The following will also be useful:

$$\sigma s_i \Delta^+ \cap \Delta^- = \sigma \Delta^+ \cap \Delta^- \cup \{-\sigma \alpha_i\}$$

which corresponds to

$$(6.2) \quad \sigma s_i \mathfrak{n} \cap \mathfrak{n}^* = \sigma \mathfrak{n} \cap \mathfrak{n}^* \oplus \mathbb{R} X_{-\sigma \alpha_i}.$$

By applying the inverse of σs_i we obtain

$$\mathfrak{n} \cap s_i \sigma^{-1} \mathfrak{n}^* = s_i \mathfrak{n} \cap \sigma^{-1} \mathfrak{n}^* \oplus \mathbb{R} X_{\alpha_i}.$$

This version was used in [8] but the s_i on the right hand side of the equation above was inadvertently left out in the Proof of Proposition 5.1 in [8]. We then can correct the simple proof of Proposition 5.1 in [8]:

Proposition 6.1. *For $\epsilon(\sigma, \mathcal{L}) = (\tilde{\epsilon}_1, \dots, \tilde{\epsilon}_l)$, we have $\epsilon(s_i \sigma, \mathcal{L}) = (\tilde{\epsilon}'_1, \dots, \tilde{\epsilon}'_l)$ where $\tilde{\epsilon}'_j = \tilde{\epsilon}_j \tilde{\epsilon}_i^{C_{i,j}}$.*

Proof. We set $\sigma = w^{-1}$ and start with (6.2): $\sigma s_i \mathfrak{n} \cap \mathfrak{n}^* = \sigma \mathfrak{n} \cap \mathfrak{n}^* \oplus \mathbb{R} X_{-\sigma \alpha_i}$ where X_{α_i} is a root vector associated to the simple root α_i . Therefore

$$(6.3) \quad \bigwedge^{l(w)+1} \sigma s_i \mathfrak{n} \cap \mathfrak{n}^* = \bigwedge^{l(w)} (\sigma \mathfrak{n} \cap \mathfrak{n}^*) \wedge \mathbb{R} X_{-\sigma \alpha_i}$$

In terms of characters of T we then have : $\tilde{\epsilon}'_j = -\chi_{s_i w}(\exp(\pi \sqrt{-1} w s_i h_{\alpha_j}))$ (by definition). Using (6.3) this becomes $-(\chi_w \chi_{-\sigma \alpha_i})(\exp(\pi \sqrt{-1} h_{\sigma \alpha_j}))$. We evaluate $-\chi_w(\exp(\pi \sqrt{-1} \sigma s_i h_{\alpha_j}))$ and using (6.1), this becomes

$$\begin{aligned} & -\chi_w(\exp(\pi \sqrt{-1} \sigma h_{\alpha_j}))(\chi_w(\exp(\pi \sqrt{-1} \sigma h_{\alpha_i}))^{C_{i,j}} \\ &= -\chi_w(\exp(\pi \sqrt{-1} \sigma h_{\alpha_j}))(-1)^{C_{i,j}}(-\chi_w(\exp(\pi \sqrt{-1} \sigma h_{\alpha_i}))^{C_{i,j}} \\ &= \tilde{\epsilon}_j \tilde{\epsilon}_i^{C_{i,j}} (-1)^{C_{i,j}}. \end{aligned}$$

Now we consider the additional factor $\chi_{-w \alpha_i}(\exp(\pi \sqrt{-1} \sigma s_i h_{\alpha_j}))$. This is just

$$\exp(\pi \sqrt{-1} \langle -\sigma \alpha_i; \sigma h_{\alpha_j} \rangle) = \exp(\pi \sqrt{-1} \langle -\alpha_i; h_{\alpha_j} \rangle) = (-1)^{C_{i,j}}.$$

Hence we obtain $\tilde{\epsilon}_j \rightarrow \tilde{\epsilon}_j \tilde{\epsilon}_i^{C_{i,j}}$. \square

Example 6.3. In the case of $\mathrm{SL}_3(\mathbb{R})$ we have $\epsilon(\sigma, \mathcal{L}) = (\tilde{\epsilon}_1, \tilde{\epsilon}_2)$ then $\epsilon(s_1 \sigma, \mathcal{L}) = (\tilde{\epsilon}_1, \tilde{\epsilon}_1 \tilde{\epsilon}_2)$ and $\epsilon(s_2 \sigma, \mathcal{L}) = (\tilde{\epsilon}_1 \tilde{\epsilon}_2, \tilde{\epsilon}_1)$.

In the general case of $\mathrm{SL}_n(\mathbb{R})$, this has a very simple description and defines an action of the Weyl group on a set of signs,

$$(\tilde{\epsilon}_1, \dots, \tilde{\epsilon}_{j-1}, \tilde{\epsilon}_j, \tilde{\epsilon}_{j+1}, \dots, \tilde{\epsilon}_{n-1}) \xrightarrow{s_j} (\tilde{\epsilon}_1, \dots, \tilde{\epsilon}_j \tilde{\epsilon}_{j-1}, \tilde{\epsilon}_j, \tilde{\epsilon}_j \tilde{\epsilon}_{j+1}, \dots, \tilde{\epsilon}_{n-1}).$$

Example 6.4. In the case of $\mathrm{Gr}(2, 4)$ we consider the cells $\sigma \in \{e, s_2, s_3 s_2\}$ which correspond to a copy of $\mathbb{R}P^2$ (as in Remark 4.2 item (ii)). We compute the structure of the line bundles $\mathcal{E}(j)$ defined in (4.4) and associated to the vector bundles $\mathcal{V}(j)$. As in Remark 4.2 the fibers of $\mathcal{V}(j)$ correspond to the cells of $\mathbb{R}P^2$.

We start with the Toda sign $\epsilon(\sigma, \mathcal{L}(1)) = (-, -, -)$ and apply these Weyl group elements σ to it. We obtain

$$\begin{array}{ccccc} \epsilon(e, \mathcal{L}(1)) & \xrightarrow{s_2} & \epsilon(s_2, \mathcal{L}(1)) & \xrightarrow{s_3} & \epsilon(s_3 s_2, \mathcal{L}(1)) \\ \updownarrow & & \updownarrow & & \updownarrow \\ (-, -, -) & \xrightarrow{s_2} & (+, -, +) & \xrightarrow{s_3} & (+, -, +) \end{array}$$

The fact that a $+$ appears in the first spot in the second and third of the Toda signs discussed means that in the incidence graph of $\mathrm{Gr}(2, 4)$, *twisted* coefficients will have to be used along the columns i.e. along $Y(3) \cong \mathrm{Gr}(1, 2)$ and $Y(4) \cong \mathrm{Gr}(1, 3)$.

Remark 6.3. The general case of $\mathrm{Gr}(k, n)$ is similar. There are two local systems \mathcal{L} to consider, that is, the constant one and a second twisted local system. The signs that correspond are $\epsilon(\sigma, \mathcal{L}) = (\tilde{\epsilon}_1, \dots, \tilde{\epsilon}_n)$ where $\tilde{\epsilon}_i = -$ for all i in the constant coefficient case, and $\tilde{\epsilon}_i = -$ for all $i \neq k$, $\tilde{\epsilon}_k = +$ for the twisted case. We now consider the signs obtained by applying the elements s_k, s_{k+1}, \dots . For convenience we can regard $\mathrm{Gr}(k, n)$ as embedded inside $\mathrm{Gr}(k, n+1)$. This simply adds one more $-$ at the end e.g. $\epsilon(\sigma, \mathcal{L}(1)) = (-, -, -, -)$ instead of $(-, -, -)$.

Note that in the constant coefficient case when s_{k+2r} is applied, a new $+$ sign appears in the $k+2r+1$ spot *for the first time*. All the preceding signs $s_m \cdots s_{k+1} s_k \epsilon(\sigma, \mathcal{L}(1)) = (\tilde{\epsilon}'_1, \tilde{\epsilon}'_2, \dots, \tilde{\epsilon}'_n)$ with $m \leq k+2r-1$, are such that $\tilde{\epsilon}'_{k+2r+1} = -$. When elements in $\mathcal{S}_{k+2r}^{(k-1)} \subset \langle s_1, \dots, s_{k+2r-1} \rangle$ are applied in this constant coefficient case, the $+$ sign in the $k+2r+1$ spot remains unchanged by the definition of the Weyl group action on signs.

In the twisted case when s_{k+2r-1} is applied, a new $+$ sign appears in the $k+2r$ spot. When elements in $\mathcal{S}_{k+2r-1}^{(k-1)} \subset \langle s_1, \dots, s_{k+2r-1} \rangle$ this $+$ sign remains unchanged.

Example 6.5. For example, we have for the local system $\mathcal{L}(1)$,

$$\begin{array}{ccccc} \epsilon(e, \mathcal{L}(1)) & \longrightarrow & \epsilon(s_2, \mathcal{L}(1)) & \longrightarrow & \epsilon(s_3 s_2, \mathcal{L}(1)) \\ \updownarrow & & \updownarrow & & \updownarrow \\ (-, -, -, -) & \xrightarrow{s_2} & (+, -, +, -) & \xrightarrow{s_3} & (+, -, +, -) \end{array}$$

and for \mathcal{L}^* ,

$$\begin{array}{ccccc} \epsilon(e, \mathcal{L}^*) & \longrightarrow & \epsilon(s_2, \mathcal{L}^*) & \longrightarrow & \epsilon(s_3 s_2, \mathcal{L}^*) \\ \updownarrow & & \updownarrow & & \updownarrow \\ (-, +, -, -) & \xrightarrow{s_2} & (-, +, -, -) & \xrightarrow{s_3} & (-, -, -, +) \end{array}$$

Remark 6.4. The general structure of all graphs involved can be loosely described by a diagram (see Example 6.1):

$$\begin{array}{ccccccc} j = k & & j = k + 1 & & j = k + 2 & & j = k + 3 \\ \circ & \xrightarrow{s_k} & \circ & \xrightarrow{s_{k+1}} & \circ & \xrightarrow{s_{k+2}} & \circ \\ \downarrow & & \downarrow & & \downarrow & & \downarrow \\ \mathcal{S}_{k-1}^{(k-1)} & & \mathcal{S}_k^{(k-1)} & & \mathcal{S}_{k+1}^{(k-1)} & & \mathcal{S}_{k+2}^{(k-1)} \\ \downarrow & & \downarrow & & \downarrow & & \downarrow \\ \{e\} & & \langle s_1, \dots, s_{k-1} \rangle & & \langle s_1, \dots, s_k \rangle & & \langle s_1, \dots, s_{k+1} \rangle \end{array}$$

Here \circ may correspond to $(\sigma_1, \dots, \sigma_k) \rightsquigarrow E_{\sigma_1} \wedge \dots \wedge E_{\sigma_k}$ so that edges \Rightarrow are defined by agreement of eigenvalues of the matrix $h(\pm)$ on $\wedge^k V(E_1, \dots, E_n)$. They can also be replaced with l tuples $\epsilon(\sigma, \mathcal{L}) = (\tilde{\epsilon}_1, \dots, \tilde{\epsilon}_l)$, and the edges \Rightarrow then correspond to non-zero co-boundaries.

We then note that for the two possible types of graphs being considered:

- (i) The columns associated to j (e.g. to $Y(j)$) depend only on the simple reflections $\{s_1, \dots, s_{j-2}\}$
- (ii) Any edges \Rightarrow involve vertices in adjacent columns.
- (iii) Any edge \Rightarrow between vertices labeled $j, j+1$ along the top column (corresponding to the incidence graph of $\mathbb{R}P^{n-k}$) induces edges \Rightarrow connecting the cells in one column (vertices in $\mathcal{G}(k-1, j-1)$) to the cells in the next (corresponding vertices in $\mathcal{G}(k-1, j)$).

Note that in the case of the the graph $\mathcal{G}(k, n)$ (ii) is true by definition. We then briefly discuss (ii) in the case of the incidence graph of $\text{Gr}(k, n)$. Using Definition 3.3 (d) of [8] which gives \Rightarrow , it is known that whenever there is a coboundary \Rightarrow relating σ and σ' , the corresponding signs must agree: $\epsilon(\sigma, \mathcal{L}) = \epsilon(\sigma', \mathcal{L})$. We consider first the case in which we start with $\tilde{\epsilon}_i = -$ for all i . We note (Remark 6.3) that when s_j is applied to this Toda sign, either there is a $+$ in the j th spot or a new $+$ sign appears in the $j+1$ spot *for the first time* and this sign remains along the column since it is unaffected by the action of s_1, \dots, s_{j-2} . Therefore the \Rightarrow can only involve adjacent $\mathcal{G}_j^{(k-1)}$ i.e. the cells associated to $Y(j)$ and $Y(j+1)$. The argument in the other case is similar. This establishes (ii).

Again (iii) is true in the case of $\mathcal{G}(k, n)$ by definition. In the case of the incidence graph of $\text{Gr}(k, n)$ the connection between vertices in the top row labeled $j, j+1$ is given by the j th simple reflection. In terms of signs $\epsilon(\sigma, \mathcal{L})$ it then depends only on the j th sign. However this sign doesn't change along the j th column (along $Y(j)$). Therefore an edge \Rightarrow on the top row extends to the entire column.

6.7. Proof of Theorem. The two distinguished n -tuples of signs are encoded in two diagonal matrices $h(-)$ and $h(+)$ acting on $V(E_1, \dots, E_n)$ and all the spaces $\wedge^k V(E_1, \dots, E_n)$. An edge \Rightarrow corresponds to the agreement of eigenvalues. The main theorem 1.1 can be restated as follows:

Theorem 6.2. *The graph $\mathcal{G}(k, n)$ of $h(\pm)$ acting on $\bigwedge^k V(E_1, \dots, E_n)$ agrees with the incidence graph of $\text{Gr}(k, n)$. More precisely, we have the following:*

- (a) *If k is odd and the choice of signs corresponds to the matrix $h(-)$ (respectively $h(+)$) then $\mathcal{G}(k, n)$ agrees with the incidence graph with constant coefficients (respectively non trivial local coefficients).*
- (b) *If k is even and the choice of signs corresponds to the matrix $h(+)$ (respectively $h(-)$) then $\mathcal{G}(k, n)$ agrees with the incidence graph with constant coefficients (respectively non trivial local coefficients).*

Proof. We proceed by induction on k . We then assume the statements (a) and (b) of the Theorem for smaller values of k , the cases $k = 1$ are already clear.

There are several similar cases which are handled in identical manner within an inductive proof. We then focus, for simplicity of exposition, on (b) and the case when k is even and consider cohomology of $\text{Gr}(k, n)$ with constant coefficients. Hence we consider the KP sign $(+, +, -, -, +, \dots)$ corresponding to $h(+)$ as in Lemma 5.3. This is the sign that guarantees that the top row of the graph of the action of $h(\pm)$ on $\bigwedge^k V(E_1, \dots, E_n)$ is the incidence graph of $\mathbb{R}P^{n-k}$ with constant coefficients (Lemma 5.3).

The two graphs that we are comparing have the same set of vertices and by Remark 6.4 ii) edges involve adjacent columns only. We need to show that there is a non-zero co-boundary in the incidence graph (given in terms of Toda signs), that is, $\sigma \Rightarrow s_i \sigma$ appears, exactly when in the graph $\mathcal{G}(k, n)$ (defined in terms of the KP signs, i.e. edges crossing $\tau_k = 0$) there is a corresponding edge.

We start with the decomposition $\text{Gr}(k, n) = Y(k) \cup Y(k+1) \cup \dots \cup Y(j) \dots$ and as in the example of $\text{Gr}(2, 4)$ in subsection 6.1 observe that, by induction, pieces of the incidence graph are already available and agree with corresponding pieces of the graph $\mathcal{G}(k, n)$. We can then assume that we know the graphs corresponding to the $Y(j) \rightsquigarrow \text{Gr}(k-1, j-1), j = k, k+1, \dots$. We also know the top row, i.e the subgraph associated to a copy of $\mathbb{R}P^{n-k}$.

We now deal with issue (a) brought up in the $\text{Gr}(2, 4)$ example in subsection 6.1. The spaces $Y(j)$, have some *additional structure of a vector bundle* $\mathcal{V}(j)$ over $\text{Gr}(k-1, j-1)$ (subsection 4.2). Then the line bundle $\mathcal{E}(j)$ defined in (4.4), $\mathcal{E}(j) := \bigwedge^{j-k} \mathcal{V}(j)$, determines the local system that we need over $Y(j)$. It turns out that we need to consider the incidence graphs of the $Y(j) \rightsquigarrow \text{Gr}(1, j-1), j = 2, 3, \dots, n$ with *twisted* coefficients. This follows by noting that the first $j-1$ signs of $\epsilon(\sigma, \mathcal{L}(1))$ on the top row always include one $+$.

Applying $\sigma = s_k, s_{k+1}, s_{k+2}, s_{k+3}, \dots$ as occurring in Proposition 4.1 to the Toda sign $(-, \dots, -)$ we have in the first step

$$\{\tilde{\epsilon}_i = - (\forall i)\} \xrightarrow{s_j} \{\tilde{\epsilon}'_{j-1} = \tilde{\epsilon}'_{j+1} = +, \tilde{\epsilon}'_i = \tilde{\epsilon}_i (i \neq j \pm 1)\}$$

Note here that the $+$ sign in the $(j-1)$ -th place does not disappear when additional simple reflections are applied. Hence along the columns we have twisted coefficients. All that remains is to show that the arrows \Rightarrow along the top row are “constant” along the columns between cells in $Y(j)$ and cells in $Y(j+1)$ related by s_j . This is Remark 6.4 (ii), (iii). \square

Remark 6.5. Recall that each space $Y(j)$ corresponds to a Grasmannian:

$$Y(j) \rightsquigarrow \text{Gr}(k-1, j-1), \quad \text{for } j = k, k+1, \dots, n.$$

For the purpose of describing the incidence graphs it is harmless to replace $\text{Gr}(k-1, j-1)$ instead of $Y(j)$. In order to keep track of the two possible incidence graphs on $\text{Gr}(k-1, j-1)$ (constant and twisted coefficients) we write $\mathcal{G}(k-1, j-1)^*$ when twisted coefficients are involved. This way $\mathcal{G}(k-1, j-1)$ or $\mathcal{G}(k-1, j-1)^*$ corresponds to $Y(j)$ at the level of incidence graphs.

We use this shorthand notation to indicate the structure of the incidence graphs in Theorem 6.2: $\mathcal{G}(k-1, r) \rightarrow \mathcal{G}(k-1, r+1)$ or $\mathcal{G}(k-1, r) \Rightarrow \mathcal{G}(k-1, r+1)$ or $\mathcal{G}(k-1, r)^* \rightarrow \mathcal{G}(k-1, r+1)^*$ or

$\mathcal{G}(k-1, r)^* \Rightarrow \mathcal{G}(k-1, r+1)^*$. For example the incidence graph of $\text{Gr}(4, 9)$ with local coefficients becomes

$$\mathcal{G}(3, 3) \Rightarrow \mathcal{G}(3, 4) \rightarrow \mathcal{G}(3, 5) \Rightarrow \mathcal{G}(3, 6) \rightarrow \mathcal{G}(3, 7) \Rightarrow \mathcal{G}(3, 8).$$

With constant coefficients this is indicated as

$$\mathcal{G}(3, 3)^* \rightarrow \mathcal{G}(3, 4)^* \Rightarrow \mathcal{G}(3, 5)^* \rightarrow \mathcal{G}(3, 6)^* \Rightarrow \mathcal{G}(3, 7)^* \rightarrow \mathcal{G}(3, 8)^*.$$

This can be further decomposed. For example $\text{Gr}(3, 4)^*$ can be described as: $\mathcal{G}(2, 2) \Rightarrow \mathcal{G}(2, 3)$. Then $\mathcal{G}(2, 3)$ corresponds to $\mathcal{G}(1, 1)^* \rightarrow \mathcal{G}(1, 2)^*$.

With this notation, Theorem 6.2 can be restated as follows:

Theorem 6.3. *We have the following.*

(i) *The incidence graph of $\text{Gr}(k, n)$ with constant coefficients is:*

$$\mathcal{G}(k-1, k-1)^* \rightarrow \mathcal{G}(k-1, k)^* \Rightarrow \mathcal{G}(k-1, k+1)^* \rightarrow \cdots \mathcal{G}(k-1, n-1)^*.$$

(ii) *The incidence graph of $\text{Gr}(k, n)$ with twisted coefficients is:*

$$\mathcal{G}(k-1, k-1) \Rightarrow \mathcal{G}(k-1, k) \rightarrow \mathcal{G}(k-1, k+1) \Rightarrow \cdots \mathcal{G}(k-1, n-1).$$

This theorem leads to the well-known statement on the orientability.

Corollary 6.4. *The real Grassmannian $\text{Gr}(k, n)$ is orientable if and only if n is even.*

Proof. We first show that if n is even then $\text{Gr}(k, n)$ is orientable. We proceed by induction on $n = 2j$. The case of $j = 1$ corresponds to $\text{Gr}(1, 2)$ which is a circle.

Using Theorem 6.3 we can write the incidence graph of $\text{Gr}(k, n)$ as

$$\mathcal{G}(k-1, k-1)^* \rightarrow \mathcal{G}(k-1, k)^* \Rightarrow \cdots \mathcal{G}(k-1, n-1)^*.$$

At the same time the incidence graph of $\text{Gr}(k-1, n-1)$ with twisted coefficients can be written as:

$$\mathcal{G}(k-2, k-2) \Rightarrow \mathcal{G}(k-2, k-1)^* \rightarrow \cdots \mathcal{G}(k-2, n-2).$$

Therefore the top element (determining orientability) corresponds to the top vertex of the graph $\mathcal{G}(k-2, n-2)$. Since n is even, by induction the top vertex from the graph $\mathcal{G}(k-2, n-2)$ contributes to cohomology and $\text{Gr}(k, n)$ is orientable.

In the same way, one can easily see that if n is odd then $\text{Gr}(k, n)$ is not orientable. Note that we have $\text{Gr}(1, 3) \cong \text{Gr}(2, 3) \cong \mathbb{R}P^2$. \square

Remark 6.6. The homology group of the Grassmannian $\text{Gr}(k, n)$ can be found by Poincaré duality, if the variety is orientable ($n = \text{even}$), i.e.

$$H_j(\text{Gr}(k, n), \mathbb{Z}) = H^{k(n-k)-j}(\text{Gr}(k, n), \mathbb{Z}) \quad \text{if } n = \text{even}.$$

In the non-orientable case ($n = \text{odd}$), the homology group can be obtained using the incidence graph of $\text{Gr}(k, n)$ with twisted coefficients \mathcal{L}^* , that is, the graph $\mathcal{G}(k, n)^*$. This is a consequence of a generalization of Poincaré duality (IX.4 and VI.3 in [16], and it is sometimes called the Poincaré-Lefschetz duality) and that the so-called orientation sheaf (V.3 in [16]) $\mathcal{O}r_X$ with $X = \text{Gr}(k, n)$, corresponds, in the non-orientable cases, to the twisted coefficients \mathcal{L}^* .

For example, consider $\text{Gr}(2, 5)$. The graph $\mathcal{G}(2, 5)^*$ is given by

$$\begin{array}{ccccccc}
 (1, 2) & \Rightarrow & (1, 3) & \rightarrow & (1, 4) & \Rightarrow & (1, 5) \\
 & & \downarrow & & \downarrow & & \downarrow \\
 & & (2, 3) & \rightarrow & (2, 4) & \Rightarrow & (2, 5) \\
 & & & & \downarrow & & \downarrow \\
 & & & & (3, 4) & \Rightarrow & (3, 5) \\
 & & & & & & \downarrow \\
 & & & & & & (4, 5)
 \end{array}$$

which is obtained by taking the action of $h(-)$ instead of $h(+)$ for the constant coefficients. The cohomology obtained from this graph is

$$\begin{aligned}
 H^0(\text{Gr}(2, 5), \mathcal{L}^*) &= 0, & H^4(\text{Gr}(2, 5), \mathcal{L}^*) &= \mathbb{Z}_2, \\
 H^1(\text{Gr}(2, 5), \mathcal{L}^*) &= \mathbb{Z}_2, & H^5(\text{Gr}(2, 5), \mathcal{L}^*) &= \mathbb{Z}_2, \\
 H^2(\text{Gr}(2, 5), \mathcal{L}^*) &= \mathbb{Z}, & H^6(\text{Gr}(2, 5), \mathcal{L}^*) &= \mathbb{Z}. \\
 H^3(\text{Gr}(2, 5), \mathcal{L}^*) &= \mathbb{Z}_2,
 \end{aligned}$$

Then the homology group $H_*(\text{Gr}(2, 5), \mathbb{Z})$ can be obtained as $H_j(\text{Gr}(2, 5), \mathbb{Z}) = H^{6-j}(\text{Gr}(2, 5), \mathcal{L}^*)$. In general, we have

$$H_j(\text{Gr}(k, n), \mathbb{Z}) = H^{k(n-k)-j}(\text{Gr}(k, n), \mathcal{L}^*) \quad \text{if } n = \text{odd}.$$

The homology groups of $\text{Gr}(k, n)$ have been computed explicitly for lower dimensional examples in [17] (see Table IV in this reference).

7. THE POINCARÉ POLYNOMIALS

From the incidence graphs $\mathcal{G}(k, n)$ (trivial coefficients) and $\mathcal{G}(k, n)^*$ (twisted coefficients) constructed in the previous section, we here consider the Poincaré polynomials $P_{(k, n)}(t)$ and $P_{(k, n)}^*(t)$ for those graphs. Since our formulas for the Poincaré polynomials will be expressed in terms of q -analog of the binomial coefficients $\begin{bmatrix} m \\ j \end{bmatrix}_q$, let us first list some of their properties:

- (q1) Pascal's triangle formula: $\begin{bmatrix} m \\ j \end{bmatrix}_q = \begin{bmatrix} m-1 \\ j \end{bmatrix}_q + q^{m-j} \begin{bmatrix} m-1 \\ j-1 \end{bmatrix}_q$.
- (q2) The polynomial $\begin{bmatrix} m \\ j \end{bmatrix}_q$ is of degree $j(m-j)$.
- (q3) Poincaré duality: $\begin{bmatrix} m \\ j \end{bmatrix}_q = \sum_{j=0}^{j(m-j)} n_j q^j = \sum_{j=0}^{j(m-j)} n_j q^{j(m-j)-j} = q^{j(m-j)} \begin{bmatrix} m \\ j \end{bmatrix}_{q^{-1}}$.

7.1. The polynomials $P_{(k, n)}^*(t)$. We first note the following Lemma of the recursion relations of the polynomials.

Lemma 7.1. *The polynomials $P_{(k, n)}^*(t)$ satisfy*

- (a*) $P_{(2j, 2m+1)}^*(t) = P_{(2j, 2m-1)}^*(t) + t^{4(m-j)+2} P_{(2j-2, 2m-1)}^*(t),$
- (b*) $P_{(2j+1, 2m)}^*(t) = P_{(2j+1, 2m-2)}^*(t) + t^{4(m-j)-2} P_{(2j-1, 2m-2)}^*(t),$
- (c*) $P_{(2j, 2m)}^*(t) = P_{(2j, 2m-1)}^*(t) + t^{2(m-j)} P_{(2j-1, 2m-1)}^*(t),$
- (d*) $P_{(2j+1, 2m+1)}^*(t) = P_{(2j+1, 2m)}^*(t) + t^{2(m-j)} P_{(2j, 2m)}^*(t).$

Before giving the proof of this Lemma, notice that this already gives the following explicit formulas.

Proposition 7.2. *The Poincaré polynomials $P_{(k,n)}^*(t)$ have the following explicit form for $(k, n) = (2j+1, 2m)$ or $(k, n) = (2j, 2m+1)$:*

$$\begin{aligned} \text{(i)* } P_{(2j+1, 2m)}^*(t) &= 0, \\ \text{(ii)* } P_{(2j, 2m+1)}^*(t) &= t^{2j} \begin{bmatrix} m \\ j \end{bmatrix}_{t^4}. \end{aligned}$$

Proof. We prove (i*) by induction on m . For $m = 1$, we have the case of $\text{Gr}(1, 2)$ with local coefficients and $P_{(1,2)}^*(t) = 0$. Then by induction using (a) in Lemma 7.1, we obtain (i*).

To prove (ii*), we also use induction on m . Again the case of $m = 1$ is simple. We first note that the relation (a) in Lemma 7.1 gives

$$\begin{aligned} P_{(2j, 2m+1)}^* &= P_{(2j, 2m-1)}^*(t) + t^{4(m-j)+2} P_{(2j-2, 2m-1)}^*(t) \\ &= t^{2j} \begin{bmatrix} m-1 \\ j \end{bmatrix}_{t^4} + t^{4(m-j)+2} t^{2(j-1)} \begin{bmatrix} m-1 \\ j-1 \end{bmatrix}_{t^4}. \end{aligned}$$

We then use the property (q1) above to obtain $t^{2j} \left(\begin{bmatrix} m-1 \\ j \end{bmatrix}_{t^4} + t^{4(m-j)} \begin{bmatrix} m-1 \\ j-1 \end{bmatrix}_{t^4} \right) = t^{2j} \begin{bmatrix} m \\ j \end{bmatrix}_{t^4}$. \square

We now prove Lemma 7.1:

Proof.

(a*) The incidence graph $\mathcal{G}(2j, 2m+1)^*$ (twisted coefficients) has the following description corresponding to the decomposition in terms of the spaces $Y(j)$ (Theorem 6.3).

$$\begin{aligned} \{ \mathcal{G}(2j-1, 2j-1) \Rightarrow \mathcal{G}(2j-1, 2j) \rightarrow \cdots \rightarrow \mathcal{G}(2j-1, 2m-3) \Rightarrow \mathcal{G}(2j-1, 2m-2) \} \\ \rightarrow \mathcal{G}(2j-1, 2m-1) \Rightarrow \mathcal{G}(2j-1, 2m). \end{aligned}$$

The portion inside of $\{\cdots\}$ corresponds to $\mathcal{G}(2j, 2m-1)^*$. The lowest degree of terms in the last graph denoted by $\mathcal{G}(2j-1, 2m)$ is $2m - (2j-1) = 2(m-j) + 1$. The incidence graph $\mathcal{G}(2j-1, 2m)$ is in turn given by

$$\begin{aligned} \{ \mathcal{G}(2j-2, 2j-2)^* \rightarrow \mathcal{G}(2j-2, 2j-1)^* \Rightarrow \cdots \rightarrow \mathcal{G}(2j-2, 2m-3)^* \Rightarrow \mathcal{G}(2j-2, 2m-2) \}^* \\ \rightarrow \mathcal{G}(2j-2, 2m-1)^*. \end{aligned}$$

Here the part $\{\cdots\}$ is $\mathcal{G}(2j-1, 2m-1)$. The lowest degree of terms associated to the graph indicated by $\mathcal{G}(2j-2, 2m-1)^*$ is $2m-1 - (2j-2) = 2(m-j) + 1$. Altogether, taking into account the lowest degree in $\mathcal{G}(2j-1, 2m)$, there is a degree shift of: $2(m-j) + 1 + 2(m-j) + 1 = 4(m-j) + 2$. Thus the incidence graph can be represented as follows:

$$\begin{array}{ccc} \mathcal{G}(2j, 2m-1)^* & \rightarrow & \mathcal{G}(2j-1, 2m-1) \\ & \Downarrow & \\ & \mathcal{G}(2j-1, 2m-1) & \rightarrow \mathcal{G}(2j-2, 2m-1)^* \end{array}$$

The vertical \Downarrow causes the cancellation of all cohomology associated to $\text{Gr}(2j-1, 2m-1)$. Also the horizontal \rightarrow correspond to multiplication by zero. We obtain $P_{(2j, 2m+1)}^*(t) = P_{(2j, 2m-1)}^*(t) + t^N P_{(2j-2, 2m-1)}^*(t)$ and N is the dimension shift which was already computed and is given by $4(m-j) + 2$.

(b*) The incidence graph $\mathcal{G}(2j+1, 2m)^*$ (twisted coefficients) has the following description (Theorem 6.3).

$$\begin{aligned} \{ \mathcal{G}(2j, 2j) \Rightarrow \mathcal{G}(2j, 2j+1) \rightarrow \cdots \rightarrow \mathcal{G}(2j, 2m-4) \Rightarrow \mathcal{G}(2j, 2m-3) \} \\ \rightarrow \mathcal{G}(2j, 2m-2) \Rightarrow \mathcal{G}(2j, 2m-1). \end{aligned}$$

The part $\{\dots\}$ corresponds to $\mathcal{G}(2j+1, 2m-2)^*$. The lowest degree of the terms in the chain complex corresponding to $\mathcal{G}(2j, 2m-1)$ is $2m-1-2j = 2(m-j)-1$. The incidence graph $\mathcal{G}(2j, 2m-1)$ is in turn given by

$$\begin{aligned} & \{\mathcal{G}(2j-1, 2j-1)^* \Rightarrow \mathcal{G}(2j-1, 2j)^* \rightarrow \dots \Rightarrow \mathcal{G}(2j-1, 2m-4)^* \rightarrow \mathcal{G}(2j-1, 2m-3)^*\} \\ & \Rightarrow \mathcal{G}(2j-1, 2m-2)^*. \end{aligned}$$

The part $\{\dots\}$ corresponds to $\mathcal{G}(2j, 2m-1)$. The lowest degree of the terms in $\mathcal{G}(2j-1, 2m-2)^*$ is $2m-2-2j+1 = 2(m-j)-1$. Altogether we have a degree shift of $2(m-j)-1+2(m-j)-1 = 4(m-j)-2$.

We thus have a graph that can be indicated by the diagram:

$$\begin{array}{ccc} \mathcal{G}(2j+1, 2m-2)^* & \rightarrow & \mathcal{G}(2j, 2m-1) \\ & \Downarrow & \\ & \mathcal{G}(2j, 2m-1) & \rightarrow \mathcal{G}(2j-1, 2m-2)^* \end{array}.$$

This gives the recursive formula. The value of r is $4(m-j)-2$.

(c*) The incidence graph $\mathcal{G}(2j, 2m)^*$ has the following description:

$$\begin{aligned} & \{\mathcal{G}(2j-1, 2j-1) \Rightarrow \mathcal{G}(2j-1, 2j) \rightarrow \dots \rightarrow \mathcal{G}(2j-1, 2m-3) \Rightarrow \mathcal{G}(2j-1, 2m-2)\} \\ & \rightarrow \mathcal{G}(2j-1, 2m-1). \end{aligned}$$

This then can be represented as:

$$\mathcal{G}(2j, 2m-1)^* \rightarrow \mathcal{G}(2j-1, 2m-1).$$

This gives rise to (c*).

(d*) The incidence graph $\mathcal{G}(2j+1, 2m+1)^*$ has the following description:

$$\begin{aligned} & \{\mathcal{G}(2j, 2j) \Rightarrow \mathcal{G}(2j, 2j+1) \rightarrow \dots \rightarrow \mathcal{G}(2j, 2m-2) \Rightarrow \mathcal{G}(2j, 2m-1)\} \\ & \rightarrow \mathcal{G}(2j, 2m). \end{aligned}$$

This then can be represented as

$$\mathcal{G}(2j+1, 2m)^* \rightarrow \mathcal{G}(2j, 2m).$$

From here (d*) follows.

This completes the proof. \square

Similarly, we can derive the formulas for $P_{(2j, 2m)}^*$ and $P_{(2j+1, 2m+1)}^*(t)$.

Proposition 7.3. *We have*

$$\begin{aligned} \text{(iii*) } P_{(2j+1, 2m+1)}^*(t) &= t^{2(m-j)} \left[\begin{matrix} m \\ j \end{matrix} \right]_{t^4}, \\ \text{(iv*) } P_{(2j, 2m)}^*(t) &= (t^{2j} + t^{2(m-j)}) \left[\begin{matrix} m \\ j \end{matrix} \right]_{t^4}. \end{aligned}$$

7.2. The polynomials $P_{(k,n)}(t)$. Let us note the following Lemma for the additional recursion relations of the Poincaré polynomials.

Lemma 7.4. *The polynomials $P_{(k,n)}(t)$ satisfy*

- (a) $P_{(2j, 2m+1)}(t) = P_{(2j, 2m)}(t) + t^{2(m-j)+1} P_{(2j-1, 2m)}^*(t),$
- (b) $P_{(2j+1, 2m)}(t) = P_{(2j+1, 2m-1)}(t) + t^{2(m-j)-1} P_{(2j, 2m-1)}^*(t),$
- (c) $P_{(2j, 2m)}(t) = P_{(2j, 2(m-1))}(t) + t^{4(m-j)} P_{(2j-2, 2(m-1))}(t),$
- (d) $P_{(2j+1, 2m+1)}(t) = P_{(2j+1, 2m-1)}(t) + t^{4(m-j)} P_{(2j-1, 2m-1)}(t).$

Before going through the proof, notice that this gives rise to explicit formulas for the polynomials $P_{(k,n)}(t)$.

Theorem 7.5. *We have the explicit form of the Poincaré polynomials $P_{(k,n)}(t)$,*

$$\begin{aligned} \text{(i)} \quad & P_{(2j,2m)}(t) = P_{(2j,2m+1)}(t) = P_{(2j+1,2m+1)}(t) = \begin{bmatrix} m \\ j \end{bmatrix}_{t^4} \\ \text{(ii)} \quad & P_{(2j+1,2m)}(t) = (1 + t^{2m-1}) \begin{bmatrix} m-1 \\ j \end{bmatrix}_{t^4} \end{aligned}$$

Proof. We use (c) of Lemma 7.4 and induction on m . We then can rewrite this recursive formula as

$$\begin{bmatrix} m-1 \\ j \end{bmatrix}_{t^4} + t^{4(m-j)} \begin{bmatrix} m-1 \\ j-1 \end{bmatrix}_{t^4}.$$

By the property (q1) above, this is just $\begin{bmatrix} m \\ j \end{bmatrix}_{t^4}$. Using (a) of Lemma 7.4 and (i*) of Proposition 7.2 we have $P_{(2j,2m+1)}(t) = P_{(2j,2m)}(t) + t^{2(m-j)+1} P_{(2j-1,2m)}^*(t) = P_{(2j,2m)}(t)$. Using (d) of Lemma 7.4 and induction on m , we have $P_{(2j+1,2m+1)}(t) = P_{(2j+1,2m-1)}(t) + t^{4(m-j)} P_{(2j,2m-1)}(t)$. This gives

$$\begin{bmatrix} m-1 \\ j \end{bmatrix}_{t^4} + t^{4(m-j)} \begin{bmatrix} m-1 \\ j-1 \end{bmatrix}_{t^4},$$

which again corresponds to $\begin{bmatrix} m \\ j \end{bmatrix}_{t^4}$.

Finally we use (b) of Lemma 7.4 and (ii*) of Proposition 7.2 to obtain

$$\begin{bmatrix} m-1 \\ j \end{bmatrix}_{t^4} + t^{2m-1} \begin{bmatrix} m-1 \\ j \end{bmatrix}_{t^4},$$

which gives (2). \square

We now prove Lemma 7.4.

Proof.

(a) We have a graph of the form,

$$\begin{aligned} & \{\mathcal{G}(2j-1, 2j-1)^* \rightarrow \mathcal{G}(2j-1, 2j)^* \Rightarrow \cdots \rightarrow \mathcal{G}(2j-1, 2m-2)^* \Rightarrow \mathcal{G}(2j-1, 2m-1)^*\} \\ & \rightarrow \mathcal{G}(2j-1, 2m)^*. \end{aligned}$$

The part $\{\cdots\}$ corresponds to $\mathcal{G}(2j, 2m)$. The lowest degree of the terms in the last graph denoted by $\mathcal{G}(2j-1, 2m-1)$ is $2m-2j+1 = 2(m-j)+1$. We then have a graph which can be summarized as follows:

$$\mathcal{G}(2j, 2m) \rightarrow \mathcal{G}(2j-1, 2m)^*.$$

From here $P_{(2j,2m+1)} = P_{(2j,2m)}(t) + t^r P_{(2j-1,2m)}^*(t)$ follows and $r = 2(m-j) + 1$.

(b) We have:

$$\begin{aligned} & \{\mathcal{G}(2j, 2j)^* \rightarrow \mathcal{G}(2j, 2j)^* \Rightarrow \cdots \rightarrow \mathcal{G}(2j, 2m-3)^* \Rightarrow \mathcal{G}(2j, 2m-2)^*\} \\ & \rightarrow \mathcal{G}(2j, 2m-1)^*. \end{aligned}$$

The portion inside $\{\cdots\}$ corresponds to $\mathcal{G}(2j+1, 2m-1)^*$. We then end up with a diagram that can be summarized as:

$$\mathcal{G}(2j+1, 2m-1) \rightarrow \mathcal{G}(2j, 2m-1)^*.$$

The lowest degree in the chain complex corresponding to $\mathcal{G}(2j, 2m-1)^*$ is then: $2(m-j) - 1$

(c) The incidence graph $\mathcal{G}(2j, 2m)$ has the following description (Theorem 6.3).

$$\{\mathcal{G}(2j-1, 2j-1)^* \rightarrow \mathcal{G}(2j-1, 2j)^* \Rightarrow \cdots \rightarrow \mathcal{G}(2j-1, 2m-4)^* \Rightarrow \mathcal{G}(2j-1, 2m-3)^*\} \\ \rightarrow \mathcal{G}(2j-1, 2m-2)^* \Rightarrow \mathcal{G}(2j-1, 2m-1)^*.$$

The portion inside of $\{\cdots\}$ corresponds to $\mathcal{G}(2j, 2m-2)$. The lowest degree of the terms in the last graph denoted by $\mathcal{G}(2j-1, 2m-1)$ is $2m-2j = 2(m-j)$. The incidence graph $\mathcal{G}(2j-1, 2m-1)^*$ is in turn given by

$$\{\mathcal{G}(2j-2, 2j-2) \Rightarrow \mathcal{G}(2j-2, 2j-1) \rightarrow \cdots \rightarrow \mathcal{G}(2j-2, 2m-4) \Rightarrow \mathcal{G}(2j-2, 2m-3)\} \\ \rightarrow \mathcal{G}(2j-2, 2m-2).$$

Here the part $\{\cdots\}$ is now $\mathcal{G}(2j-1, 2m-2)^*$. The lowest degree of terms associated to the graph indicated by $\mathcal{G}(2j-2, 2m-2)^*$ is $2m-2-(2j-2) = 2(m-j)$. Altogether, taking into account the lowest degree in $\mathcal{G}(2j-2, 2m-2)$, there is a degree shift of: $4(m-j)$. We thus have a graph that can be indicated by the diagram:

$$\begin{array}{ccc} \mathcal{G}(2j, 2m-2) & \rightarrow & \mathcal{G}(2j-1, 2m-2)^* \\ & \Downarrow & \\ & \mathcal{G}(2j-1, 2m-2)^* & \rightarrow \mathcal{G}(2j-2, 2m-2) \end{array}$$

From here we obtain the recursive formula.

(d) We start with the corresponding graph that can be represented by a diagram:

$$\begin{array}{ccc} \mathcal{G}(2j+1, 2m-1) & \rightarrow & \mathcal{G}(2j, 2m-1)^* \\ & \Downarrow & \\ & \mathcal{G}(2j, 2m-1)^* & \rightarrow \mathcal{G}(2j-1, 2m-1) \end{array}$$

The lowest degree in the piece corresponding to $\mathcal{G}(2j-1, 2m-1)$ is $4(m-j)$. This becomes the formula $P_{(2j+1, 2m+1)}(t) = P_{(2j+1, 2m-1)}(t) + t^{4(m-j)}P_{(2j, 2m-1)}(t)$.

This completes the proof of Lemma 7.4. \square

Remark 7.1. We note the similarity in the formulae of the Poincaré polynomials for the real and complex Grassmannians. That is, in the case of (i) in Theorem 7.5, we have

$$P_{(k, n)}(t) = P_{(\lfloor k/2 \rfloor, \lfloor n/2 \rfloor)}^{\mathbb{C}}(t^2).$$

Also, in particular, if we take the limit $n \rightarrow \infty$ for the case $|t| < 1$, we have for both cases (i) and (ii)

$$P_{(k, \infty)}(t) = P_{(\lfloor k/2 \rfloor, \infty)}^{\mathbb{C}} = \prod_{j=1}^{\lfloor k/2 \rfloor} \frac{1}{1 - t^{4j}}.$$

This is a consequence of the structure of the cohomology ring of the Grassmannians in terms of the characteristic classes (see for example [3, 24]): It is well known that the real cohomology ring of the complex Grassmannian $\text{Gr}(k, n, \mathbb{C})$ can be described by

$$H^*(\text{Gr}(k, n, \mathbb{C}), \mathbb{R}) \cong \frac{\mathbb{R}[c_1, \dots, c_{n-k}, \bar{c}_1, \dots, \bar{c}_k]}{\{c \cdot \bar{c} = 1\}},$$

where $c := 1 + c_1 + \cdots + c_{n-k}$ and $\bar{c}_i = 1 + \bar{c}_1 + \cdots + \bar{c}_k$ with the Chern classes c_j 's defined by

$$c_j \in H^{2j}(\text{Gr}(k, n, \mathbb{C}), \mathbb{R}).$$

The Poincaré polynomial $P_{(k, n)}^{\mathbb{C}}(t)$ is then given by

$$P_{(k, n)}^{\mathbb{C}}(t) = \left[\begin{matrix} n \\ k \end{matrix} \right]_{t^2} = \prod_{j=0}^{k-1} \frac{1 - t^{2(n-j)}}{1 - t^{2(k-j)}}.$$

In particular, for the classifying space $BU(k)$ as the infinite Grassmannian $\text{Gr}(k, n, \mathbb{C})$ with $n = \infty$, the cohomology ring is given by

$$H^*(BU(k), \mathbb{R}) \cong \mathbb{R}[c_1, c_2, \dots, c_k], \quad \text{with } c_j \in H^{2j}(BU(k), \mathbb{R}).$$

and the Poincaré polynomial becomes the series given by

$$P_{(k, \infty)}^{\mathbb{C}}(t) = \prod_{j=1}^k \frac{1}{1 - t^{2j}}.$$

For the classifying space $BO(k)$ as the infinite Grassmannian $\text{Gr}(k, \infty)$, the cohomology ring is known to be

$$H^*(BO(k), \mathbb{R}) \cong \mathbb{R}[p_1, p_2, \dots, p_{\lfloor k/2 \rfloor}],$$

where the generators of the ring are given by the Potrjagin classes $p_j \in H^{4j}(\text{Gr}(k, n), \mathbb{R})$. The Poincaré series of $BO(k)$ is

$$P_{(k, \infty)}(t) = \prod_{j=1}^{\lfloor k/2 \rfloor} \frac{1}{1 - t^{4j}} = \lim_{n \rightarrow \infty} P_{(k, n)}(t),$$

where the limit of course make sense for $|t| < 1$.

8. THE \mathbb{F}_q POINTS ON $\text{Gr}(k, n)$ AND THE POINCARÉ POLYNOMIALS

Here we first introduce the *weighted* Schubert cell where the weight is given by the $q^{\eta(w_\sigma)}$ (and $q^{\eta(w_\sigma)^*}$) defined in subsection 6.3. Then we define a polynomial $p_{(k, n)}(q)$ (and $p_{(k, n)}^*(q)$) from the incidence graph $\mathcal{G}(k, n)$ (and $\mathcal{G}(k, n)^*$) based on the weights of the Schubert cells. It turns out that the polynomial $p_{(k, n)}(q)$ is related to the number of points on $\text{Gr}(k, n)$ over the finite field \mathbb{F}_q , and also related to the Poincaré polynomials $P_{(k, n)}(t)$ found in the previous section. The point here is that the notion of the weighted Schubert cells gives a simple method to compute the Poincaré polynomials and the \mathbb{F}_q points on $\text{Gr}(k, n)$.

Remark 8.1. As in the case of the Toda-flow for the real flag variety discussed in [8], those polynomials $p_{(k, n)}(q)$ can be computed by counting the number of blow-ups along the KP flow.

8.1. The q -weighted Schubert cells. Let us first recall that the Schubert cell $(\sigma_1, \dots, \sigma_k)$ can be identified as an element w_σ in $\mathcal{S}_n^{(k)}$. Hence the vertices of the incidence graph $\mathcal{G}(k, n)$ correspond to certain minimal length Weyl group representatives w_σ . As shown in subsection 6.3, given \mathcal{L} local system on $\text{Gr}(k, n)$ certain powers of q can be associated to each vertex w_σ . Since there are only two local systems two consider, we can simplify the notation of [8], and just denote by $q^{\eta(w_\sigma)}$ the power of q assigned in the case when \mathcal{L} is constant and $q^{\eta(w_\sigma)^*}$ the power of q in the case when \mathcal{L} is twisted. We then associate powers $q^{\eta(w_\sigma)}$ to each vertex w_σ of $\mathcal{G}(k, n)$ and powers $q^{\eta(w_\sigma)^*}$ to each vertex w_σ of $\mathcal{G}(k, n)^*$. We call the Schubert cells X_{w_σ} with those powers $q^{\eta(w)}$ the *weighted* Schubert cells, denoted by $(w_\sigma, q^{\eta(w_\sigma)})$ for each $w_\sigma \in \mathcal{S}_n^{(k)}$.

Here we consider only the $\eta(w)$ (the $\eta(w)^*$ can be treated in a similar way). Let us first define the following set of weighted vectors.

(a) For odd k ,

$$\left\{ e_j(q) = (E_j; q^{\lfloor \frac{j}{2} \rfloor}) : j = 1, \dots, n \right\}.$$

(i.e. the weights are assigned as $(1, q, q, q^2, q^2, \dots, q^{\lfloor \frac{n}{2} \rfloor})$),

(b) For even k ,

$$\left\{ e_j(q) = (E_j; q^{\lfloor \frac{j-1}{2} \rfloor}) : j = 1, \dots, n \right\}.$$

(i.e. the weights are assigned as $(1, 1, q, q, \dots, q^{\lfloor \frac{n-1}{2} \rfloor})$).

This is a q -deformation of the signed vector e_j , and the sign for each vector E_j is given by setting $q = -1$. Then we can find the explicit form of the $\eta(w_\sigma)$.

Lemma 8.1. *The function $\eta(w_\sigma)$ with the representation $w_\sigma = (\sigma_1, \dots, \sigma_k)$ is given by*

$$\begin{aligned} \eta(w_\sigma) &= \sum_{j=1}^k \lfloor \frac{\sigma_j - j}{2} \rfloor & \text{if } k = \text{odd}, \\ \eta(w_\sigma) &= \sum_{j=1}^k \lfloor \frac{\sigma_j - j - 1}{2} \rfloor & \text{if } k = \text{even}. \end{aligned}$$

To show this, we note that the $\eta(w_\sigma)$ satisfies the following conditions which uniquely determine $\eta(w_\sigma)$ for given Schubert cell $w_\sigma = (\sigma_1, \dots, \sigma_k)$.

- (i) To the top cell $e = (1, 2, \dots, k)$ we associate $\eta(e) = 0$.
- (ii) If two Schubert cells w and w' are joined by \Rightarrow , i.e. $w \Rightarrow w'$, then $\eta(w) = \eta(w')$.
- (iii) If two Schubert cells w and w' are joined by \rightarrow (not \Rightarrow), then $\eta(w') = \eta(w) + 1$.

We then define a polynomial $p_{(k,n)}(q)$ as an alternating sum,

$$p_{(k,n)}(q) := \sum_{w \in \mathcal{S}_n^{(k)}} (-1)^{\ell(w)} q^{\eta(w)}$$

We now offer a direct construction of the polynomials $p_{(k,n)}(q)$ which leads to their direct calculation. An alternative way to proceed is through arguments similar to those leading to the recursive formulas for Poincaré polynomials. We have the following Theorem:

Theorem 8.2. *The polynomials $p_{(k,n)}(q)$ take the forms,*

$$\begin{aligned} p_{(2j,2m)}(q) &= p_{(2j,2m+1)}(q) = p_{(2j+1,2m+1)}(q) = \begin{bmatrix} m \\ j \end{bmatrix}_{q^2} \\ p_{(2j+1,2m)}(q) &= (1 - q^m) \begin{bmatrix} m-1 \\ j \end{bmatrix}_{q^2}. \end{aligned}$$

Proof. Let us first consider the case $\text{Gr}(2j, 2m)$. In this case we have

$$\{(E_1; 1), (E_2; 1), (E_3, q), (E_4; q), \dots, (E_{2m-1}; q^{m-1}), (E_{2m}; q^{m-1})\}.$$

We compute $p_{(2j,2m)}(q)$ by computing all wedge products $(\sigma_1, \dots, \sigma_{2j}) \leftrightarrow e_{\sigma_1}(q) \wedge \dots \wedge e_{\sigma_{2j}}(q)$. It is immediate that if a cell contains only one term from a pair $\{(E_{2i-1}; q^{i-1}), (E_{2i}; q^{i-1})\}$, then this cell is canceled by the cell containing the same terms except the term from the pair replaced by the other one. Thus the cells which contribute to $p_{(2j,2m)}(q)$ are given by the wedge products containing pairs $\{(E_{2i-1}; q^{i-1}), (E_{2i}; q^{i-1})\}$ for some i , i.e.

$$(E_{2a_1-1} \wedge E_{2a_1} \wedge \dots \wedge E_{2a_j-1} \wedge E_{2a_j}; q^{j(j-1)+4|Y(a)|}).$$

Here $Y(a)$ represents the Young diagram corresponding to (a_1, \dots, a_j) , and 4 implies that each box in $Y(a)$ consists of 2×2 cube of the boxes for the original Young diagram Y_λ with

$$\lambda = (2(a_1 - 1) + 1, 2(a_1 - 1) + 2, \dots, 2(a_j - j) + 2j - 1, 2(a_j - j) + 2j).$$

Since the generating function of the number of cells in $\text{Gr}(j, m)$ is given by (2.2), we obtain the formula $p_{(2j,2m)}(q)$.

Now let us consider the case $\text{Gr}(2j, 2m+1)$. In this case we have,

$$\{(E_1; 1), (E_2; 1), \dots, (E_{2m-1}; q^{m-1}), (E_{2m}; q^{m-1}), (E_{2m+1}; q^m)\}.$$

It is easy to see that if a cell contains E_{2m+1} in $2j$ -wedge product, then this cell has no contribution in $p_{(2j, 2m+1)}(q)$. Then the situation is the same as the case $\text{Gr}(2j, 2m+1)$. A similar argument can be applied for the case of $\text{Gr}(2k+1, 2n+1)$ (in this case, all the terms containing E_1 vanish).

Finally we consider the case $\text{Gr}(2j+1, 2m)$. We start with

$$\{(E_1; 1), (E_2; q), (E_3; q), \dots, (E_{2m-2}; q^{m-1}), (E_{2m-1}; q^{m-1}), (E_{2m}; q^m)\}.$$

We note that the cells containing both E_1 and E_{2m} have no contribution. There are two types of cells which contribute; (i) those consisting of E_1 and pairs $\{E_{2i}, E_{2i+1}\}$ of the same degree q^i , and (ii) those consisting of E_{2n} and pairs of the same degrees. The first case (i), i.e. without E_{2m} , gives the same polynomial as in the case $\text{Gr}(2j+1, 2m-1)$. The second case (ii), i.e. without E_1 , we have the same polynomial times $-q^m$ due to the degree of E_{2m} and $(-1)^{l(w)} = (-1)^{2m-1}$. We thus obtain the result for $p_{(2j+1, 2m)}(q)$. \square

Remark 8.2. The polynomials $p_{(k,n)}(q)$ in Theorem 8.2 are related to the Poincaré polynomials $P_{(k,n)}(t)$ found in Theorem 7.5.

- (a) For $\text{Gr}(k, n)$ with $(k, n) = (2j, 2m)$ or $(2j, 2m+1)$ or $(2j+1, 2m+1)$, the Poincaré polynomial is given by $P_{(k,n)}(t) = p_{(k,n)}(q = t^2)$, i.e.

$$P_{(k,n)}(t) = \begin{bmatrix} m \\ j \end{bmatrix}_{t^4} = \prod_{i=0}^{j-1} \frac{1 - t^{4(m-i)}}{1 - t^{4(j-i)}}.$$

For example, $P_{(2,4)}(t) = P_{(2,5)}(t) = P_{(3,5)}(t) = 1 + t^4$.

- (b) For $\text{Gr}(k, n)$ with $(k, n) = (2j+1, 2m)$, $P_{(k,n)}(t)$ is given by

$$P_{(k,n)}(t) = (1 + t^{2m-1}) \begin{bmatrix} m-1 \\ j \end{bmatrix}_{t^4}.$$

Namely, the factor $(1 - q^m)$ in the polynomial $p_{(k,n)}(q)$ is replaced by $(1 + t^{2m-1})$ and $\begin{bmatrix} m-1 \\ j \end{bmatrix}_{q^2}$ with $q = t^2$. For example, $p_{(3,6)}(q) = (1 - q^3) \begin{bmatrix} 2 \\ 1 \end{bmatrix}_{q^2}$ and $P_{(3,6)}(t) = (1 + t^5)(1 + t^4) = 1 + t^4 + t^5 + t^9$.

Example 8.1. Following the constructive arguments in the proof of Theorem 8.2, we directly find the polynomials $p_{(k,n)}(q)$ for the cases $\text{Gr}(4, 8)$ and $\text{Gr}(5, 12)$:

- (a) For $\text{Gr}(4, 8)$, we have the following cells which contribute the polynomial $p_{(4,8)}(q)$,

$$\begin{aligned} (1, 2, 3, 4) &= e, \\ (1, 2, 5, 6) &= s_4 s_5 s_3 s_4, \\ (1, 2, 7, 8) &= s_6 s_7 s_5 s_6 s_4 s_5 s_3 s_4, \\ (3, 4, 5, 6) &= s_2 s_3 s_1 s_2 s_4 s_5 s_3 s_4, \\ (3, 4, 7, 8) &= s_2 s_3 s_1 s_2 s_6 s_7 s_5 s_6 s_4 s_5 s_3 s_4, \\ (5, 6, 7, 8) &= s_4 s_5 s_3 s_4 s_2 s_3 s_1 s_2 s_6 s_7 s_5 s_6 s_4 s_5 s_3 s_4 \end{aligned}$$

Here the cells are represented by the elements of $\mathcal{S}_8^{(4)}$. Then the polynomial is given by

$$p_{(4,8)}(q) = 1 + q^2 + 2q^4 + q^6 + q^8 = \begin{bmatrix} 4 \\ 2 \end{bmatrix}_{q^2}.$$

The Young diagrams of those cells are given by

$$\begin{aligned} (1, 2, 3, 4) &= \emptyset, & (1, 2, 5, 6) &= \begin{array}{|c|c|} \hline \square & \square \\ \hline \end{array}, & (1, 2, 7, 8) &= \begin{array}{|c|c|c|c|} \hline \square & \square & \square & \square \\ \hline \end{array} \\ (3, 4, 5, 6) &= \begin{array}{|c|c|} \hline \square & \square \\ \hline \end{array}, & (3, 4, 7, 8) &= \begin{array}{|c|c|c|c|} \hline \square & \square & \square & \square \\ \hline \end{array}, & (5, 6, 7, 8) &= \begin{array}{|c|c|c|c|} \hline \square & \square & \square & \square \\ \hline \end{array} \end{aligned}$$

Note here that the box \square gives the unit for those diagrams and each diagram represents the Pontrjagin class $p_j \in H^{4j}(\text{Gr}(4, 8), \mathbb{R})$ for $j = 1, 2$, and this explains the relation,

$$p_{(4,8)}(q) = |\text{Gr}(2, 4, \mathbb{F}_{q^2})|.$$

Then the cohomology ring may be expressed by

$$H^*(\text{Gr}(4, 8), \mathbb{R}) \cong \frac{\mathbb{R}[p_1, p_2, \bar{p}_1, \bar{p}_2]}{\{p \cdot \bar{p} = 1\}},$$

where $p = 1 + p_1 + p_2$ and $\bar{p} = 1 + \bar{p}_1 + \bar{p}_2$.

(b) For $\text{Gr}(5, 12)$, we have the contributing cells containing either E_1 or E_{12} ,

$$\begin{array}{ll} (1, 2, 3, 4, 5) & (2, 3, 4, 5, 12) \\ (1, 2, 3, 6, 7) & (2, 3, 6, 7, 12) \\ (1, 2, 3, 8, 9) & (2, 3, 8, 9, 12) \\ (1, 2, 3, 10, 11) & (2, 3, 10, 11, 12) \\ (1, 4, 5, 6, 7) & [1 \rightarrow 12] \quad (4, 5, 6, 7, 12) \\ (1, 4, 5, 8, 9) & (4, 5, 8, 9, 12) \\ (1, 4, 5, 10, 11) & (4, 5, 10, 11, 12) \\ (1, 6, 7, 8, 9) & (6, 7, 8, 9, 12) \\ (1, 6, 7, 10, 11) & (6, 7, 10, 11, 12) \\ (1, 8, 9, 10, 11) & (8, 9, 10, 11, 12) \end{array}$$

The cells in the left hand side gives $1 + q^2 + 2q^4 + 2q^6 + 2q^8 + q^{10} + q^{12} = (1 - q^{10})(1 - q^8)/(1 - q^4)(1 - q^2)$, and those in the right hand side gives $-q^6$ times the same polynomial, i.e.

$$p_{(5,12)}(q) = (1 - q^6) \begin{bmatrix} 5 \\ 2 \end{bmatrix}_{q^2}.$$

The Young diagrams for the cells in the left column are given by

$$\emptyset \quad \begin{array}{|c|} \hline \square \\ \hline \end{array} \quad \begin{array}{|c|c|} \hline \square & \square \\ \hline \end{array} \quad \begin{array}{|c|c|c|} \hline \square & \square & \square \\ \hline \end{array} \quad \begin{array}{|c|c|c|c|} \hline \square & \square & \square & \square \\ \hline \end{array} \quad \begin{array}{|c|c|} \hline \square & \square \\ \hline \end{array} \quad \begin{array}{|c|c|c|} \hline \square & \square & \square \\ \hline \end{array} \quad \begin{array}{|c|c|c|c|} \hline \square & \square & \square & \square \\ \hline \end{array} \quad \begin{array}{|c|c|c|c|c|} \hline \square & \square & \square & \square & \square \\ \hline \end{array}$$

The Young diagrams of the cells in the right column are given by the above ones combined with the first cell in the right column,

$$(2, 3, 4, 5, 12) = \begin{array}{|c|c|c|c|c|} \hline \square & \square & \square & \square & \square \\ \hline \end{array}.$$

That is, we have, from the second cell,

$$\begin{array}{|c|c|c|c|c|c|c|c|} \hline \square & \square & \square & \square & \square & \square & \square & \square \\ \hline \end{array} \quad \begin{array}{|c|c|c|c|c|c|} \hline \square & \square & \square & \square & \square & \square \\ \hline \end{array} \quad \begin{array}{|c|c|c|c|c|c|c|} \hline \square & \square & \square & \square & \square & \square & \square \\ \hline \end{array} \quad \begin{array}{|c|c|c|c|c|c|} \hline \square & \square & \square & \square & \square & \square \\ \hline \end{array} \quad \begin{array}{|c|c|c|c|c|c|c|} \hline \square & \square & \square & \square & \square & \square & \square \\ \hline \end{array} \quad \begin{array}{|c|c|c|c|c|c|} \hline \square & \square & \square & \square & \square & \square \\ \hline \end{array} \quad \begin{array}{|c|c|c|c|c|c|c|} \hline \square & \square & \square & \square & \square & \square & \square \\ \hline \end{array} \quad \begin{array}{|c|c|c|c|c|c|c|} \hline \square & \square & \square & \square & \square & \square & \square \\ \hline \end{array}$$

Note again that those cells are expressed by the diagrams $\begin{array}{|c|} \hline \square \\ \hline \end{array}$ and $\begin{array}{|c|c|c|c|c|} \hline \square & \square & \square & \square & \square \\ \hline \end{array}$. Each diagram of divisible by $\begin{array}{|c|} \hline \square \\ \hline \end{array}$ represents the Pontrjagin class $p_j \in H^{4j}(\text{Gr}(5, 12), \mathbb{R})$, and the hook diagram may correspond to an extra element, say r , of degree 11 with the property $r^2 = 0$. It then may be natural to conjecture that the cohomology ring of $\text{Gr}(5, 12)$ has the structure,

$$H^*(\text{Gr}(5, 12), \mathbb{R}) \cong \frac{\mathbb{R}[p_1, p_2, p_3, \bar{p}_1, \bar{p}_2, r]}{\{p \cdot \bar{p} = 1, r^2\}},$$

where $p = 1 + p_1 + p_2 + p_3$, and $\bar{p} = 1 + \bar{p}_1 + \bar{p}_2$.

The proof of the following Proposition is similar to the calculation of $P_{(2j,2m+1)}^*(t)$, $P_{(2j+1,2m+1)}^*(t)$ and is omitted.

Proposition 8.3. *We have:*

$$p_{(2j,2m+1)}^*(q) = q^j \begin{bmatrix} m \\ j \end{bmatrix}_{q^2}$$

$$p_{(2j+1,2m+1)}^*(q) = q^{m-j} \begin{bmatrix} m \\ j \end{bmatrix}_{q^2}$$

8.2. The number of \mathbb{F}_q -points on $\text{Gr}(k, n)$. The main goal of this section is to show that the \mathbb{F}_q -points on the Grassmannian $\text{Gr}(k, n)$ is given by

$$|\text{Gr}(k, n)_{\mathbb{F}_q}| = q^r |p_{(k,n)}(q)|$$

where r is given by $r = k(n - k) - \deg(p_{(k,n)}(q))$.

In order to calculate $|\text{Gr}(k, n)_{\mathbb{F}_q}|$, we first introduce the complexification $\text{Gr}(k, n)_{\mathbb{C}}$ of the real Grassmannian $\text{Gr}(k, n)$, which is not the complex Grassmannian $\text{Gr}(k, n, \mathbb{C})$, but rather, a Zariski open subset of $\text{Gr}(k, n, \mathbb{C})$ having the same homotopy type as $\text{Gr}(k, n)$. So, for instance the complexification of $\mathbb{R}P^1 = \text{Gr}(1, 2)$ is not $\text{Gr}(1, 2, \mathbb{C})$ which is $\mathbb{C}P^1$, but rather, the set of all lines in $\mathbb{C}^2 = \{(x, y)\}$ such that $x^2 + y^2 \neq 0$. This is an open subset of $\mathbb{C}P^1$ which has the homotopy type of a circle.

Definition 8.1. We fix a real vector subspace of dimension k , $V \subset \mathbb{R}^n$ and its complexification $V_{\mathbb{C}} = V \oplus_{\mathbb{R}} \sqrt{-1}V$. The group $\text{SO}_n(\mathbb{R})$ acts transitively on $\text{Gr}(k, n)$ but the orbit $\text{SO}_n(\mathbb{C}) \cdot V_{\mathbb{C}}$ of the vector space $V_{\mathbb{C}}$ does not exhaust all of $\text{Gr}(k, n, \mathbb{C})$. We define this orbit as the *complexification* of $\text{Gr}(k, n)$, and denoted by $\text{Gr}(k, n)_{\mathbb{C}}$. The real Grassmannian $\text{Gr}(k, n)$ can then be described as $K/L \cap K$, where $K = \text{SO}_n(\mathbb{R})$ and the Levi factor L of a maximal parabolic subgroup containing the Borel subgroup B of upper triangular matrices in $\text{SL}_n(\mathbb{R})$ and the complexification is $K(\mathbb{C})/L(\mathbb{C}) \cap K(\mathbb{C}) = \text{SO}_n(\mathbb{C}) \cdot V_{\mathbb{C}}$ which has the same homotopy type as $\text{Gr}(k, n)$.

This naturally extends to other semi-simple Lie groups. In brief, if $G = KAN$ (Iwasawa decomposition) and $P = LN$ is a maximal parabolic with Levi factor L containing a maximally split Cartan subgroup $H = TA$, then we have $G/P \cong K/K \cap L$ and the complexification will be $K(\mathbb{C})/L(\mathbb{C}) \cap K(\mathbb{C})$.

Example 8.2. Consider $\mathbb{R}P^{n-1}$. If we fix V a one dimensional vector subspace of \mathbb{R}^n . Then the $\text{SO}(n, \mathbb{C})$ orbit containing $V_{\mathbb{C}}$ can be described as the set of all lines in \mathbb{C}^n , denoted by $\mathbb{C}(x_1, \dots, x_n)$, such that $x_1^2 + \dots + x_n^2 \neq 0$. This is an open subset $\text{Gr}(1, n)_{\mathbb{C}}$ of the Grassmannian $\text{Gr}(1, n, \mathbb{C}) = \mathbb{C}P^{n-1}$.

Example 8.3. Let us consider $\text{Gr}(2, 4)$. Using the Plücker embedding as in Example 2.2, the complexification can be explicitly described as follows.

$$\text{Gr}(2, 4)_{\mathbb{C}} = \left\{ \mathbb{C}(z_1, z_2, z_3, w_1, w_2, w_3) : \begin{array}{l} z_1^2 + z_2^2 + z_3^2 - w_1^2 - w_2^2 - w_3^2 = 0, \\ z_1^2 + z_2^2 + z_3^2 \neq 0 \end{array} \right\}.$$

This is an open subset of $\text{Gr}(2, 4, \mathbb{C})$. This formula is useful for counting the \mathbb{F}_q -points on $\text{Gr}(k, n)$ (see below).

We consider $\overline{\mathbb{F}}_q$ an algebraic closure of a field \mathbb{F}_q with q elements, and consider Grassmannian varieties $\text{Gr}(k, n, \overline{\mathbb{F}}_q)$. As a set of points this is the set of all the k -dimensional subspaces of $\overline{\mathbb{F}}_q^n$.

However the $\text{Gr}(k, n, \overline{\mathbb{F}}_q)$ is the $\overline{\mathbb{F}}_q$ -analogue of the standard complex Grassmannian variety $\text{Gr}(k, n, \mathbb{C})$. Here we are interested instead in the $\overline{\mathbb{F}}_q$ -counterparts of the complexifications $\text{Gr}(k, n)_{\mathbb{C}}$ of real Grassmannians in counting their \mathbb{F}_q -points.

Assume that q is a power of a prime number $p \neq 2$ such that in \mathbb{F}_q the polynomial $x^2 + 1$ is reducible i.e. $\sqrt{-1} \in \mathbb{F}_q$. If p has the form $p = 4k + 1$ with k an integer, this will be the case

e.g. $q = 5$. We then consider the analogue of $\text{Gr}(k, n)$ over \mathbb{F}_q , that is, the Zariski open subset $\text{Gr}(k, n)_{\overline{\mathbb{F}}_q}$ of $\text{Gr}(k, n, \overline{\mathbb{F}}_q)$ and then the corresponding \mathbb{F}_q points. Then we have the following results for $|S^n(\mathbb{F}_q)|$, the number of \mathbb{F}_q -points on S^n :

(a) For $n = 2m - 1$, we have

$$|S^{2m-1}(\mathbb{F}_q)| = q^{m-1}(q^m - 1).$$

(b) For $n = 2m$, we have

$$|S^{2m}(\mathbb{F}_q)| = q^m(q^m + 1).$$

This can be obtained as follows: Let us first consider the case $n = 1$, i.e.

$$S^1(\mathbb{F}_q) = \{(x, y) \in \mathbb{F}_q^2 : x^2 + y^2 = 1\}.$$

Then using the formulae for the stereographic projection; $x = \frac{2u}{u^2+1}, y = \frac{u^2-1}{u^2+1}$ with $y \neq 1$ and $\{u \in \mathbb{F}_q : u^2 + 1 \neq 0\}$. Since $\sqrt{-1} \in \mathbb{F}_q$, we have 2 points in $\{u^2 + 1 = 0\}$. Counting the point $(0, 1)$, the north pole, we have $|S^1(\mathbb{F}_q)| = q - 2 + 1 = q - 1$. Now consider the case $n = 2$, we have $x = \frac{2u_1}{u_1^2+u_2^2+1}, y = \frac{2u_2}{u_1^2+u_2^2+1}, z = \frac{u_1^2+u_2^2-1}{u_1^2+u_2^2+1}$ with $z \neq 1$ and $\{(u_1, u_2) \in \mathbb{F}_q^2 : u_1^2 + u_2^2 + 1 \neq 0\}$. This gives $q^2 - (q - 1)$ points (note $(q - 1)$ is the number of points in $u_1^2 + u_2^2 + 1 = 0$). We now add the points of the north pole $(x, y, 1)$ with $x^2 + y^2 = 0$. This gives $2(q - 1) + 1$, where $2(q - 1)$ for $x = \pm\sqrt{-1}y \neq 0$ and 1 for $(0, 0, 1)$. Then we have $|S^2(\mathbb{F}_q)| = q^2 - (q - 1) + 2(q - 1) + 1 = q(q + 1)$. Using the induction, one can show that the number of points in the north pole is given by

$$(8.1) \quad \begin{cases} |\{(x_1, \dots, x_{2m-1}) \in \mathbb{F}_q^{2m-1} : x_1^2 + \dots + x_{2m-1}^2 = 0\}| = q^{2m-2}, \\ |\{(x_1, \dots, x_{2m}) \in \mathbb{F}_q^{2m} : x_1^2 + \dots + x_{2m}^2 = 0\}| = q^{2m-1} + q^m - q^{m-1}. \end{cases}$$

Then one can obtain the above formulae for $|S^n(\mathbb{F}_q)|$.

Example 8.4. We consider the analogue of $\mathbb{R}P^{n-1}$ over \mathbb{F}_q , that is, the Zariski open subset $\text{Gr}(1, n)_{\mathbb{F}_q}$ of $\text{Gr}(1, n, \mathbb{F}_q)$. Recall that we have the Schubert decomposition,

$$\mathbb{C}P^{n-1} = \text{Gr}(1, n, \mathbb{C}) = \{(*, \dots, *)\} \sqcup \{(*, \dots, *, 1, 0)\} \sqcup \dots \sqcup \{(1, 0, \dots, 0)\},$$

and we have $|\text{Gr}(1, n, \mathbb{F}_q)| = [n]_q = 1 + q + \dots + q^{n-1}$. To find $|\text{Gr}(1, n)_{\mathbb{F}_q}|$, the number of \mathbb{F}_q points on $\mathbb{R}P^{n-1}$, we have to remove the points in the Schubert cells given by

$$\{(x_1, \dots, x_k, 1, 0, \dots, 0) \in \mathbb{F}_q^n : x_1^2 + \dots + x_k^2 + 1 = 0\} \quad k = 1, \dots, n - 1.$$

Since $\sqrt{-1} \in \mathbb{F}_q$, those sets are equivalent to S^{k-1} on \mathbb{F}_q whose points can be counted from the formulae above. Thus we get

(a) For $n = 2m$,

$$|\text{Gr}(1, 2m)_{\mathbb{F}_q}| = q^{m-1}(q^m - 1).$$

(b) For $n = 2m + 1$,

$$|\text{Gr}(1, 2m + 1)_{\mathbb{F}_q}| = q^{2m}.$$

As was shown in Proposition 8.2, those polynomials are related to $p_{(1,n)}(q)$, i.e. $p_{(1,2m)}(q) = 1 - q^m$ and $p_{(1,2m+1)}(q) = 1$, and we have the form,

$$|\text{Gr}(1, n)_{\mathbb{F}_q}| = q^r |p_{(1,n)}(q)|.$$

Example 8.5. We now consider $\text{Gr}(2, 4)$. As in Example 2.2, $\text{Gr}(2, 4)$ becomes, via the Plücker embedding, the set of one dimensional isotropic vector spaces in \mathbb{R}^6 . We then have, as in Example 8.3, the following description of the \mathbb{F}_q points of the variety we are studying

$$\text{Gr}(2, 4)_{\mathbb{F}_q} = \{(x_1, x_2, x_3, y_1, y_2, y_3) \in \overline{\mathbb{F}}_q^6 : x_1^2 + x_2^2 + x_3^2 - y_1^2 - y_2^2 - y_3^2 = 0, x_1^2 + x_2^2 + x_3^2 \neq 0\}.$$

Since $\sqrt{-1} \in \mathbb{F}_q$, we can transform the equation $x_1^2 + x_2^2 + x_3^2 - y_1^2 - y_2^2 - y_3^2 = 0$ giving *isotropy* into $x_1^2 + x_2^2 + x_3^2 + y_1^2 + y_2^2 + y_3^2 = 0$. The number of solutions of $x_1^2 + x_2^2 + x_3^2 + y_1^2 + y_2^2 + y_3^2 = 0$ is given by $q^5 + q^3 - q^2$ (see (8.1)). We now must subtract those points for which $x_1^2 + x_2^2 + x_3^2 = 0$ and $y_1^2 + y_2^2 + y_3^2 = 0$. From (8.1), one can see that there are q^2 solutions of $x_1^2 + x_2^2 + x_3^2 = 0$. So with an additional q^2 solutions of $y_1^2 + y_2^2 + y_3^2 = 0$, we end up with $q^5 - q^4 + q^3 - q^2 = q^2(q-1)(q^2+1)$. We now divide by $q-1$ to count the projectivization and obtain a total of $q^2(1+q^2)$ points.

Example 8.6. Using the formulae for $|S^n(\mathbb{F}_q)|$ for the case with $\sqrt{-1} \in \mathbb{F}_q$, one can write an explicit formula giving the number of \mathbb{F}_q points of finite Chevalley group $\mathrm{SO}_n(\mathbb{F}_q)$: First recall that $\mathrm{SO}_{n+1}(\mathbb{R})/\mathrm{SO}_n(\mathbb{R}) \cong S^n$. Then one expects:

$$|\mathrm{SO}_n(\mathbb{F}_q)| = \prod_{k=1}^n |S^{n-k}(\mathbb{F}_q)|,$$

which corresponds to the results [4]:

(a) For $n = 2m$,

$$|\mathrm{SO}_{2m}(\mathbb{F}_q)| = 2q^{m(m-1)}(q^2-1)(q^4-1)\cdots(q^{2m-2}-1)(q^m-1).$$

(b) For $n = 2m+1$,

$$|\mathrm{SO}_{2m+1}(\mathbb{F}_q)| = 2q^{m^2}(q^2-1)(q^4-1)\cdots(q^{2m}-1).$$

In [8], we show that those polynomials $p(q) = (q^2-1)(q^4-1)\cdots(q^{2m-2}-1)(q^m-1)$ and $p(q) = (q^2-1)(q^4-1)\cdots(q^{2m}-1)$ are related to the cohomology of the real flag variety $\mathrm{SL}_n(\mathbb{R})/B$ through the singular solutions (blow-ups) of the Toda lattice.

We assume that q is a power of a prime p , m is relatively prime to p and $p \neq 2$. Moreover, as before we assume that $\sqrt{-1} \in \mathbb{F}_q$. As in [8] one has the following.

Proposition 8.4. *The cohomology $H^*(\mathrm{Gr}(k, n)_{\overline{\mathbb{F}}_q}; \overline{\mathbb{Q}}_m)$ has Frobenius eigenvalues of the form q^i .*

Proof. This follows from the arguments in [8] with almost no change. As can be seen from [9] or more directly by Remark 6.1 above, the incidence graph of $\mathrm{Gr}(k, n)$ is a subgraph of the flag manifold. The Frobenius eigenvalues are still computed in terms of Hecke algebra operators as in Section 5 of [8] but the Weyl group elements in the expressions $T_{w^{-1}}^{-1}$ are restricted to a smaller subset corresponding to representatives of cells in a Grassmanian. This is also implicit in Section 9 of [9] but notation is more convoluted.

One may also consider the spectral sequence associated to the fibration

$$(K \cap L)(\overline{\mathbb{F}}_q) \rightarrow (K)(\overline{\mathbb{F}}_q) \rightarrow (K/L \cap K)(\overline{\mathbb{F}}_q)$$

This reduces the argument to the cases of $K \cap L$ and K over $\overline{\mathbb{F}}_q$. The case of K and $L \cap K$ is just the case discussed in [8] of the flag manifold. \square

We now recall that from the Lefschetz fixed point formula for Fr the alternating sum is given by

$$\sum_s (-1)^s \mathrm{Tr} \left((Fr)_* |_{H_c^s(\mathrm{Gr}(k, n)_{\overline{\mathbb{F}}_q}; \overline{\mathbb{Q}}_m)} \right) = |\mathrm{Gr}(k, n)_{\overline{\mathbb{F}}_q}|$$

By Poincaré duality, $H_c^{2k(n-k)-s}(\mathrm{Gr}(k, n)_{\overline{\mathbb{F}}_q}; \overline{\mathbb{Q}}_m)$ is the dual of $H^s(\mathrm{Gr}(k, n)_{\overline{\mathbb{F}}_q}; \mathbb{V})$ where \mathbb{V} is the dual of a constant sheaf. In the orientable cases we can replace \mathbb{V} with $\overline{\mathbb{Q}}_m$ i.e. constant coefficients.

8.3. Frobenius eigenvalues calculation. This calculation is based on section 9 of [9] or on Section 6.1 [8] which is restricted to real split cases and has simpler notation. Frobenius eigenvalues q^i increase along a graph $\mathcal{G}(k, n)$ or $\mathcal{G}(k, n)^*$ as described in (i), (ii), (iii) in Subsection 8.1.

In terms of the action of the Hecke algebra in Lemma 3.5 of [23], one must apply $T_{s+i}^{-1} = q^{-1}(T_{s_i} + (1 - q))$. Now \Rightarrow corresponds to case (e) and the Frobenius eigenvalue does not change. The case of \rightarrow corresponds to (d2) and the Frobenius eigenvalue is multiplied by q .

By construction of the polynomial $p_{(k,n)}(q)$ we have

$$\sum_s (-1)^s \text{Tr} \left((Fr)_* |_{H^s(\text{Gr}(k,n)_{\mathbb{F}_q}; \bar{\mathbb{Q}}_m)} \right) = p_{(k,n)}(q)$$

This leads to the following Proposition,

Proposition 8.5. *We have*

$$|\text{Gr}(k, n)_{\mathbb{F}_q}| = \pm q^{k(n-k)-D} p_{(k,n)}(q),$$

with $D = \deg(p_{(k,n)}(q))$.

Proof. We consider the cases with $n = \text{even}$ (orientable case) and $n = \text{odd}$ (non-orientable case):

- (1) Assume that n is even. We use Poincaré duality, $H_c^{2k(n-k)-s}(\text{Gr}(k, n)_{\mathbb{F}_q}; \bar{\mathbb{Q}}_m)$ is the dual of $H^s(\text{Gr}(k, n)_{\mathbb{F}_q}; \bar{\mathbb{Q}}_m)$. This corresponds to considering the polynomial $q^{k(n-k)} p_{(k,n)}(q^{-1})$. We now used the formulas listed at the beginning of Section 7. We note that if $D = \deg(p_{(k,n)}(q))$ then, according to these formulas $q^D p_{(k,n)}(q^{-1}) = \pm p_{(k,n)}(q)$. Hence we obtain

$$\sum_s (-1)^s \text{Tr} \left((Fr)_* |_{H_c^s(\text{Gr}(k,n)_{\mathbb{F}_q}; \bar{\mathbb{Q}}_m)} \right) = |\text{Gr}(k, n)_{\mathbb{F}_q}| = \pm q^{k(n-k)-D} p_{(k,n)}(q).$$

- (2) Assume that n is odd. By Poincaré duality, $H_c^{2k(n-k)-s}(\text{Gr}(k, n)_{\mathbb{F}_q}; \bar{\mathbb{Q}}_m)$ is the dual of $H^s(\text{Gr}(k, n)_{\mathbb{F}_q}; \mathcal{L})$ where \mathcal{L} is a twisted local system. We then have $q^{k(n-k)} p_{(k,n)}^*(q^{-1})$. We then use Proposition 8.3. We obtain $q^{k(n-k)} q^r p_{(k,n)}(q^{-1})$ where $r = -j$ or $r = m - j$ if $k = 2j, 2j + 1$ and $n = 2m + 1$.

This completes the proof. \square

REFERENCES

- [1] M. J. Ablowitz and H. Segur, *Solitons and the inverse scattering transform*, SIAM Studies in Applied Mathematics, (SIAM, Philadelphia/ 1981).
- [2] A. Björner and F. Brenti, *Combinatorics of Coxeter Groups*, GTM **231** (Springer, New York, 2005).
- [3] R. Bott and L. W. Tu, *Differential forms in algebraic topology*, (Springer-Verlag, New York) (1982).
- [4] R. Carter, *Finite Groups of Lie Type, Conjugacy Classes and Complex Characters*, Wiley Classical Library Edition (1993).
- [5] L. Casian and Y. Kodama, Topology of the iso-spectral real manifold associated with the generalized Toda lattices on semisimple Lie algebras, *J. Phys. A: Math. Gen.* **33** (2000) 1-14.
- [6] L. Casian and Y. Kodama, Blow-ups of the Toda lattices and their intersections with the Bruhat cells, *Contemporary Math.* **301** (2002) 283-310.
- [7] L. Casian and Y. Kodama, Compactification of the isospectral varieties of nilpotent Toda lattices, *Surikaisekiken Kokyuroku* (RIMS Proceedings, Kyoto University), **1400** (2004) 39-87.
- [8] L. Casian and Y. Kodama, Toda lattice, cohomology of compact Lie groups and finite Chevalley groups, *Invent. Math.* **165** (2006) 163-208.
- [9] L. Casian and R. Stanton, Schubert cells and representation theory, *Invent. Math.* **137** (1999) 461-539.
- [10] S. Chakravarty and Y. Kodama, Classification of the line-solitons of KP II, *J. Phys. A: Math. Theor.* **41** (2008) 275209 (33pp).
- [11] S. Chakravarty and Y. Kodama, Soliton solutions of the KP equation and application to shallow water waves, *Stud. Appl. Math.* **123** (2009) 83-151.

- [12] I. M. Gel'fand and V. V. Sarganova, Combinatorial geometries and torus strata on homogeneous compact manifolds, *Russian Math. Surveys*, **42**:2 (1987) 133-168.
- [13] W. Fulton and J. Harris, *Representation Theory* GTM **129** (Springer, New York, 1991).
- [14] F. R. Gantmacher, *The theory of matrices*, (Chelsea Publishing Company, New York, 1990)
- [15] R Hirota, *The Direct Method in Soliton Theory* (Cambridge University Press, Cambridge, 2004)
- [16] B. Iversen, *Cohomology of sheaves*, (Springer-Verlag, New York, 1986).
- [17] S. J. Jungking, *Some computations of the homology of real Grassmannian manifolds*, Master thesis at The University of British Columbia, (September, 1979). (<https://circle.ubc.ca/handle/2429/21381>).
- [18] B B Kadomtsev and V I Petviashvili, On the stability of solitary waves in weakly dispersing media *Sov. Phys. Doklady*, **15** (1970) 539-541.
- [19] R. R. Kocherlakota, Integral Homology of Real Flag Manifolds and Loop Spaces of Symmetric Spaces, *Advances in mathematics* **110**, (1995), 1-46
- [20] Y. Kodama, KP solitons in shallow water, *J. Phys. A: Math. Gen.*, **43** (2010) 434004 (54pp).
- [21] Y. Kodama and J. Ye, Toda lattices with indefinite metric II: Topology of the iso-spectral manifolds, *Physica D* **121** (1998) 89-108.
- [22] D. Kadhane and G. Lusztig, Schubert varieties and Poincaré duality, *Proc. Symp. in Pure Math.*, AMS **36** (1980) 185-203.
- [23] G. Lusztig and D. Vogan, Singularities of Closures of K-orbits on Flag Manifolds, *Invent. Math.* **71** (1983) 365-379.
- [24] J. W. Milnor and J. D. Stasheff, *Characteristic classes*, (Princeton University Press, Princeton), (1974).
- [25] T. Miwa, M. Jimbo and E. Date, *Solitons: Differential equations, symmetries and infinite dimensional algebras*, (Cambridge University Press, 2000) Translated from the Japanese version published by Iwanami-Publication in 1993.
- [26] M. Sato, Soliton equations as dynamical systems on an infinite dimensional Grassmann manifolds, *RIMS Kokyuroku*, **439** (1981) 30-46.
- [27] H. Yeh, W. Li and Y. Kodama, *Eur. Phys. J. Special Topics*, **185** (2010) 97-111.

DEPARTMENT OF MATHEMATICS, OHIO STATE UNIVERSITY, COLUMBUS, OH 43210
E-mail address: `casian@math.ohio-state.edu`

DEPARTMENT OF MATHEMATICS, OHIO STATE UNIVERSITY, COLUMBUS, OH 43210
E-mail address: `kodama@math.ohio-state.edu`